Lecture 4

Battery Materials, Diffusion, Ionic Mobility, Voltage Calculation

Batteries

- Are key elements for energy storage
- The current state of the art are Li-batteries, while Na-batteries may represent the next viable technology (other mobile species possible, Mg, K, Sn, Al, …)
- There are many parameters that affect material choice.
- Relevant quantity are Voltage, Capacity, and Energy Density (Voltage x Capacity).
- Optimisation entails discovery/improvement of solid state materials.

Batteries: The Challenge

Capacity
Voltage
Efficiency

General Scheme

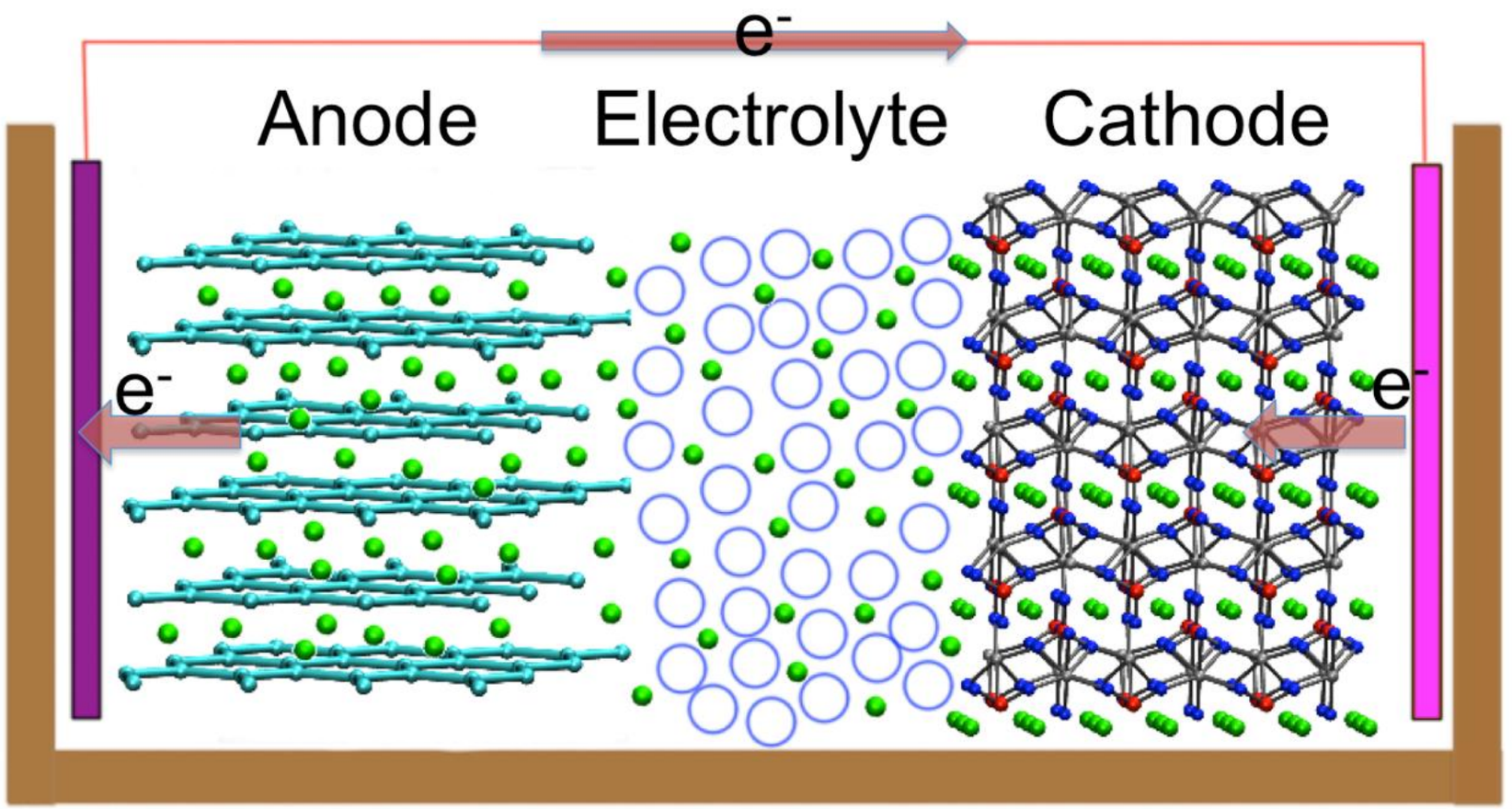

Si, C

LiMPO4, M=Fe, Mn
LiMBO3
MoO2,MoO3
V, Nb, Ti,... oxides

Battery Elements

- There are three essential constituent of a battery material:
  - A cathode (reduction reaction)
  - An electrolyte (electron transport)
  - An anode (oxidation reaction)
  - …and their interfaces!
  - $Li \rightarrow Li^{+} + e^{-}$
  - System must allow both species (Li cations and electrons) to flow - must be a ionic conductor as well as an electronic conductor – maximize interface contact!
  - Anode is the source of Lithium Ions, cathode is the sink

Battery elements

- The anode is commonly simply graphitic carbon, or silicon (recently). If Si, then solid state reactions occur.
- The electrolyte contains a lithium salt dissolved into a mixture of organic solvents ($LiPF_6$ for example, ionic liquids are also a possibility, imidazolate salts)
- The cathode is the part enjoying most attention recently, and is the one, which is being optimised & tu.ned for improved voltage and capacity (this is of less concern on the anodic side, where voltage can be low and capacity is already granted by the material itself (porosity, including the use of “molecular” C)

Properties

- Battery material contain a readily reducible/oxidisable element, normally a transition metal.
- The reaction with lithium is reversible (intercalation type of reaction)
- High free energy of reaction
  - high capacity - means that the number of lithiums per transition metal needs to be high (at least one!)
  - high intercalation voltage
  - high energy storage (voltage x capacity)
- Rapid reaction with lithium
- Good electronic conductor
- Stable
  - no degradation, no over-dischage/over-charge
  - can afford many charge/discharge types

Battery Requirements

- Energy Density
- Power density
- Cycle life, Lifetime
- Charging rate
- Temperature stability
- Safety, Cost
- Manufacturability

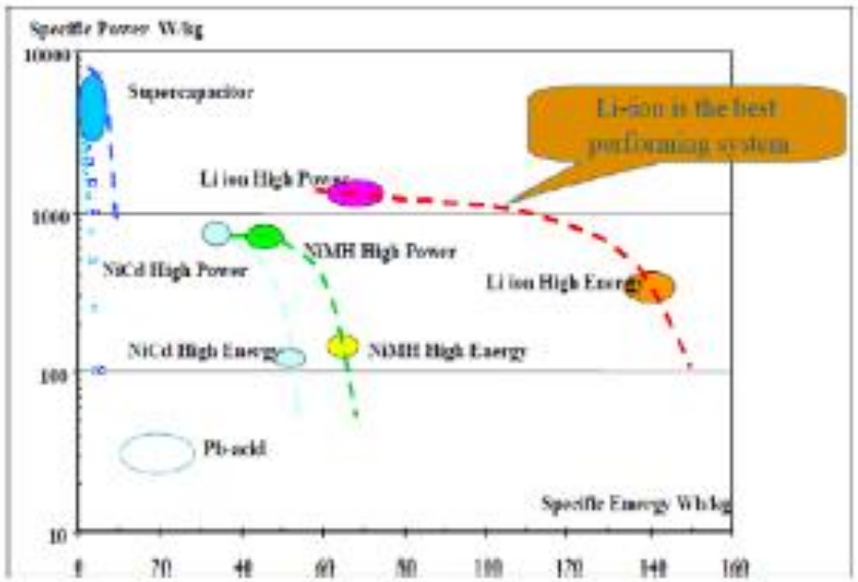

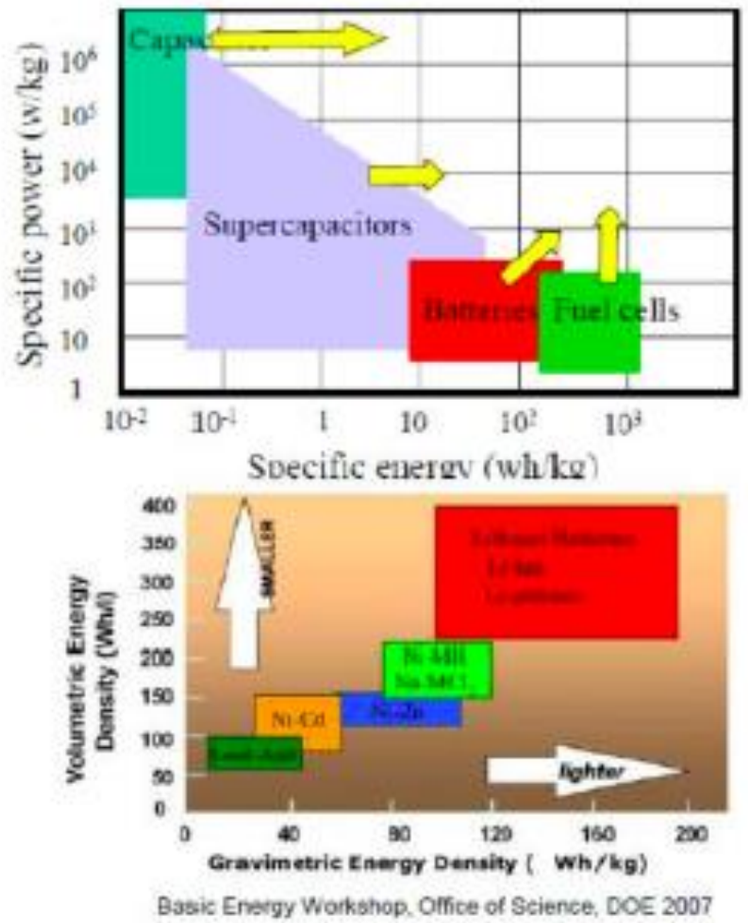

Basic Energy Workshop, Office of Science, DOE 2007

How this problem is solved…

- Use transition metals like Fe, Mn, V, Mo,…(Ti, Ni, Co,…)
- Use l**ayered or channel compounds**, such that there is an obvious means to accommodate/intercalate Li ions.
- Oxides are a good choice, also phosphates, silicates, borates.
- Normally higher Li mobility due to structural features, electrical conductivity often a problem (too low)
- Little is known about mechanisms, both for ionic and electronic conduction, interfaces are an emerging challenge.
- Relatively difficult to truly innovate in this field, advancements rather slow & cumulative.

Layered structures

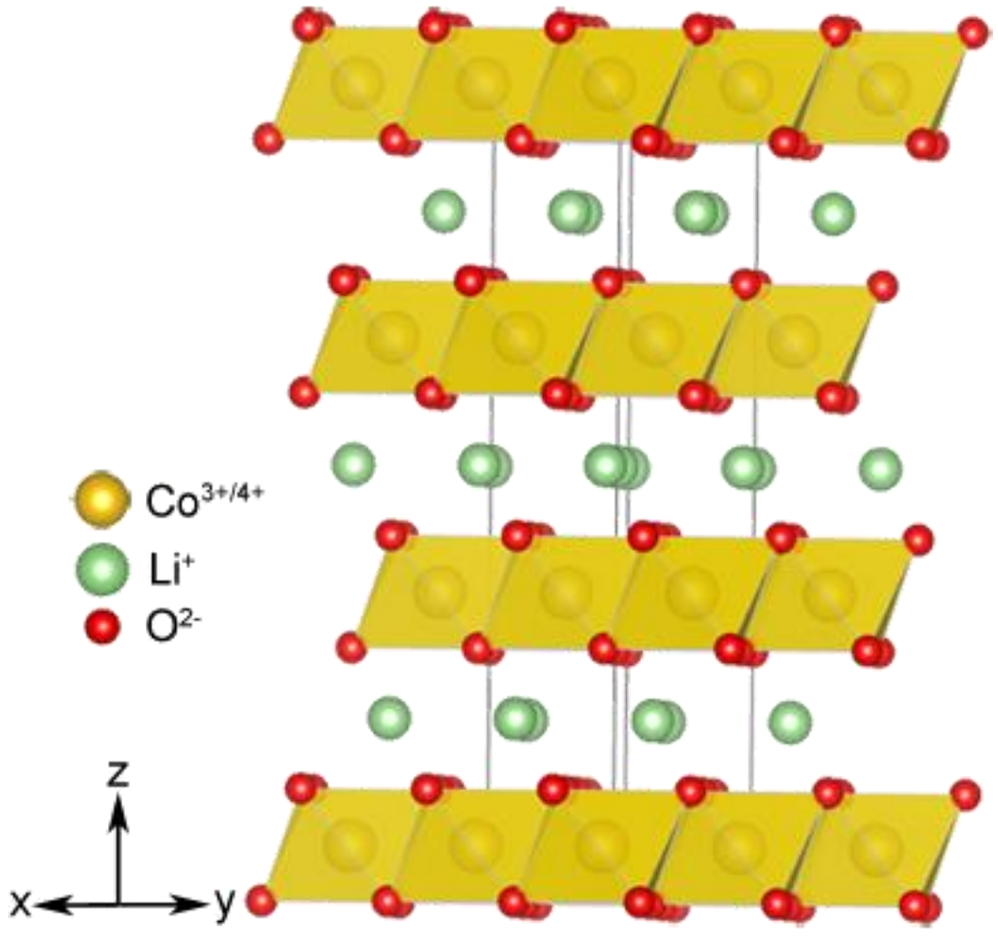

$LiCoO_2$

Layers of octahedrally coordinated Co atoms, Li intercalated

layered vanadates

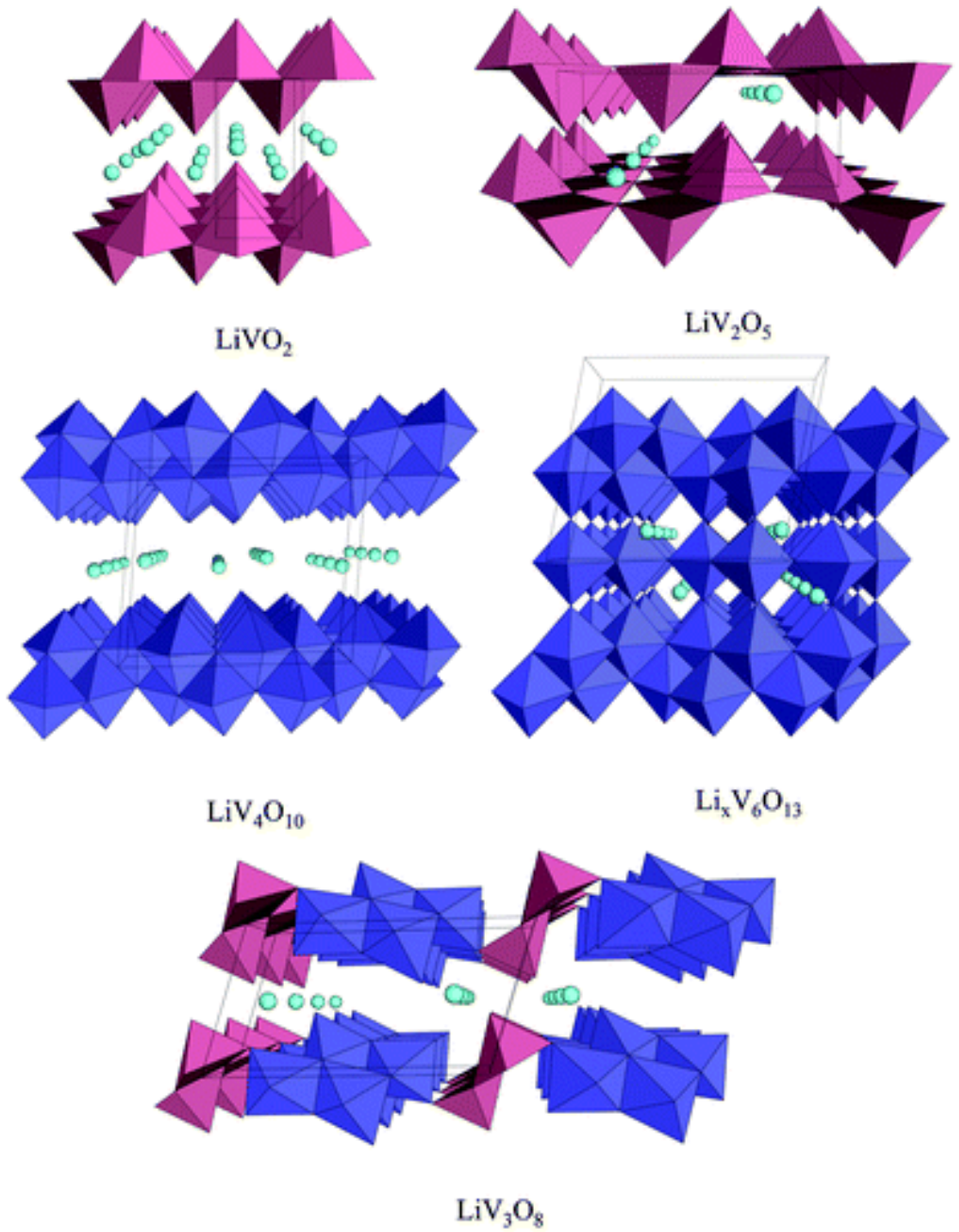

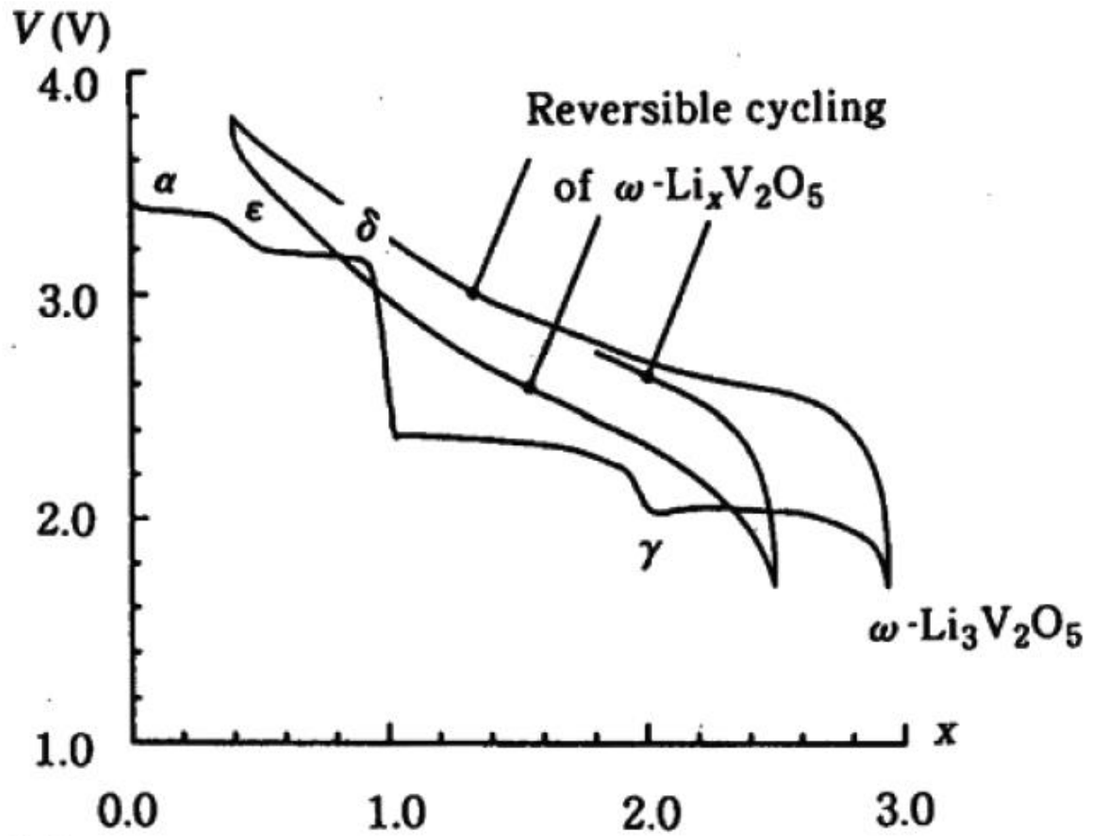

(c)

In certain compounds, increasing Li concentration leads to the formation of different structures.

The cell (half-cell) voltage is measured against a reference cell (set to zero), as a function of Li concentration (or capacity).

M. Whittingham, [*J. Mater. Chem.*](), 2005, **15**, 3362-3379
M. Whittingham, *Chem. Rev.* ***2004,*** *104, 4271-4301*

Spinels, $LiMn_2O_4$

- Class of solid state structures of composition AB2O4 - compositionally versatile
- $LiMn_2O_4$ -> Mn_2O_4 + Li

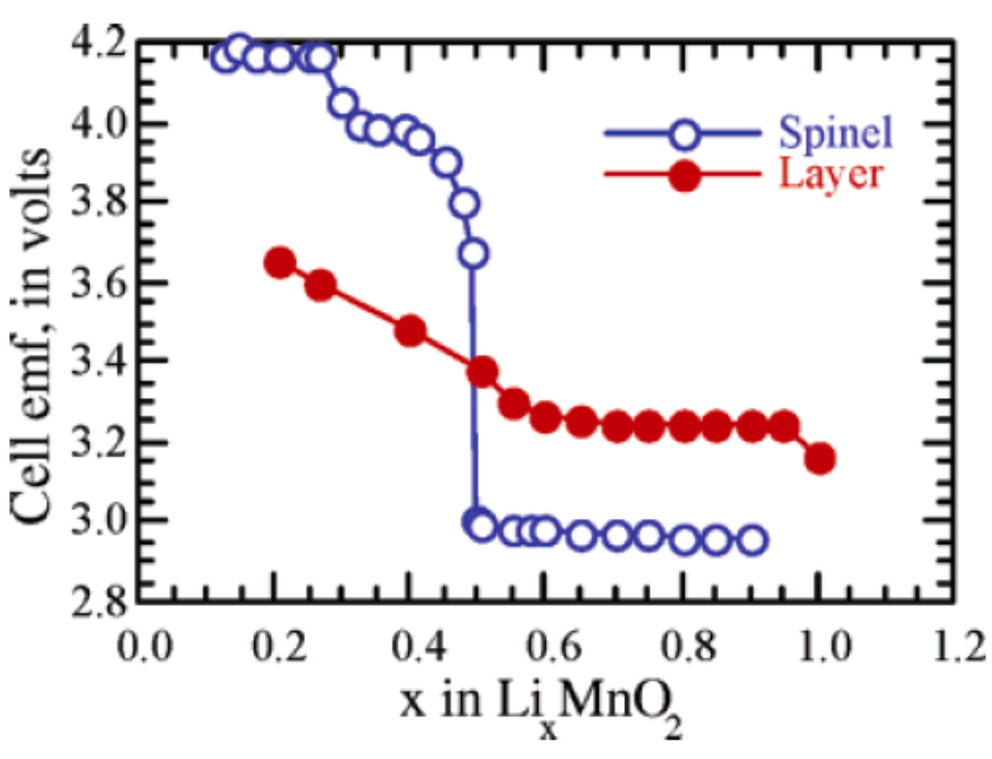

Figure 11. Potential profile of $LiMnO_2$ and spinel $LiMn_2O_4$ (data from Bruce and Whittingham).

Useful composition and voltage ranges depend on structure - also the state in which the battery material is prepared is critical

For Mn-based batteries, Jahn-Teller distortion may impair reversibility, so sensible electronic configurations shall be avoided.

Structural distortions

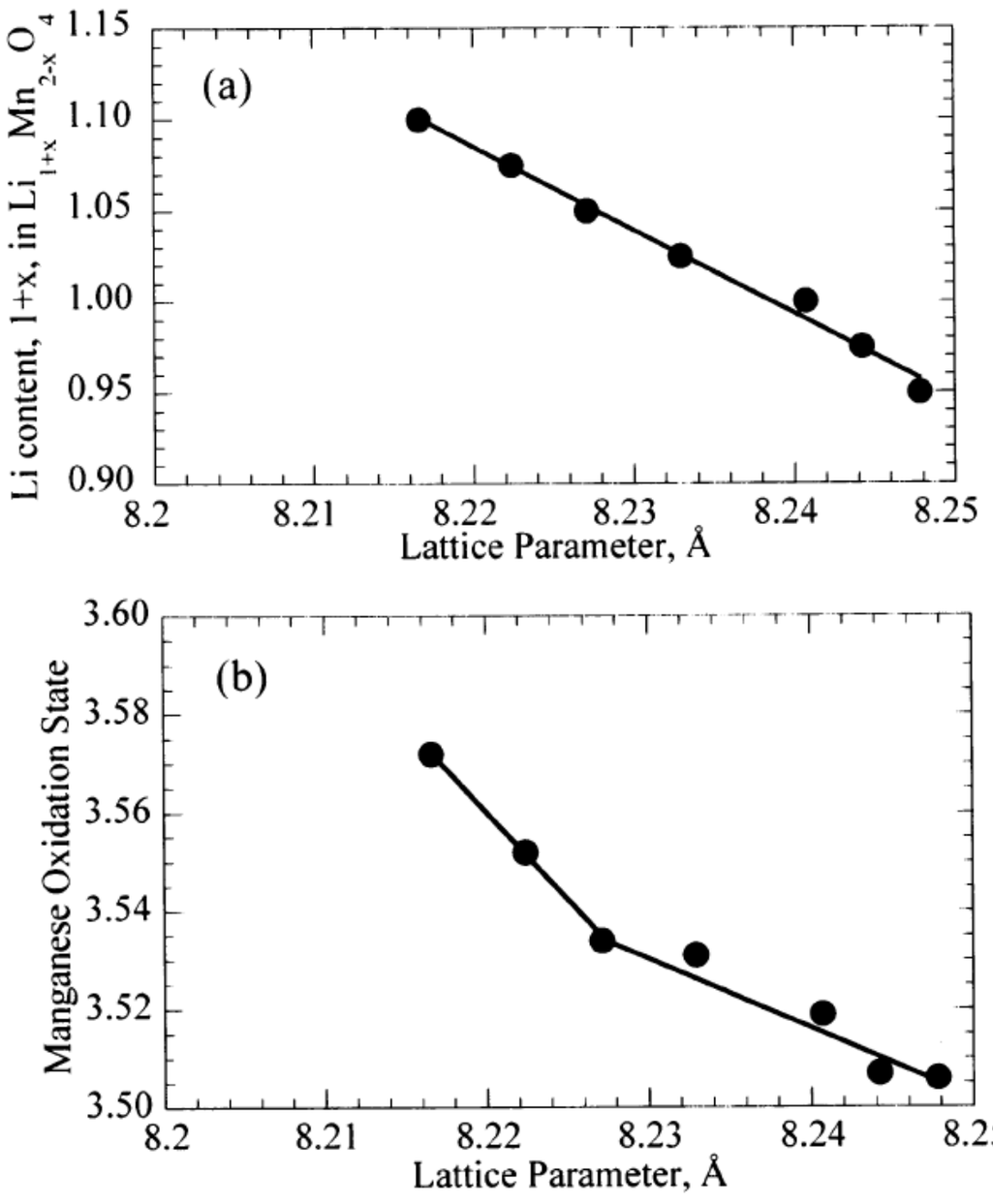

M. Whittingham, *Chem. Rev.* ***2004,*** *104, 4271-4301*

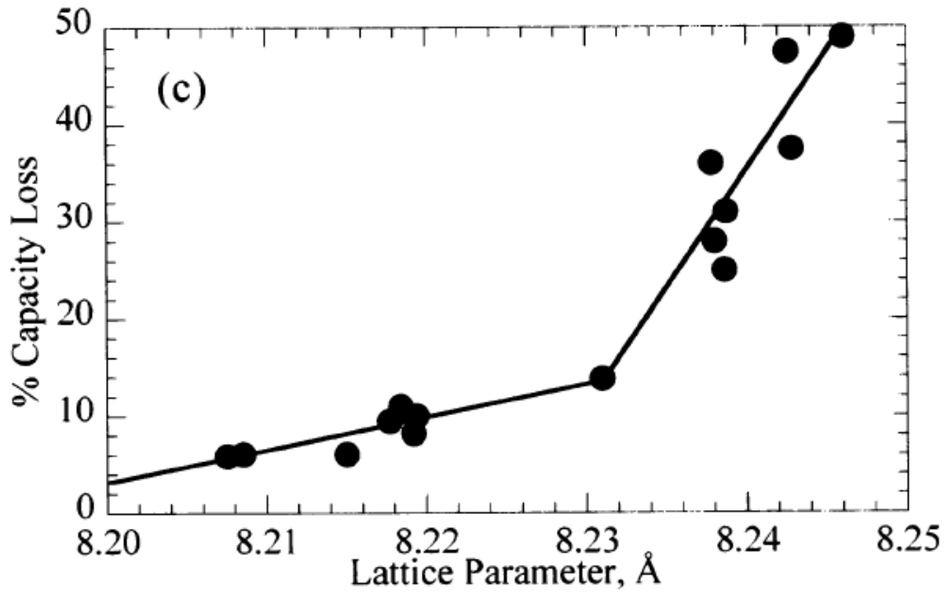

Figure 12. Correlation of the lattice parameter of the spinel $Li_{1+x}Mn_{2-x}O_4$ with (a) the lithium content, (b) manganese oxidation state, and (c) capacity loss of the cell over the first 120 cycles, after ref 157.

Li content structurally impacts structure, oxidation number of the active center, and capacity (loss). This is turns constraints the range over which a battery can operate.

Battery Type Overview

The voltage difference between the anode and cathode determines the cell power, while the anode's lithium content determines its energy density. About a million other things affect lifespan and performance

Anode and Cathode Materials(1)

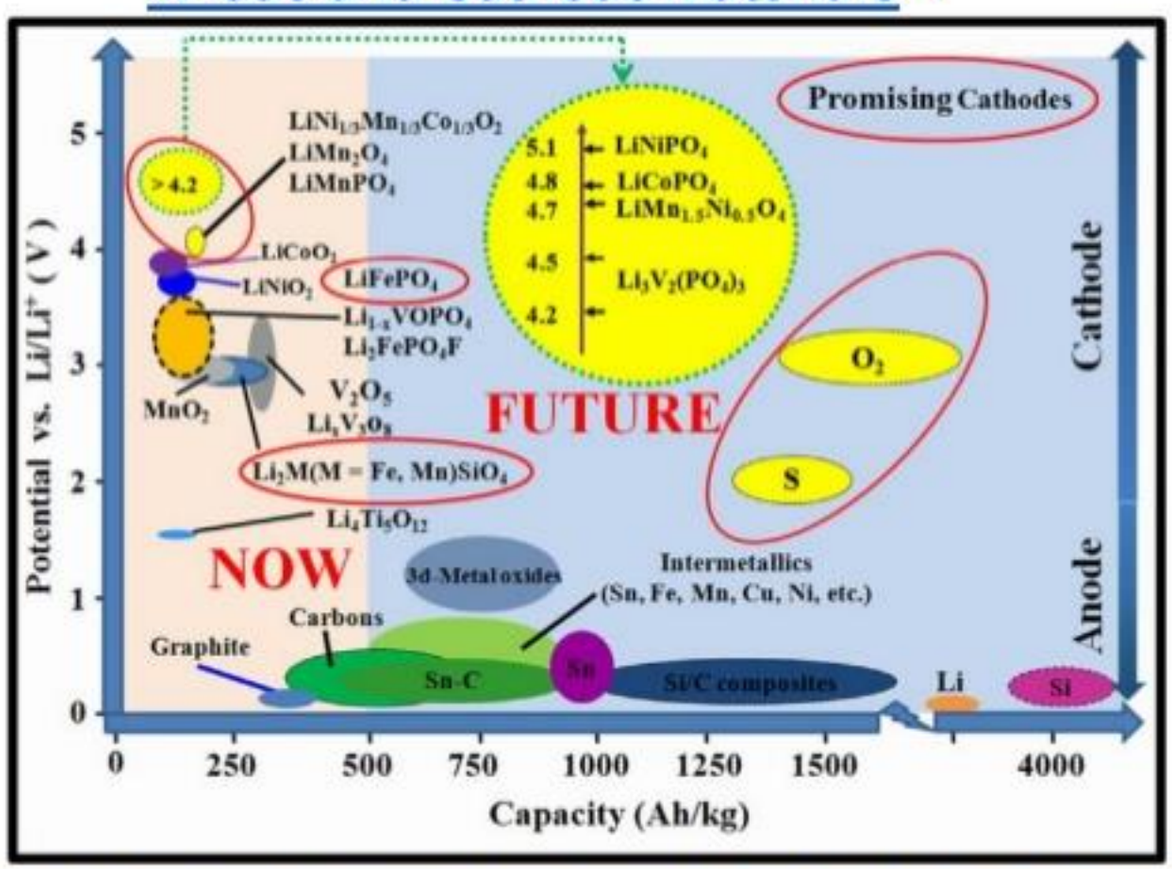

Source: Cathode materials for next generation lithium ion batteries. May 2013. Jiantie Xu , Shixue Dou , Huakun Liu , Liming Dai. Case Western.
1) Source File

Transport processes (ions/electrons)
Often coupled events

Conductivity

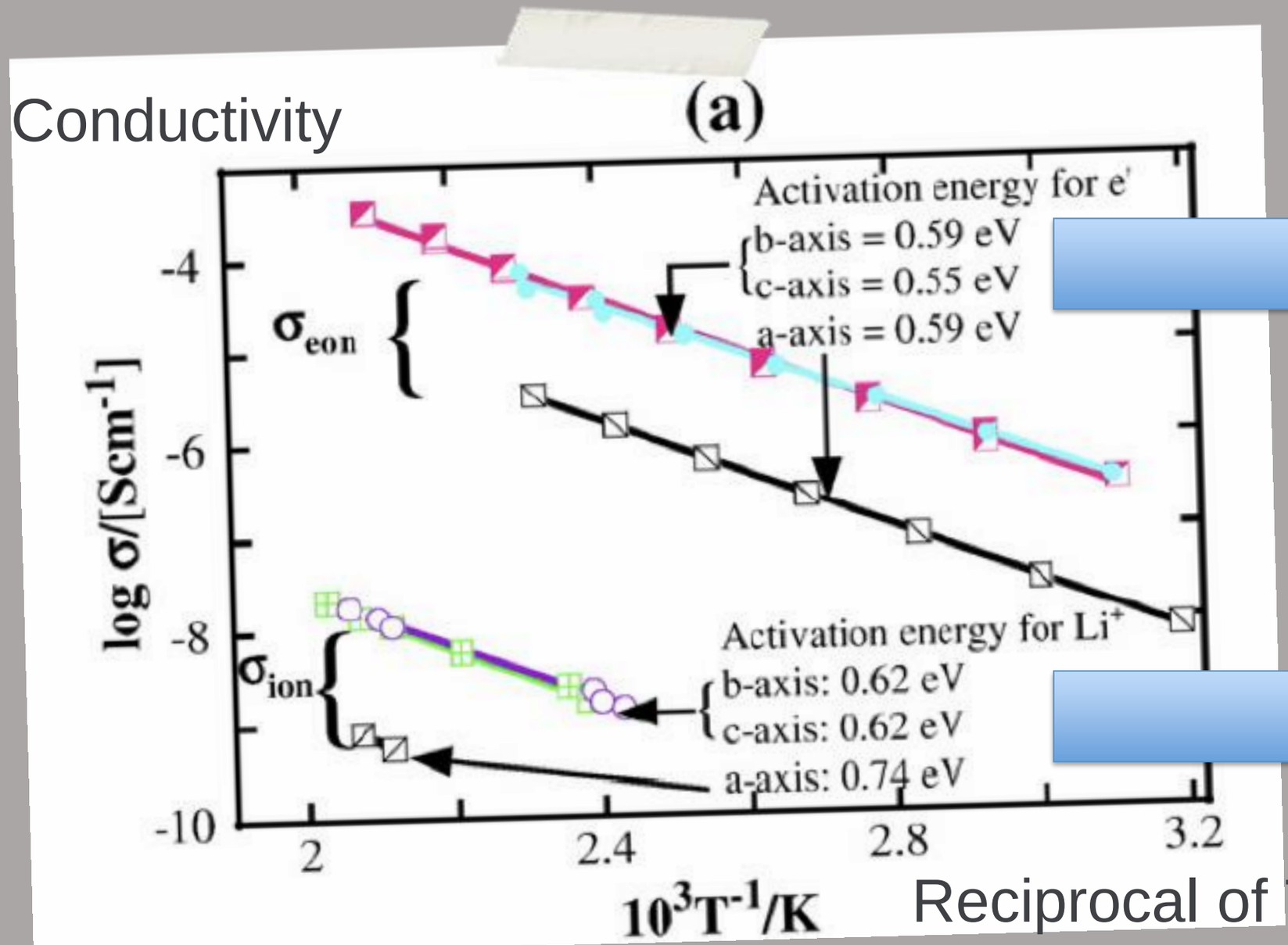

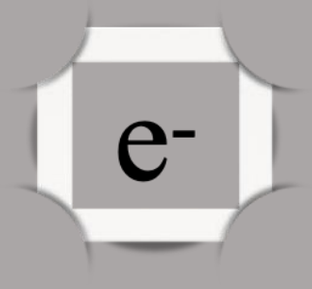

Reciprocal of Temperature

Amin et al. Solid State Ionics 179 (2008) 1683-1687 (J. Maier)

$LiFePO_4$: Channels as Li Pathways

[010], easy

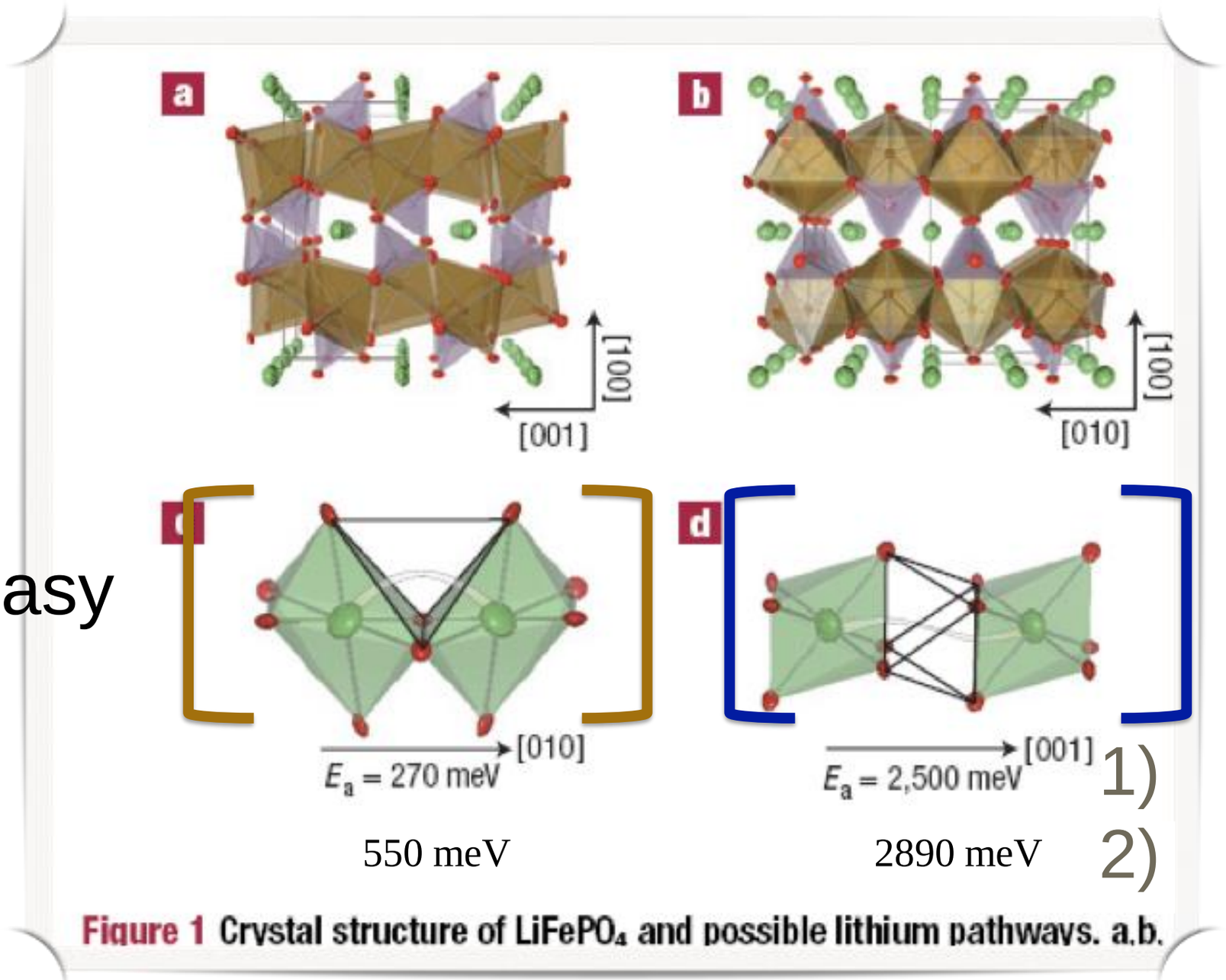

Figure 1 Crystal structure of $LiFePO_4$ and possible lithium pathways. a,b,

[001], no go

1)

550 meV

2890 meV 2)

1) Yamada *et al.*, Nat. Mater. 7, 707 (2008)

2) M. S. Islam *et al.*, Chem. Mater. 17, 5085 (2005)

$LiFePO_4$ - Olivine materials

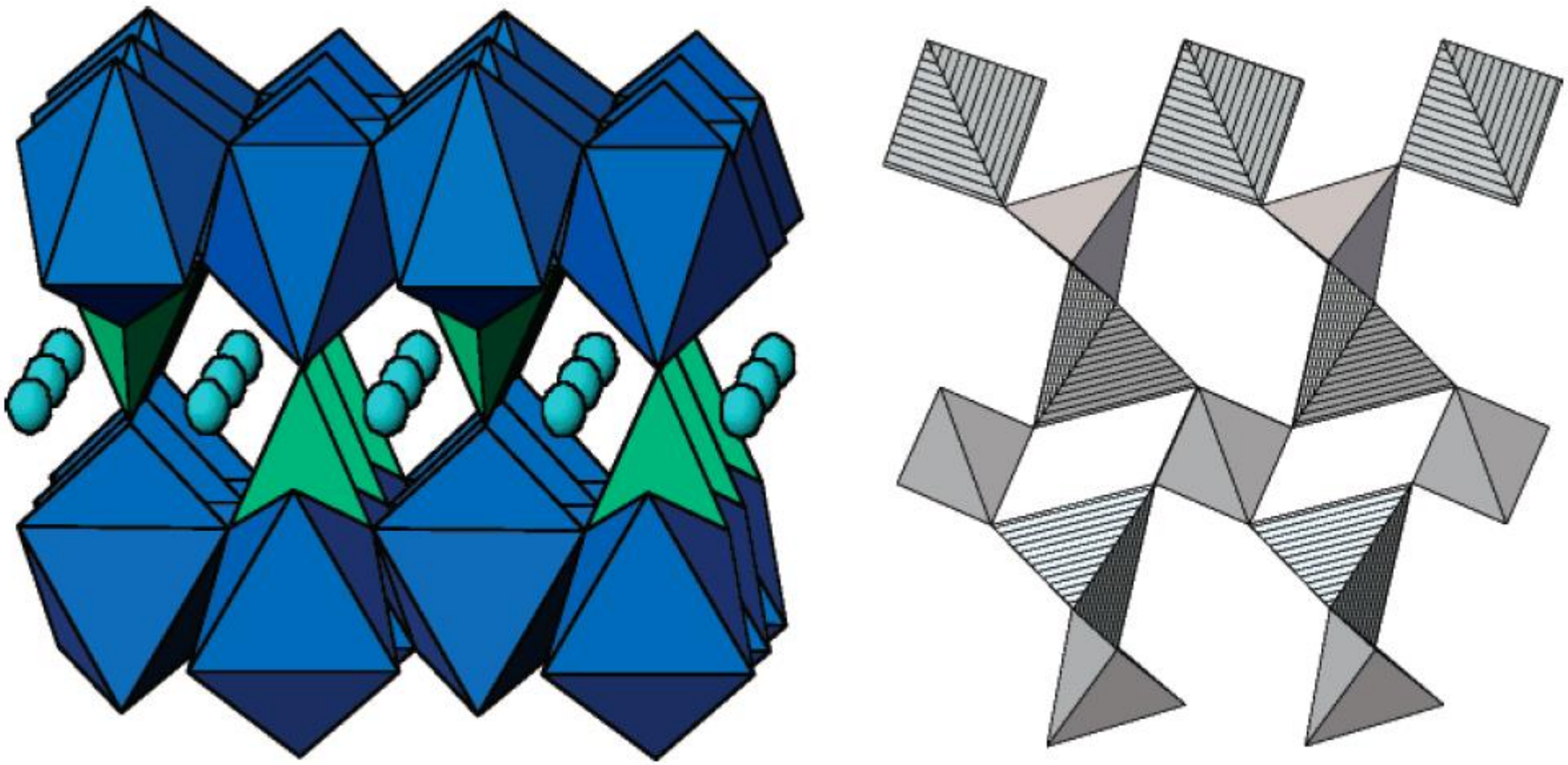

Figure 22. Structures of orthorhombic $LiFePO_4$ and trigonal quartz-like $FePO_4$.

M. Whittingham, *Chem. Rev.* ***2004,*** *104, 4271-4301*

Li_xFePO4

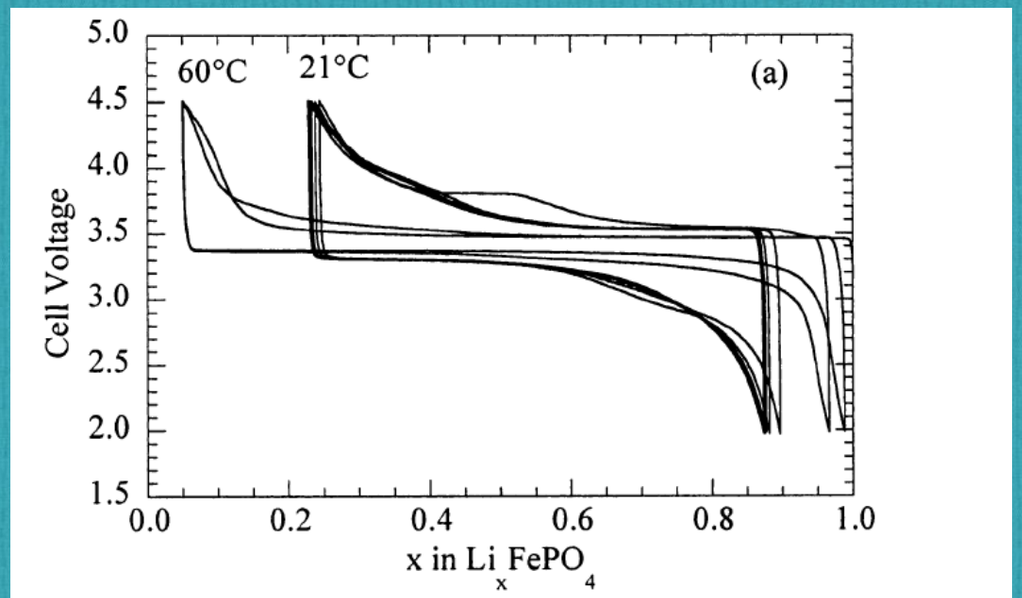

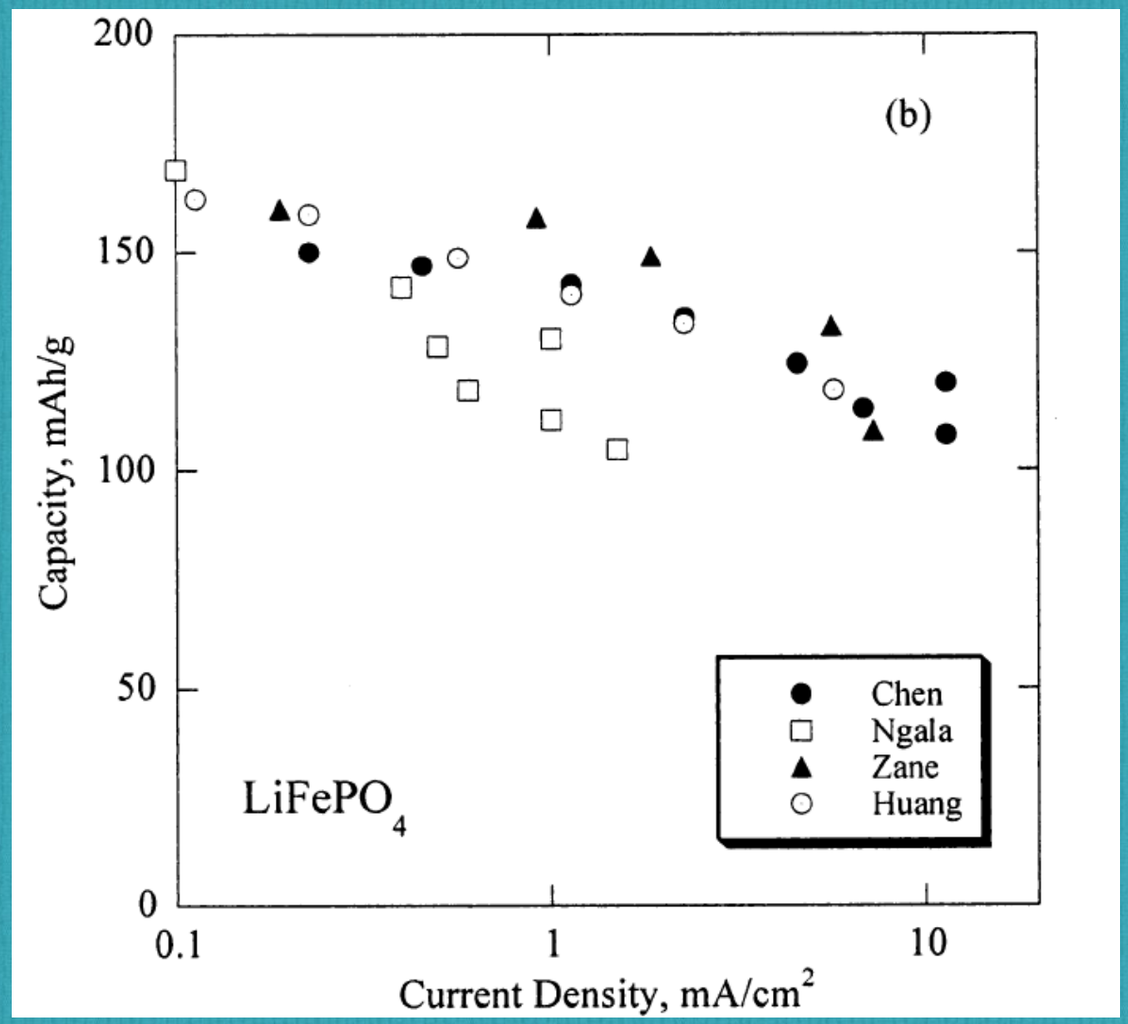

M. Whittingham, *Chem. Rev.* ***2004,*** *104, 4271-4301*

Capacity (theoretical)

Calculate the theoretical specific capacity in mAh/g of lithium iron phosphate, LiFePO4, if the molecular weight is 158 g/mol. (3.6 C = 1 mAh)

theoretical specific capacity = #molLi x #electroncharge / #molmass
(in C/g)
(divide by 3.6 for mAh/g)

LiFePO4 (LFP) intercalates one mole of lithium per mole LFP.
(1 mol Li/mol LFP) * (96487 C/mol Li) / (158 g/mol LFP) / (3.6 C/ mAh) = 170 mAh/g

https://www.unitjuggler.com/convert-electriccharge-from-C-to-mAh.html?val=3.6
http://battery.berkeley.edu/

Candidate redox active centres

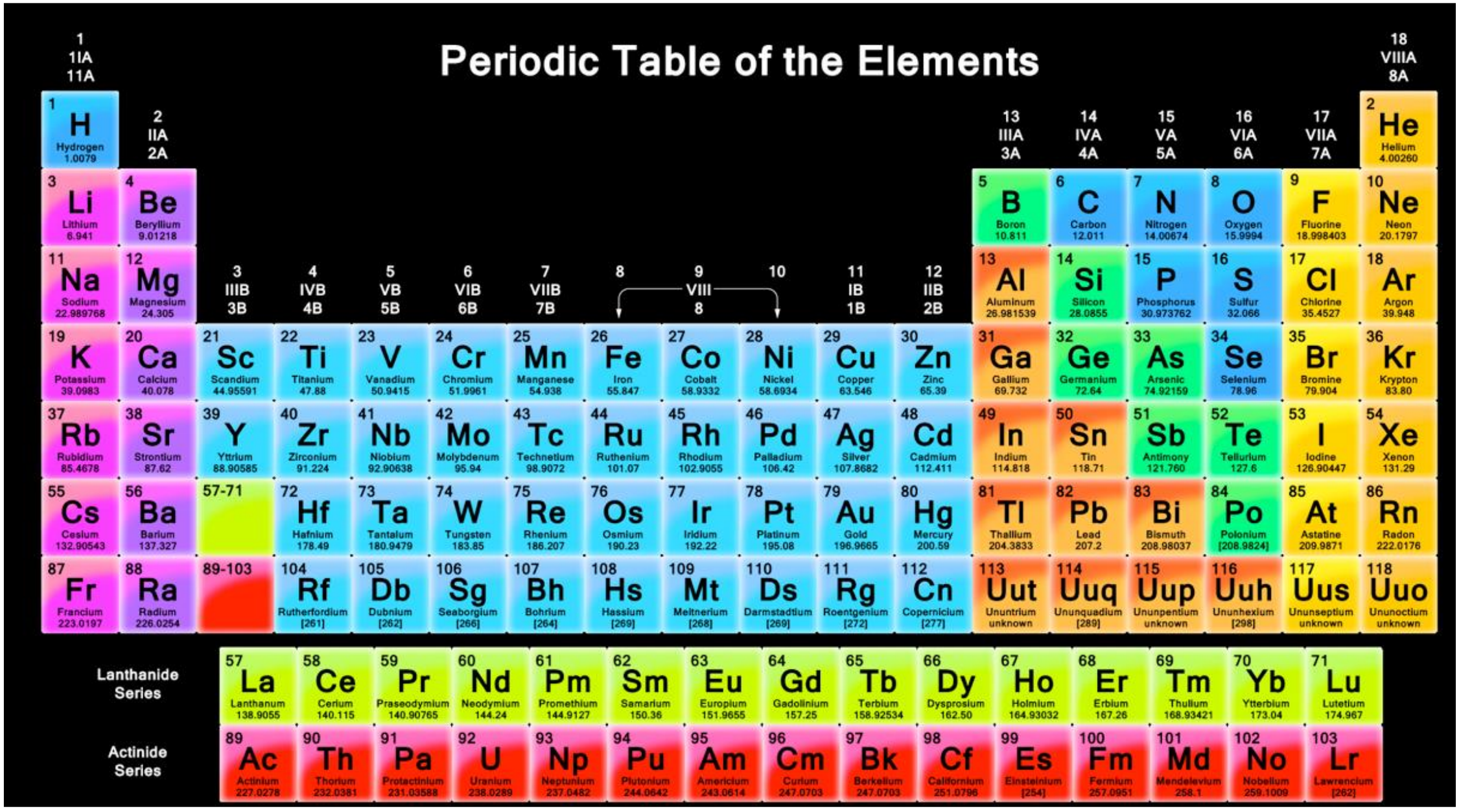

Orbitals

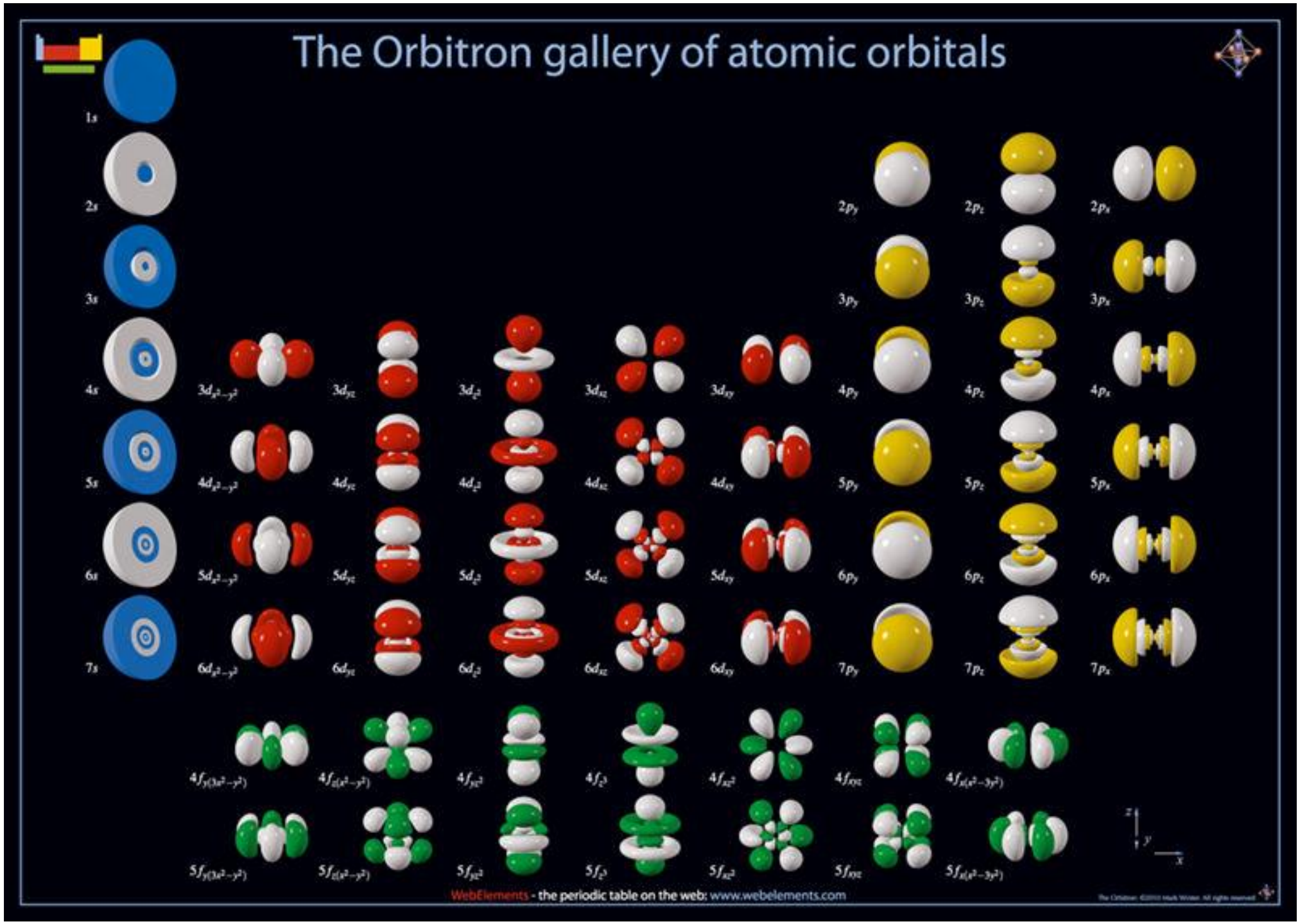
The Orbitron gallery of atomic orbitals
1s
2s
3s
4s
5s
6s
7s
2p_y
2p_z
2p_x
3p_y
3p_z
3p_x
4p_y
4p_z
4p_x
5p_y
5p_z
5p_x
6p_y
6p_z
6p_x
7p_y
7p_z
7p_x
3d_xy
3d_xz
3d_yz
4d_xy
4d_xz
4d_yz
5d_xy
5d_xz
5d_yz
6d_xy
6d_xz
6d_yz
4f_xyz
4f_xz2
4f_yz2
5f_xyz
5f_xz2
5f_yz2
WebElements - the periodic table on the web: www.webelements.com

Cathode Matherial	Voltage	Capacity
$LiCoO_2$	4.2 V	272 mAh/g
$LiFePO_4$	3.2 V	170 mAh/g
$LiMn_2O_4$	4.3 V	140 mAh/g
LiV_2O_5	3.6 V	142 mAh/g

$LiFePO_4$:Proposed domino-cascade model

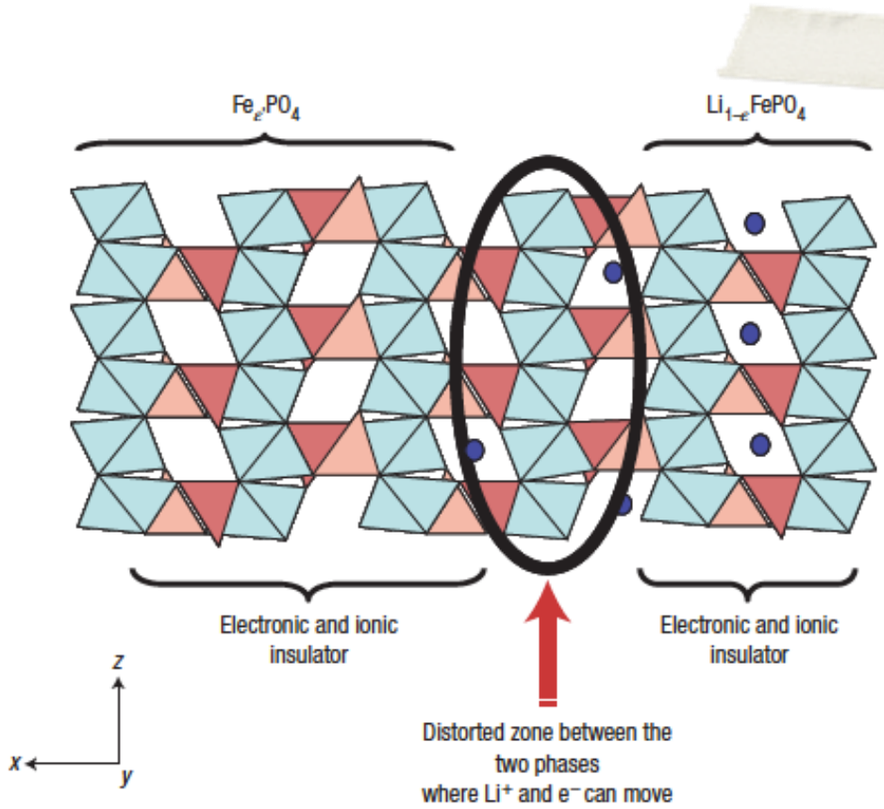

Figure 4 Distorted zone in the *ac* plane between the lithiated ($Li_{1-\varepsilon}FePO_4$) and delithiated ($Li_{\varepsilon}FePO_4$) phases during the lithium deintercalation/intercalation process in $LiFePO_4$ olivine-type material.

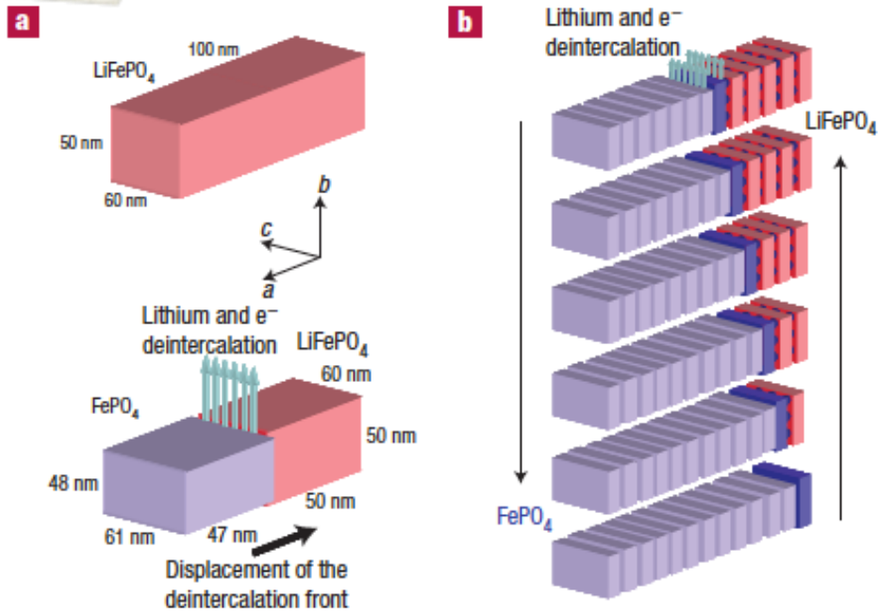

Figure 5 Schematic view of the 'domino-cascade' mechanism for the lithium deintercalation/intercalation mechanism in a $LiFePO_4$ crystallite. Distances are not accurate because studied crystallites are rather isotropic. **a**, Scheme showing a view of the strains occurring during lithium deintercalation. **b**, Layered view of the lithium deintercalation/intercalation mechanism in a $LiFePO_4$ crystallite.

C. Delmas et al., Nat. Mat. 7 (2008), 665

Sulfur

$$2Li^{+} + 2e^{-} + S(s) \longrightarrow Li_2S(s)$$ 1670 mAh/g, 2.2V.

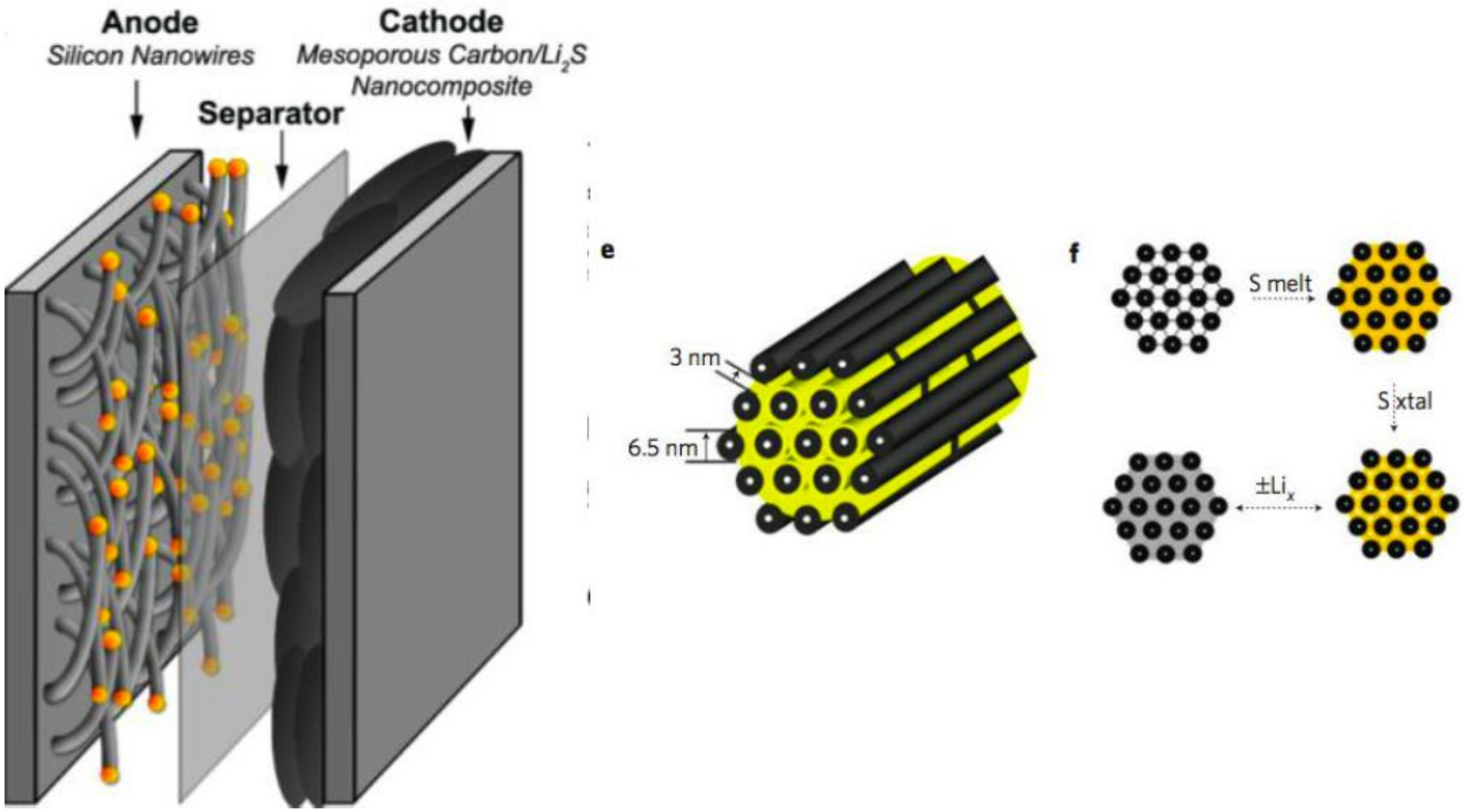

Yuan Yang, Matt McDowell, Ariel Jackson and Y. Cui (Nano Letters, 2010)

(L. Nazar, Nature Materials, 2009)

https://energy.stanford.edu/sites/default/files/YiCui.pdf

Na-Batteries

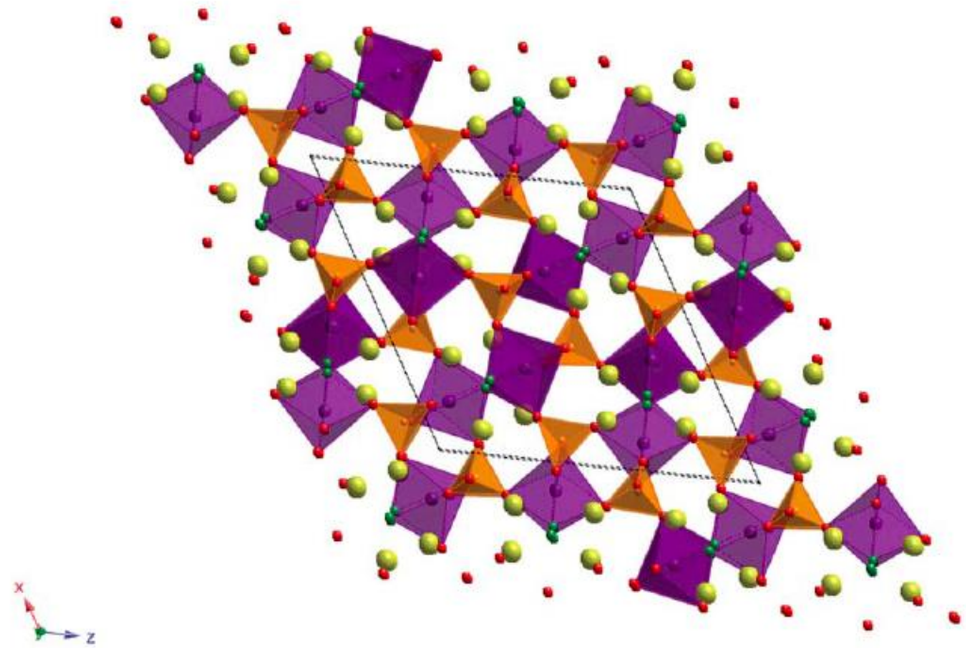

Fig. 18 Crystal structure of Na_2MnPO_4F. The manganese octahedra are plotted in purple, phosphate tetrahedra are shown in orange, fluorine atoms in green and Na ions in yellow.

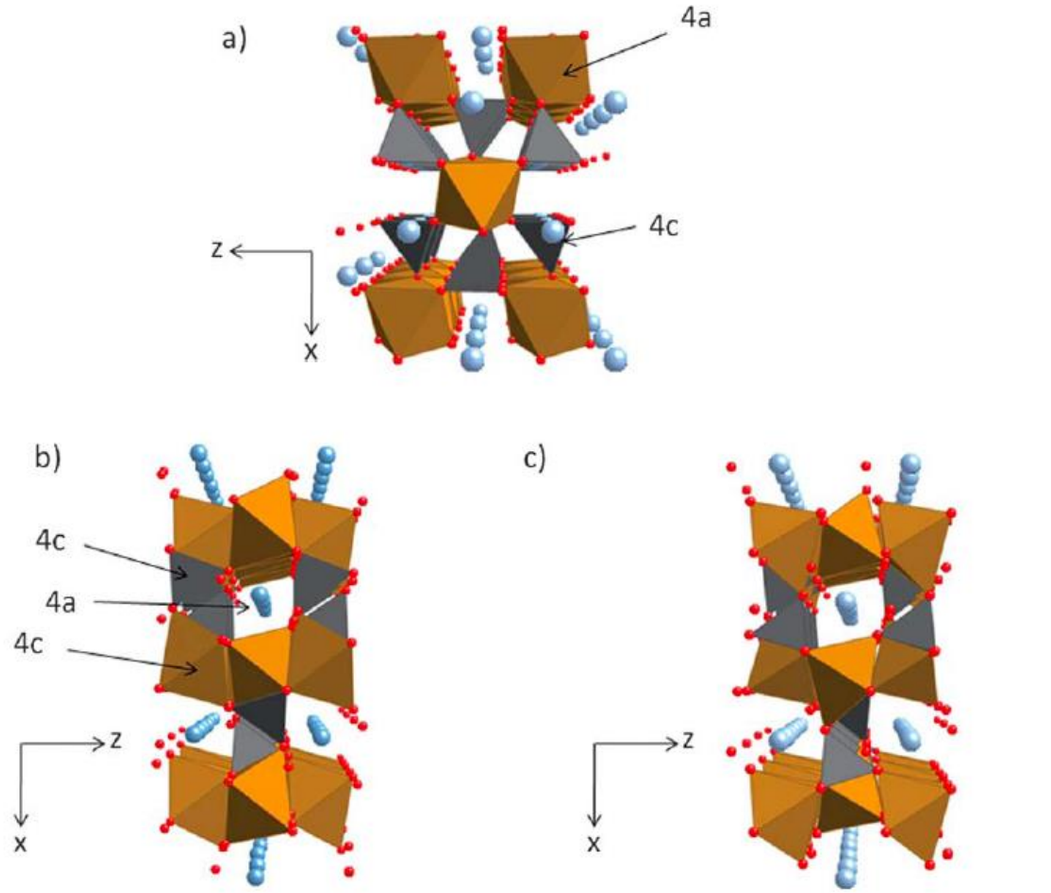

Fig. 6 Structure of (a) maricite $NaFePO_4$, (b) olivine $LiFePO_4$, and (c) olivine $NaFePO_4$. 4(a) and 4(c) crystallographic sites are marked.

V. Palomares, Energy Environ. Sci., 2012, 5, 5884

Mass Transport

“entropy CV”

“structure factor SF CV”

Batteries

Confined Crystallisation

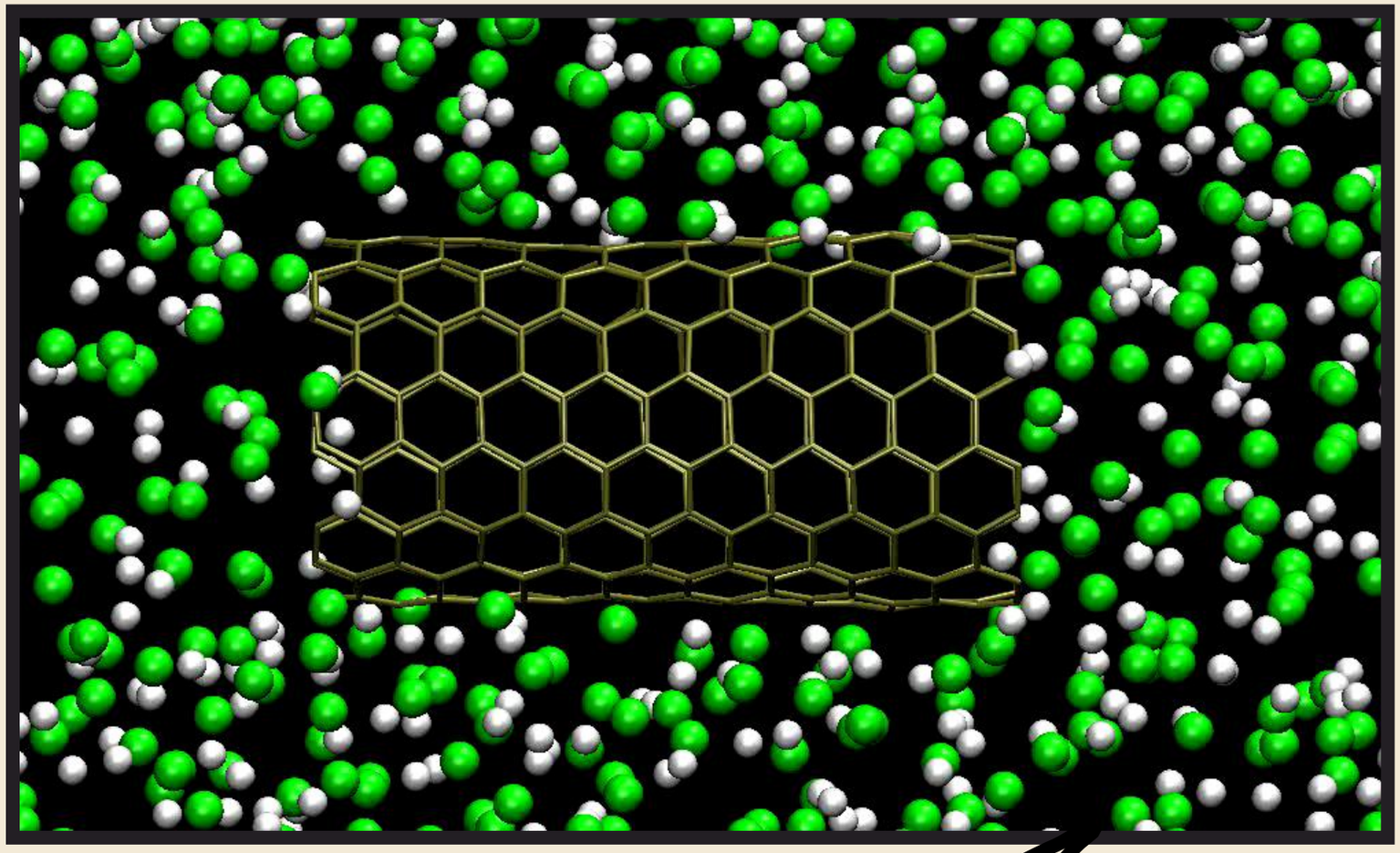

CaF_2, nanointerfaces "liquid" F^- anions

"nanoionics"

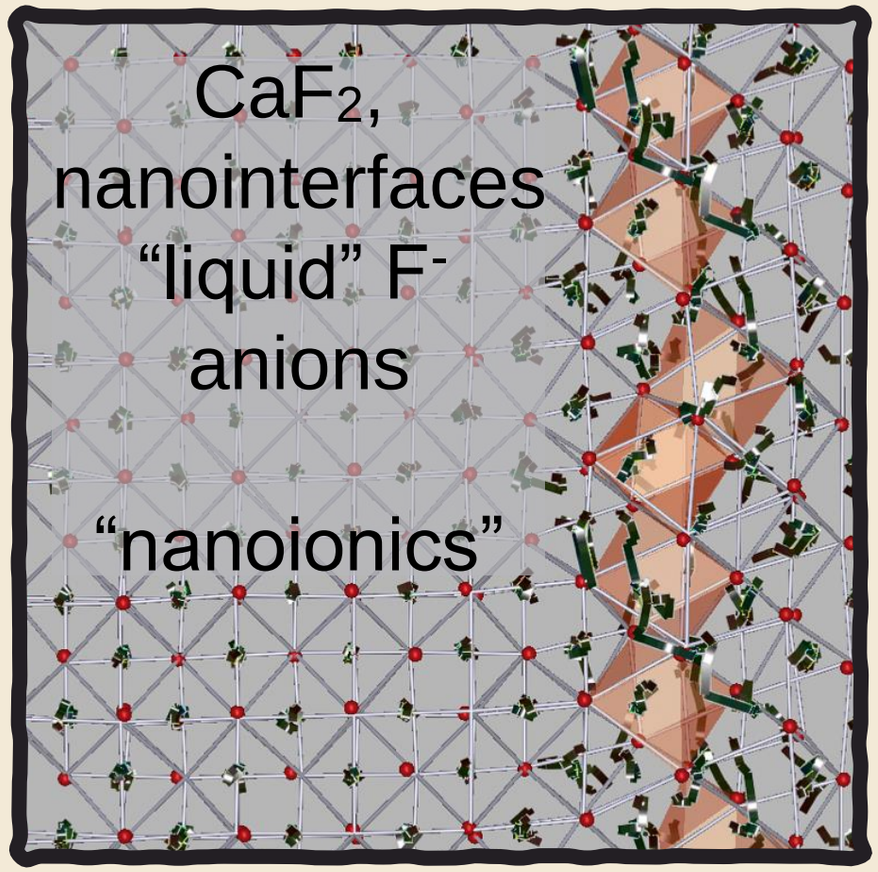

Diffusion & Defects in AgI

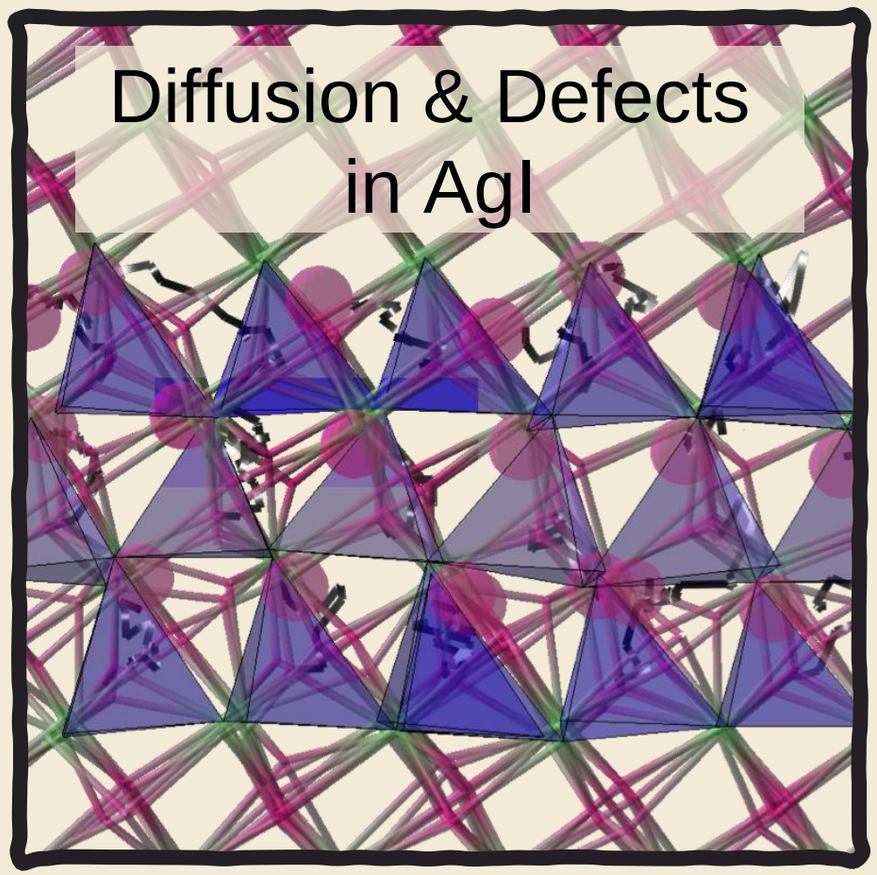

Diffusion, Crystallisation, Ionic Conduction

CARDIFF UNIVERSITY
PRIFYSGOL CAERDYDD

M. Baldoni et al., small (2007), S.E. Boulfelfel, S.Leoni, unpublisehd

Lithium-ion batteries

DFT & Molecular Dynamics

- Stabilities of different cathode materials
- Lithium uptake
- Mobility of lithium ions
- Intercalation / de-intercalation process(es)

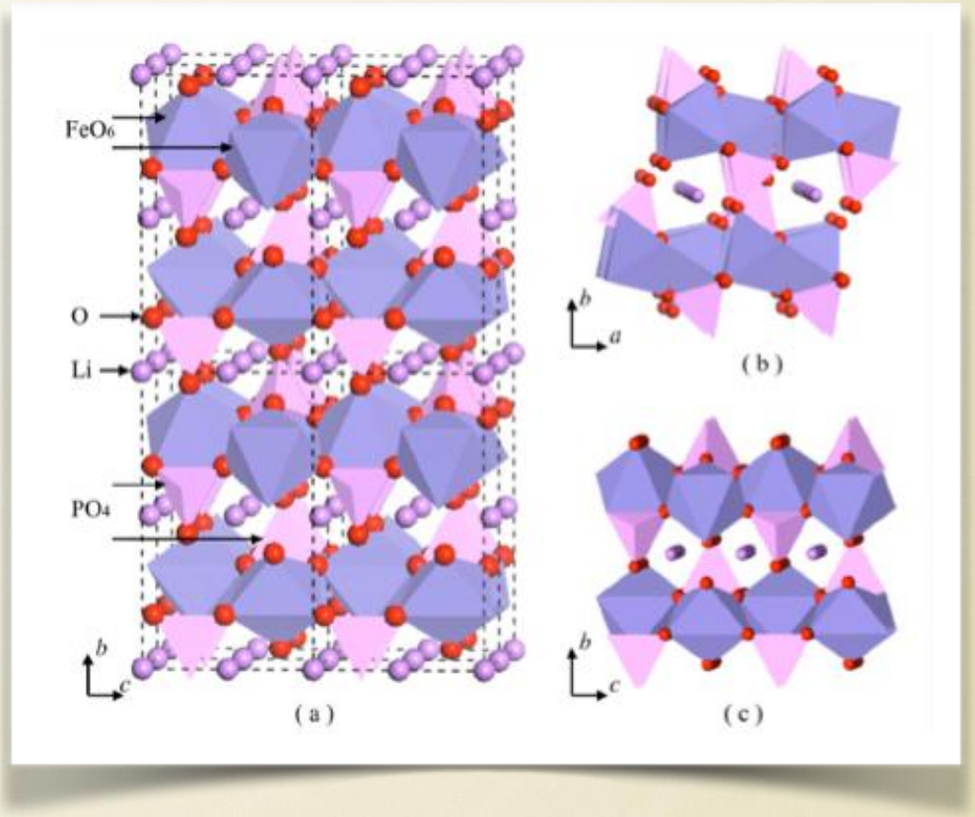

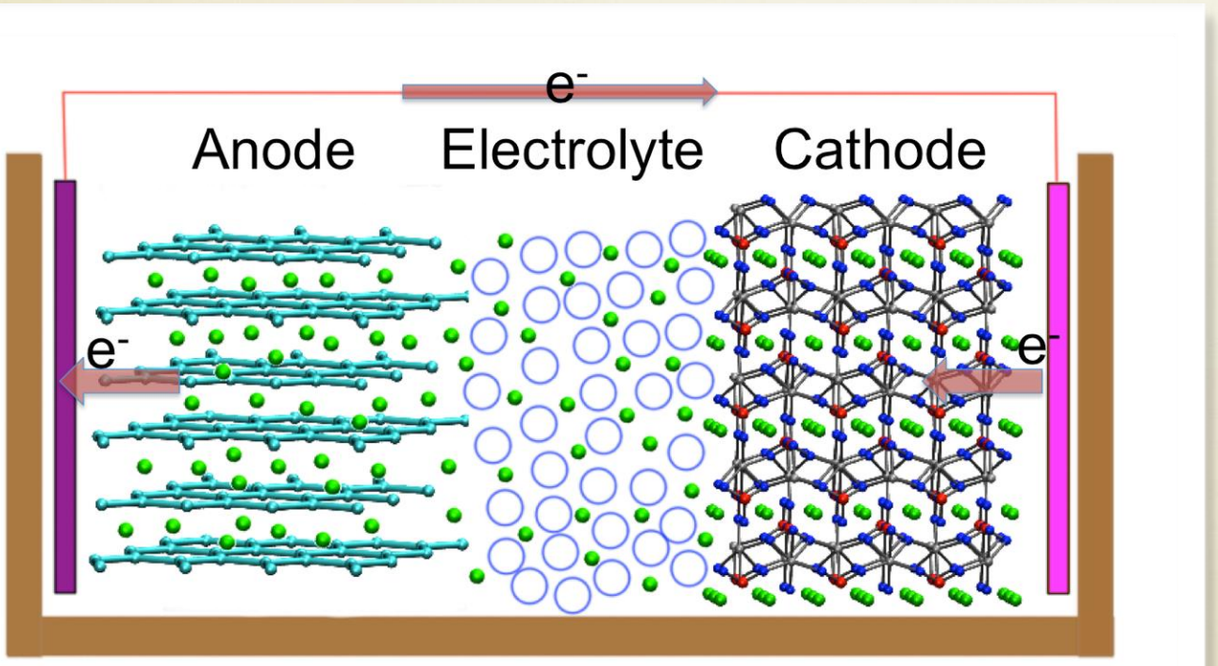

- $LiFePO_4$ crystal structure

Ouyang et al., Phys. Rev. B 69 (2004), 104303.

Which directions are relevant ?

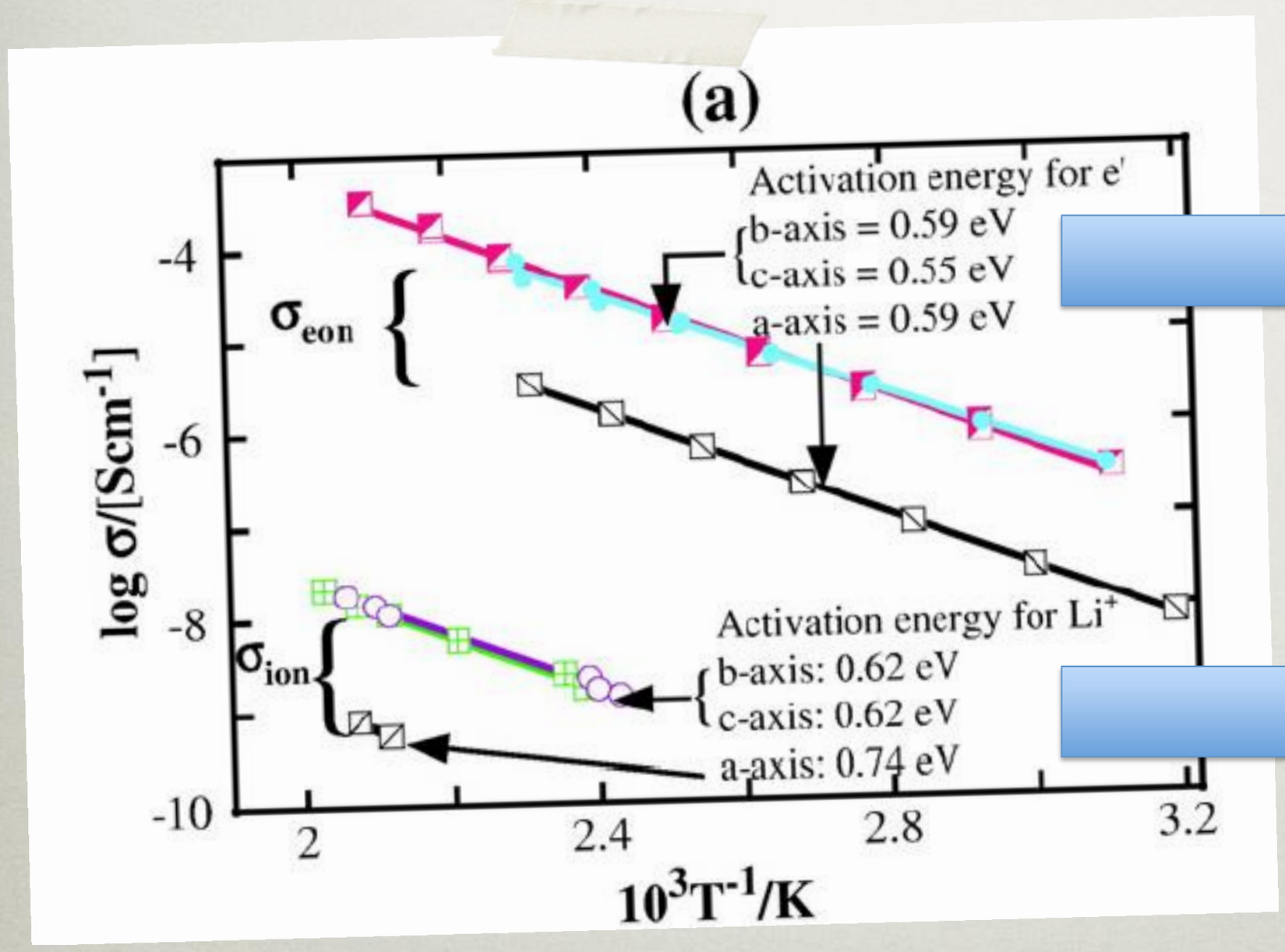

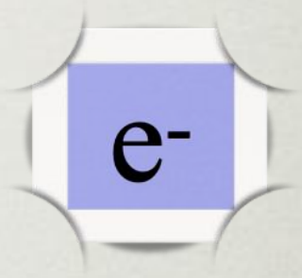

Amin et al. Solid State Ionics 179 (2008) 1683-1687

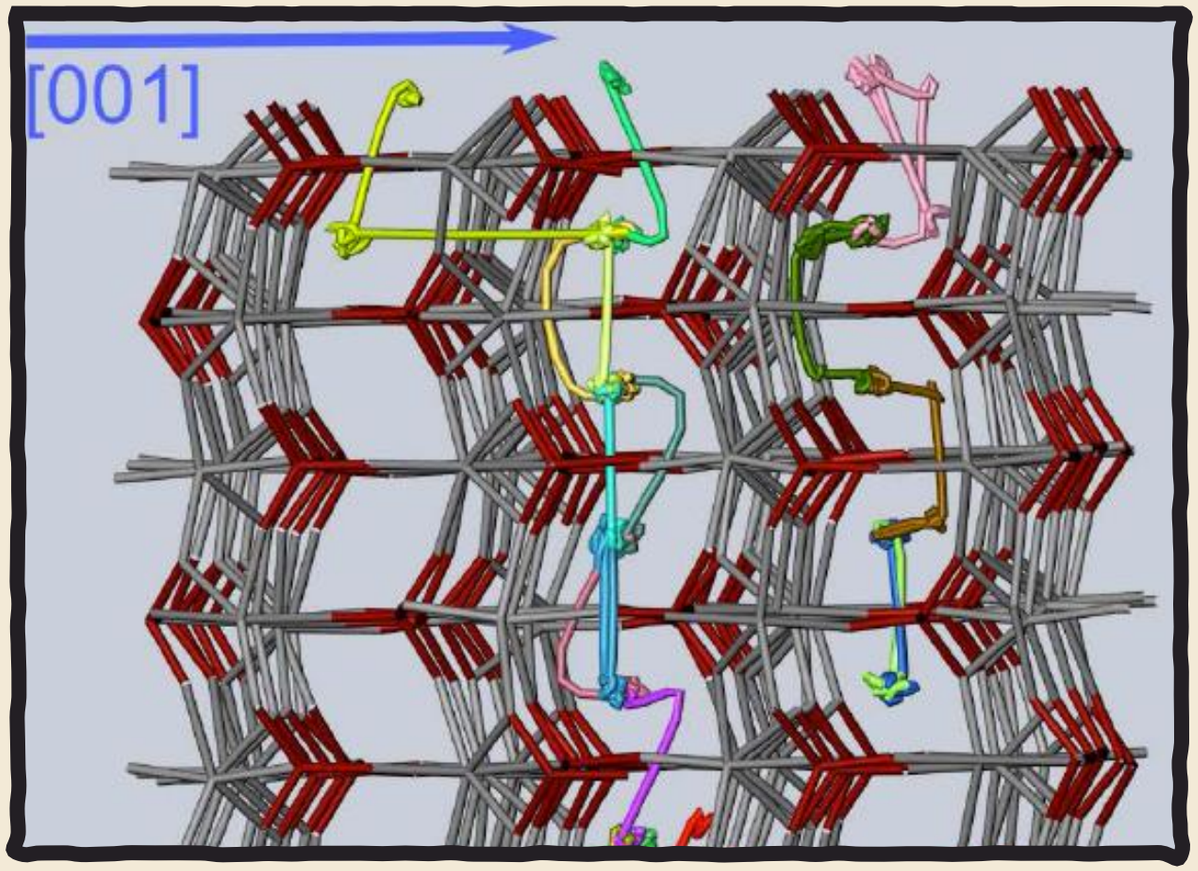

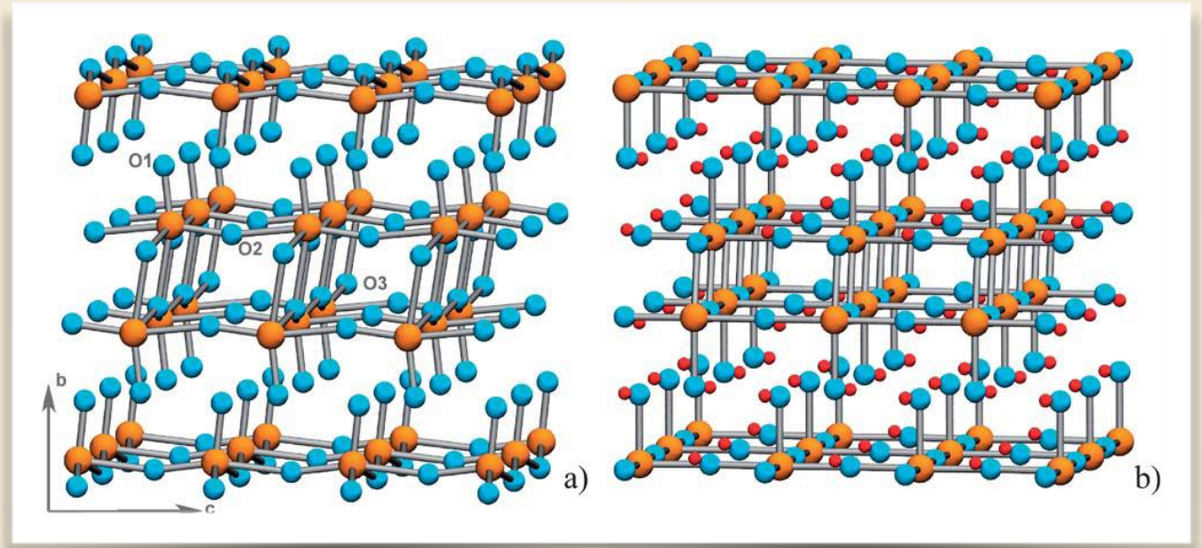

Ionic transport & Intercalation in $FePO_4$ and MoO_3

L. Craco, M. Laad, S.Leoni, Europhys. Lett 91 (2010)
L. Craco, S. Leoni, JAP 111-112 (2012).
L. Craco, S. Leoni, APL, 99, 192103 (2011).
S. Leoni et al., ZPC, 226, 95 (2012)
S.E. Boulfelfel, J. Mat Chem (2012)
M. Baldoni et al., J. Mat Chem. A, (2013)
T. Hackel et al, in preparation (2013)

Batteries: Ionic Transport, Voltage, Capacity, Electronic Transport

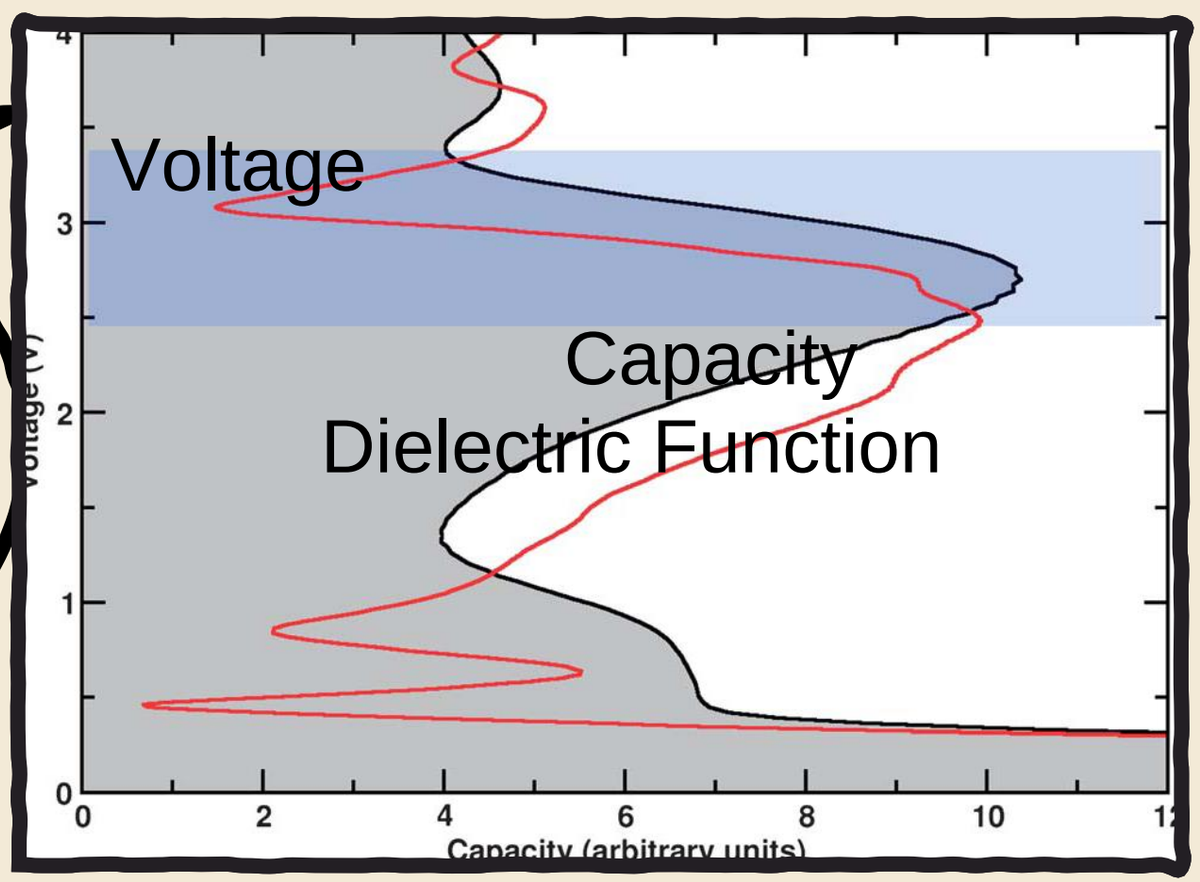

CARDIFF UNIVERSITY
PRIFYSGOL CAERDYDD

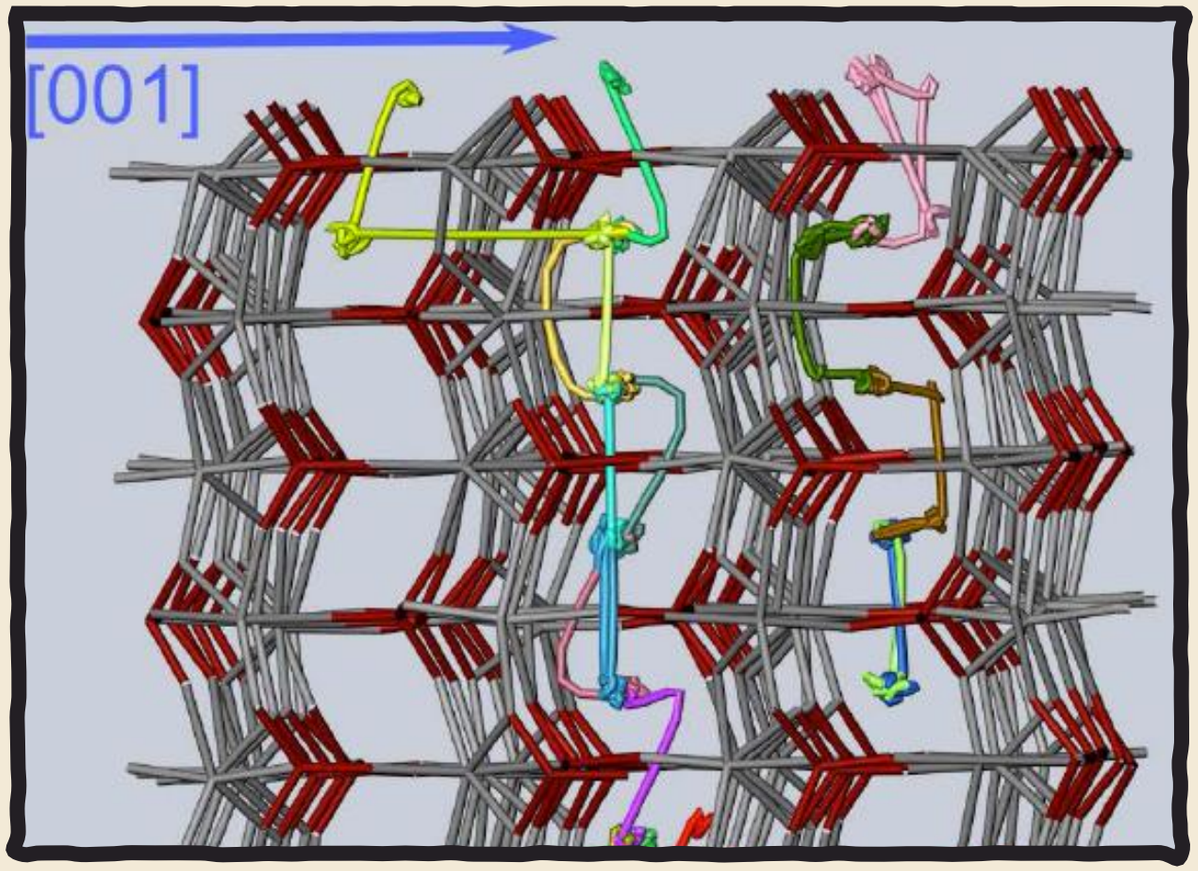

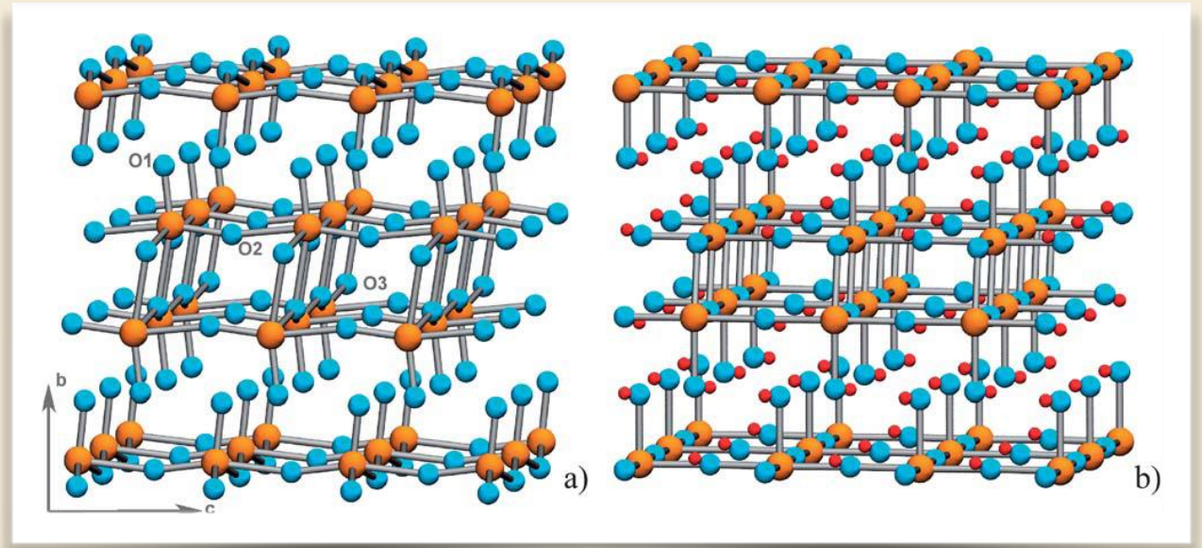

Ionic transport & Intercalation
Charge/Discharge

Ionic Transport,
Voltage, Capacity,
Electronic Transport

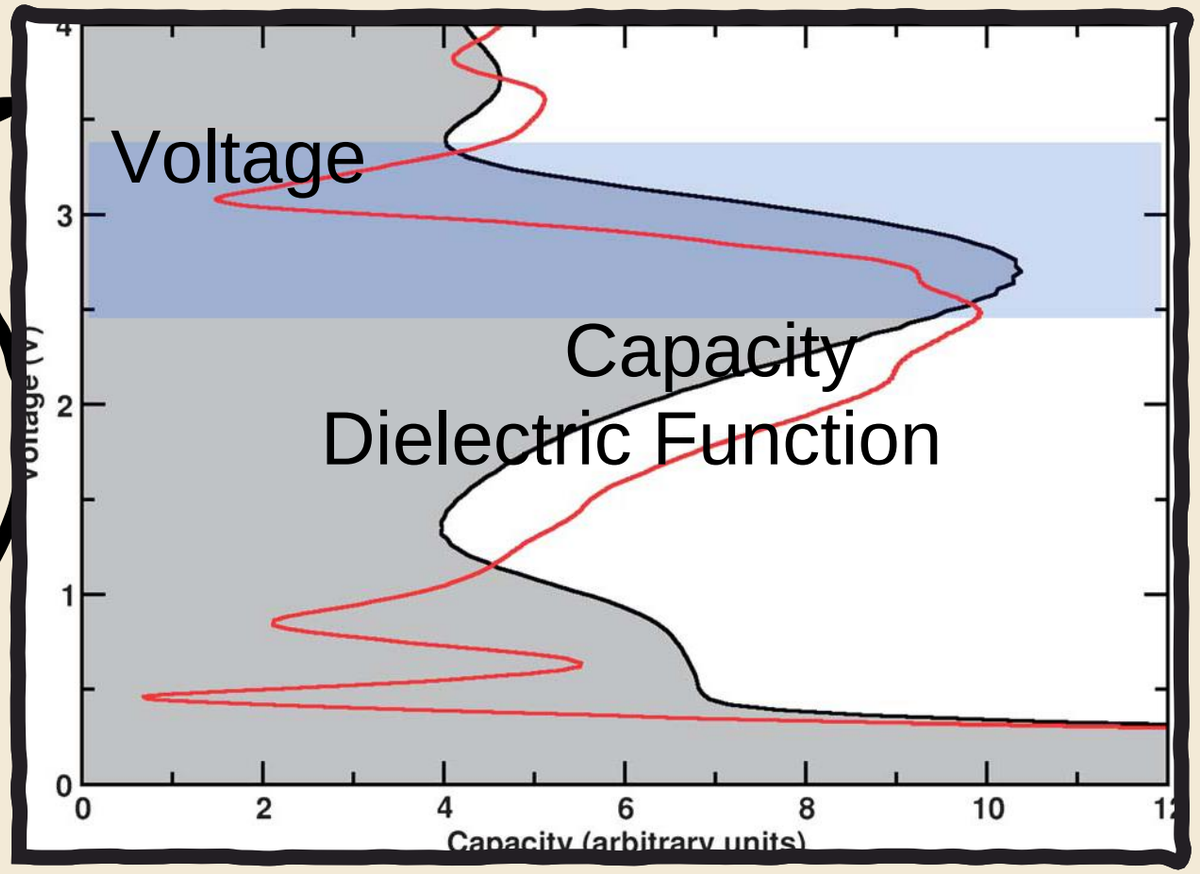

CARDIFF UNIVERSITY
PRIFYSGOL CAERDYDD
S. Leoni, S. Jobbins, Cardiff University

Ansatz: e-doped $FePO_4$

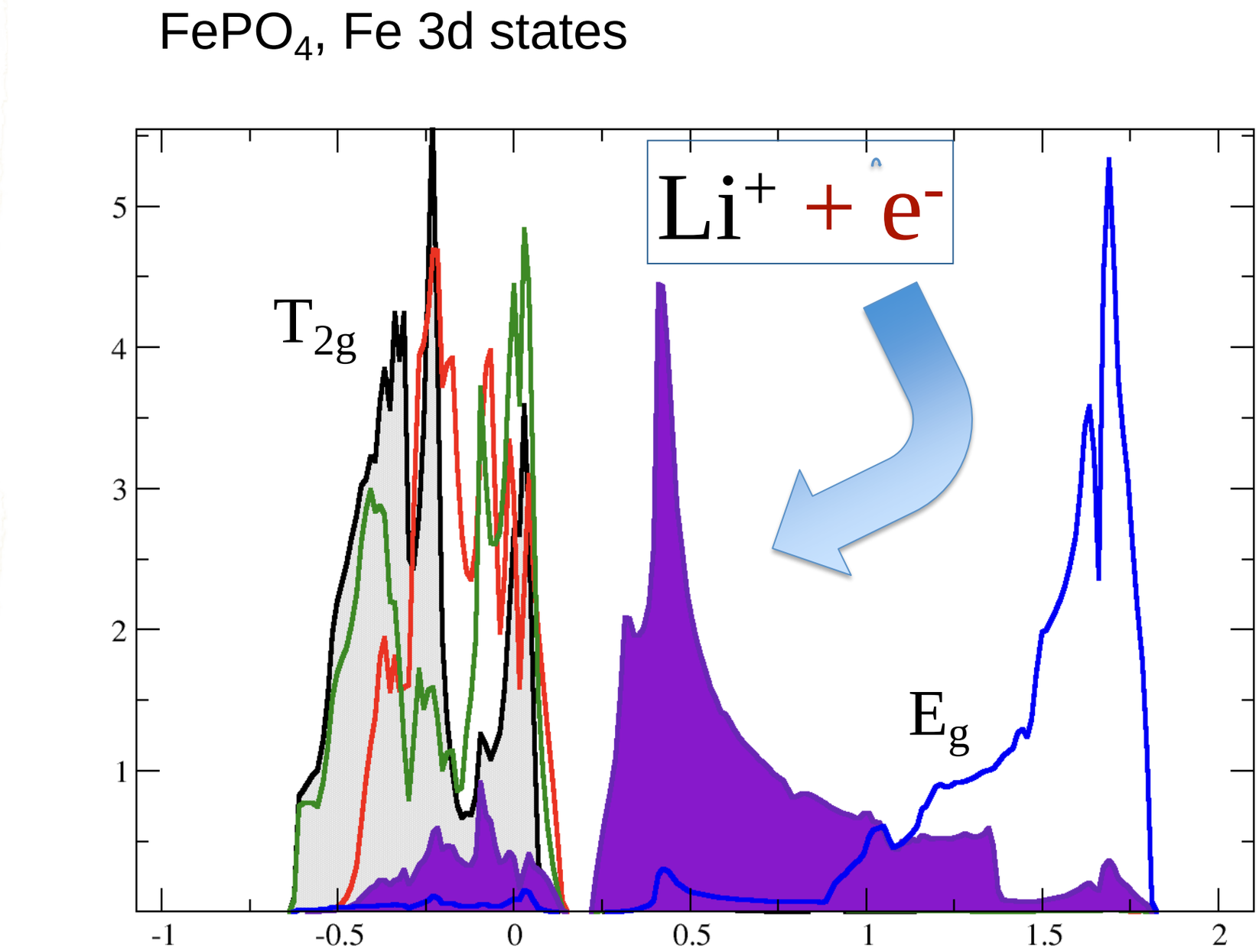

Electronic Structure and Transport

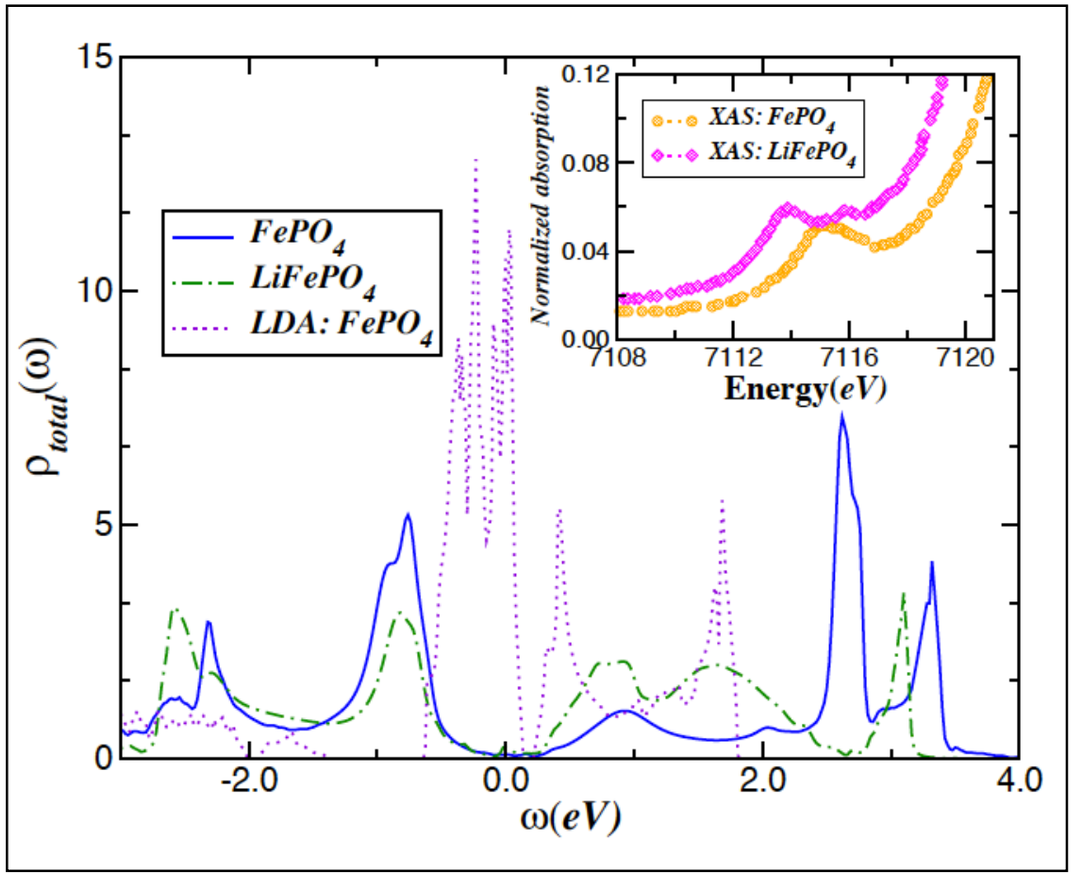

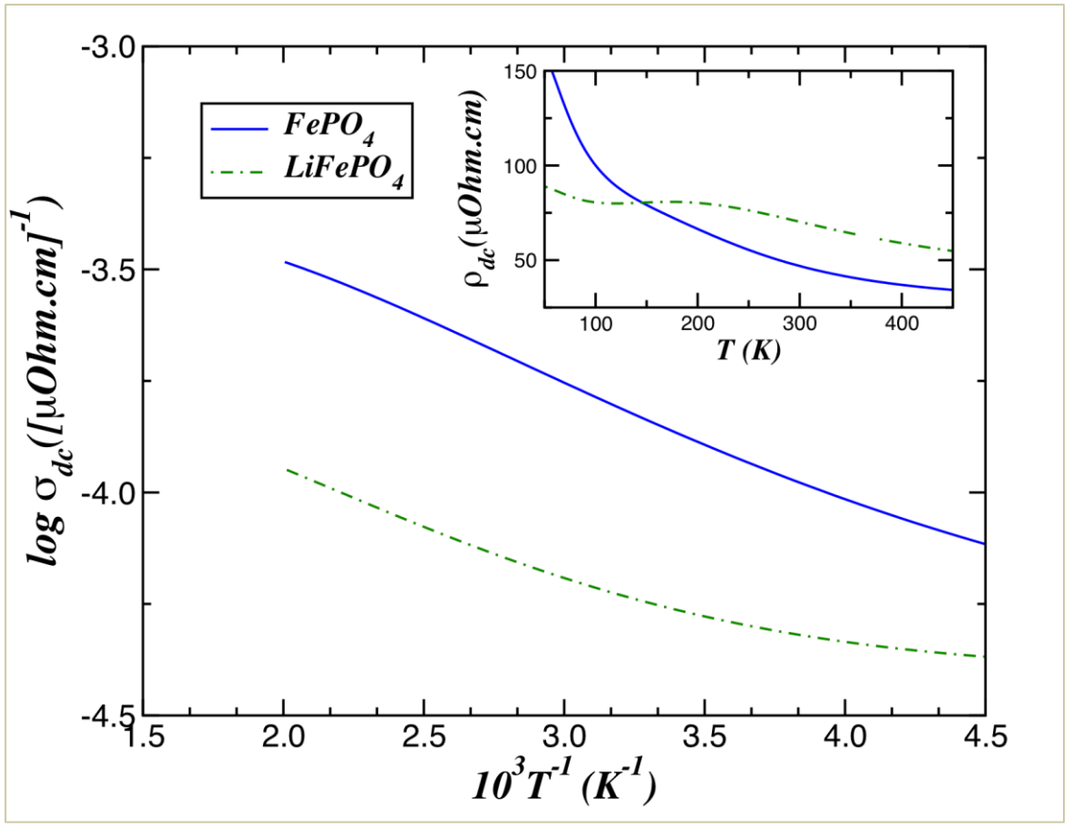

LDA+DMFT

L. Craco, M. Laad, S.Leoni, Europhys. Lett 91 (2010), 27001
L. Craco, S. Leoni, JAP 111-112 (2012).
L. Craco, S. Leoni, APL, 99, 192103 (2011).
S. Leoni et al., ZPC, 226, 95 (2012).
M. Baldoni et al., J. Mat Chem. A, (2013)
L. Craco, S. Leoni (2020)

Orbital Switch on Charging, Discharging

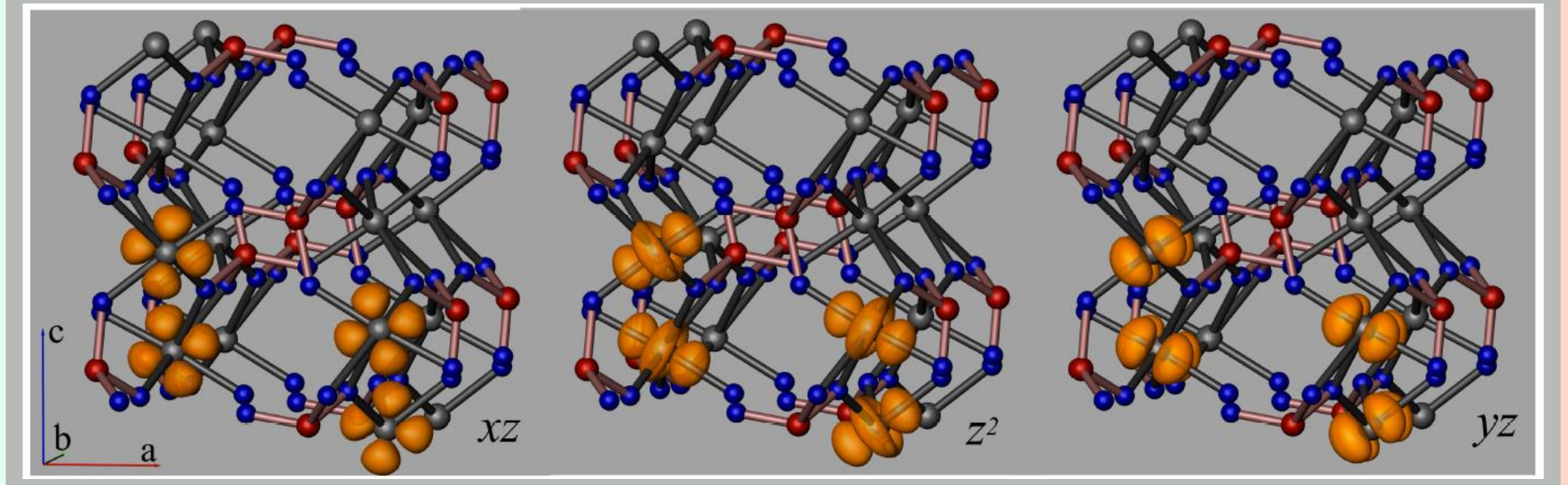

2 Orbital “States”

LDA

LDA+DMFT

$FePO_4$

$FePO_4$

$LiFePO_4$

Dielectric Constant

$$\varepsilon^a(\omega) = 1 + \frac{4\pi i \sigma^a(\omega)}{\omega}$$

dielectric function

$$R^a(\omega) = \left| \frac{\sqrt{\varepsilon^a(\omega)} - 1}{\sqrt{\varepsilon^a(\omega)} + 1} \right|^2$$

optical reflectivity

$$\sigma^a(\omega) = \sigma_1^a(\omega) + i\sigma_2^a(\omega)$$

optical conductivity
of orbital a

L. Craco, S. Leoni, Applied Phys. Lett., 99, 192103 (2011)

Voltage/Capacity

$$C(V) \cong \left|\varepsilon(\omega)\right|$$

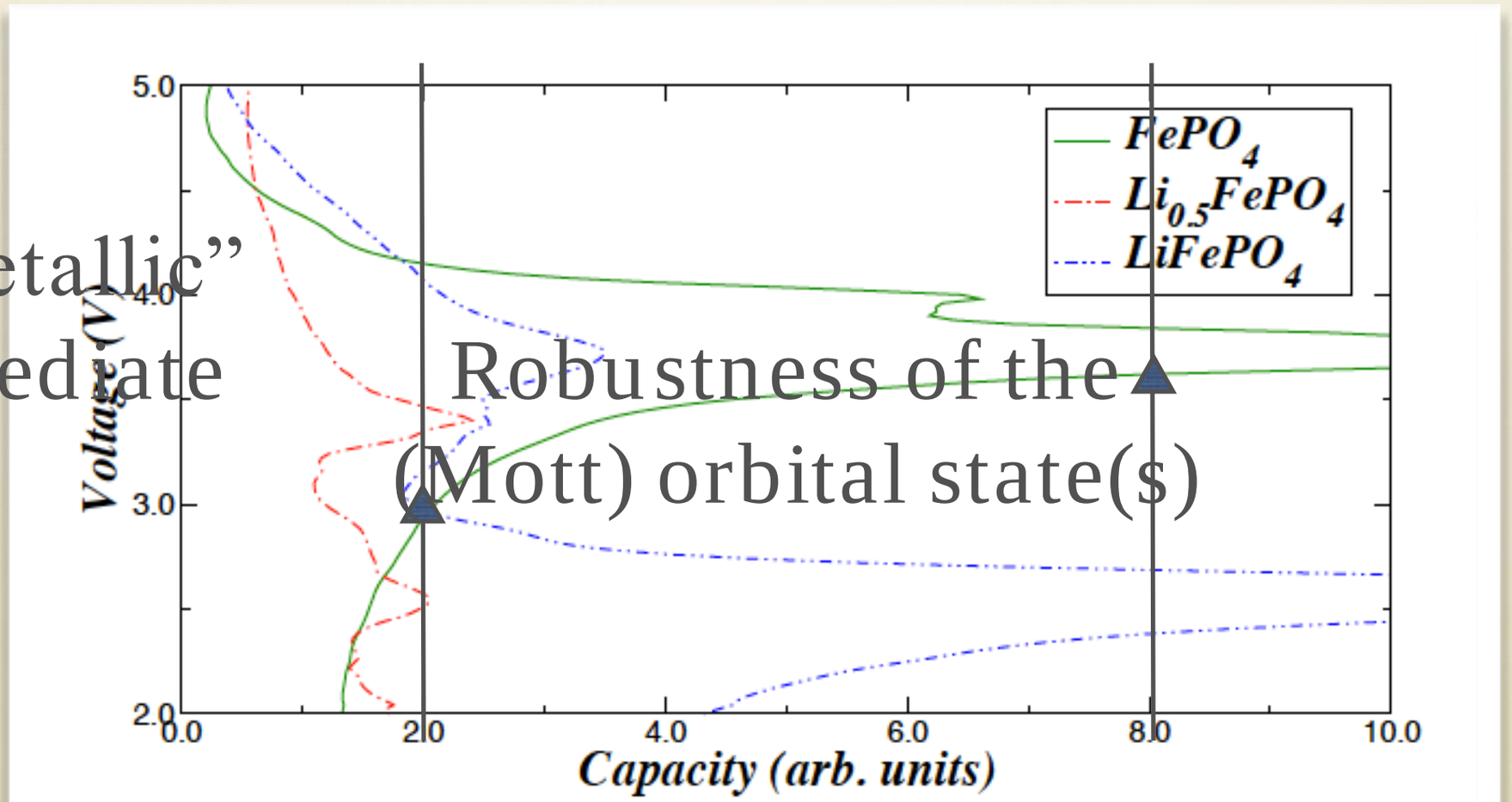

No “metallic” intermediate

Robustness of the (Mott) orbital state(s)

L. Craco, S. Leoni, APL, 99, 192103 (2011).
S. Leoni et al., ZPC, 226, 95 (2012).
M. Baldoni et al., J. Mater. Chem. A, 1, 1778 (2013).

Dielectric Function & Transport

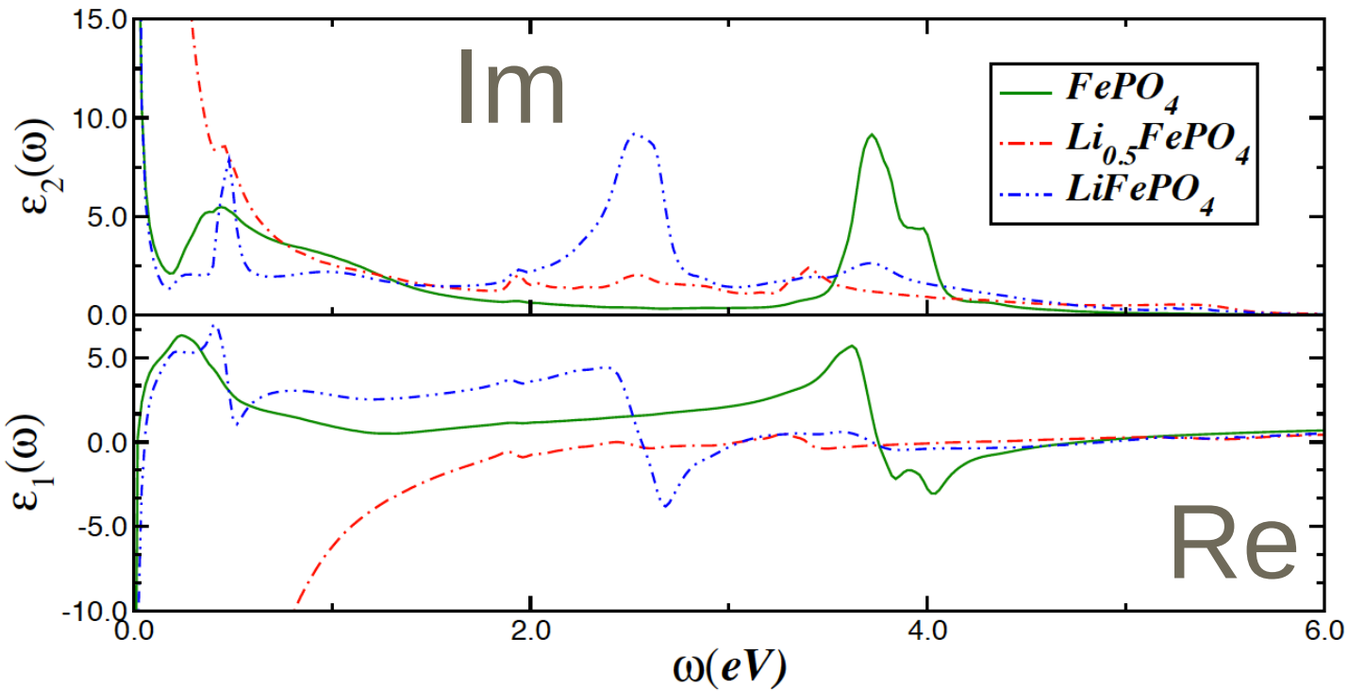

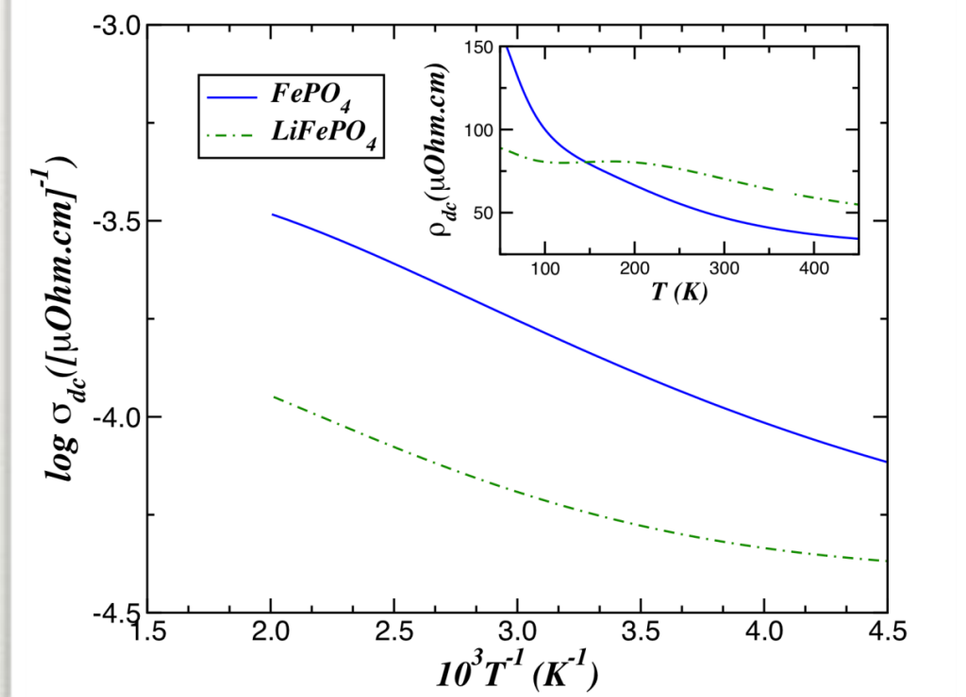

L. Craco, M. Laad, S.Leoni, Europhys. Lett 91 (2010)
L. Craco, S. Leoni, JAP, 111-112, (2012)
L. Craco, S. Leoni, APL, 99, 192103 (2011)
S. Leoni et al., ZPC, 226, 95 (2012)
M. Baldoni et. al, J. Mater. Chem. A (2013)

LDA+DMFT
(GGA+U)

Li_xMoO3

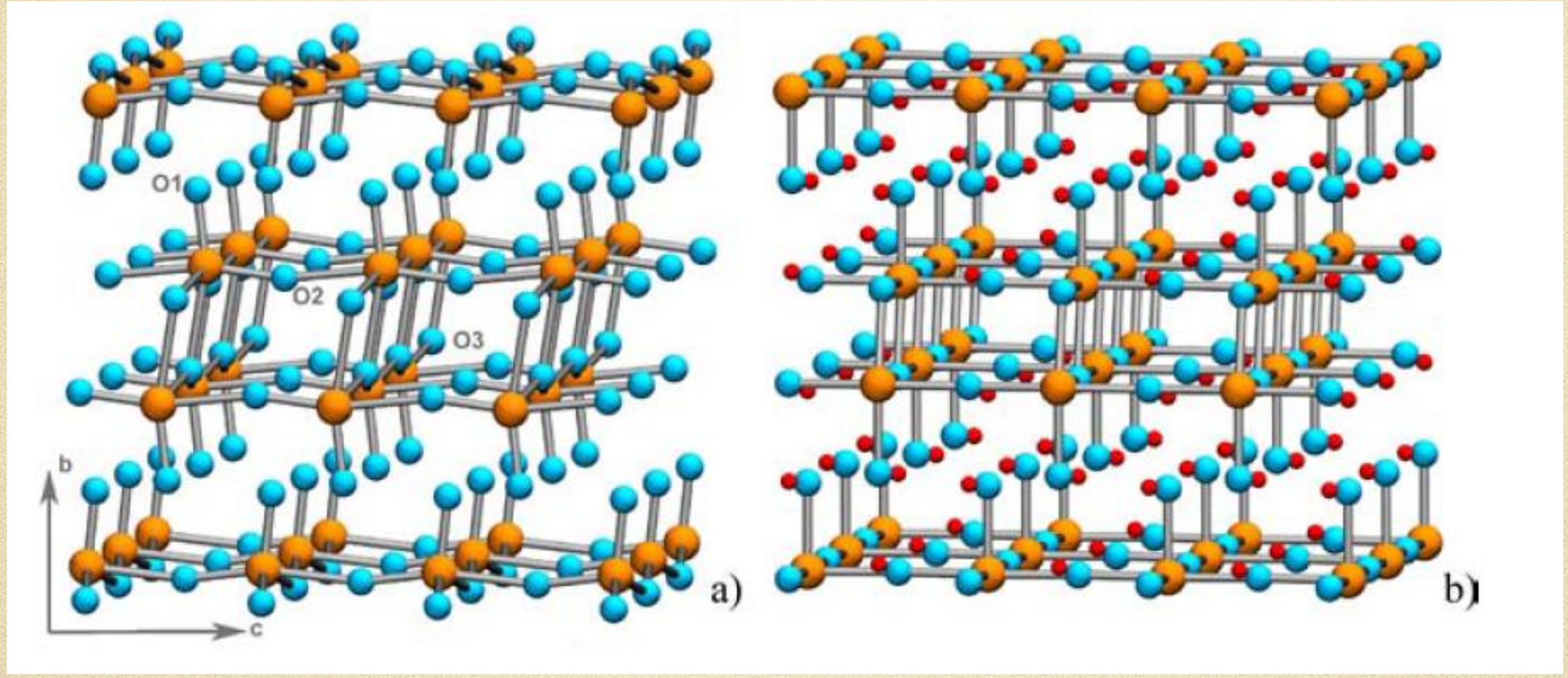

α-MoO_3 and Li_2MoO_3

DFT-GGA

GGA+U Analysis

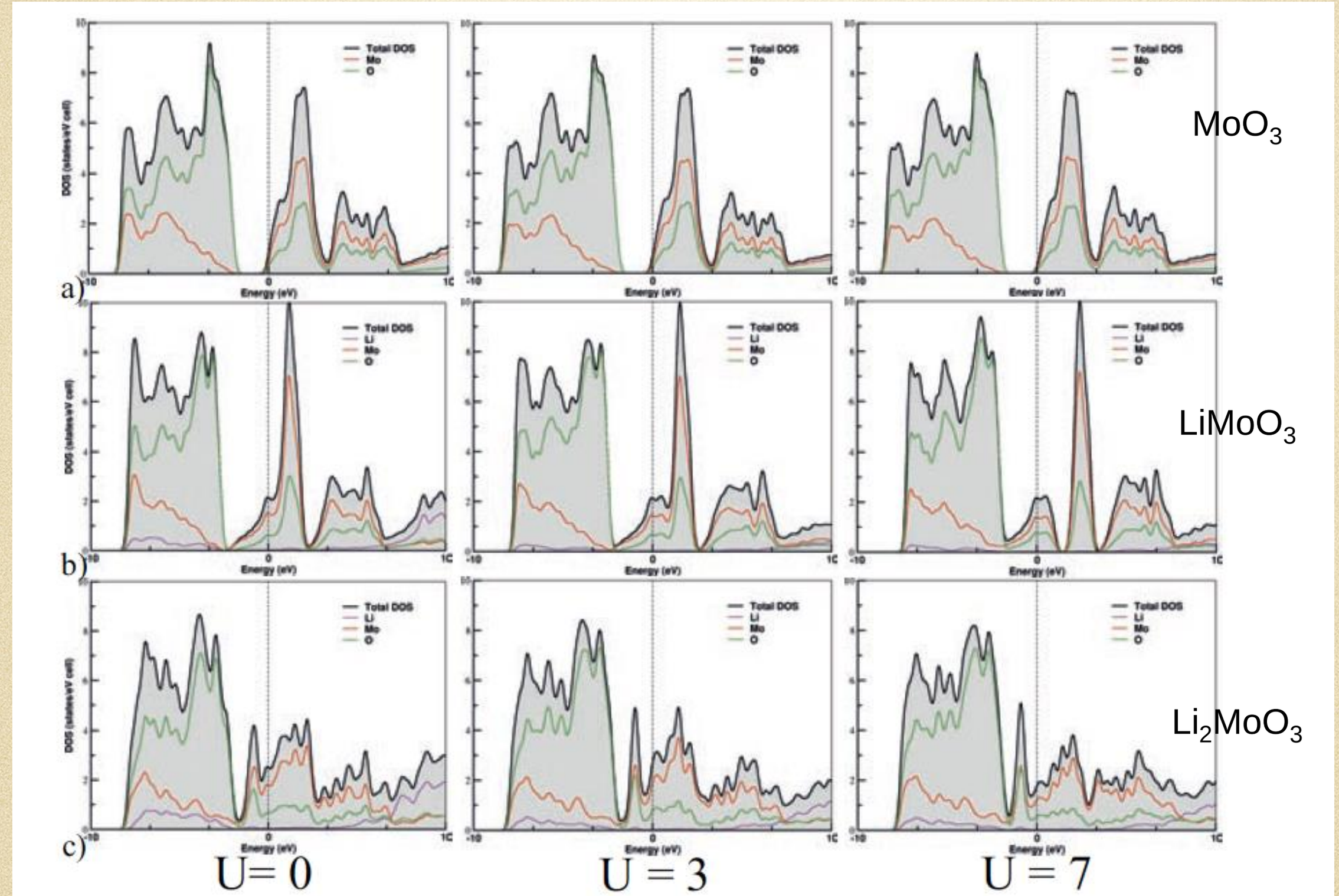

Dielectric Function ε

α-MoO_3

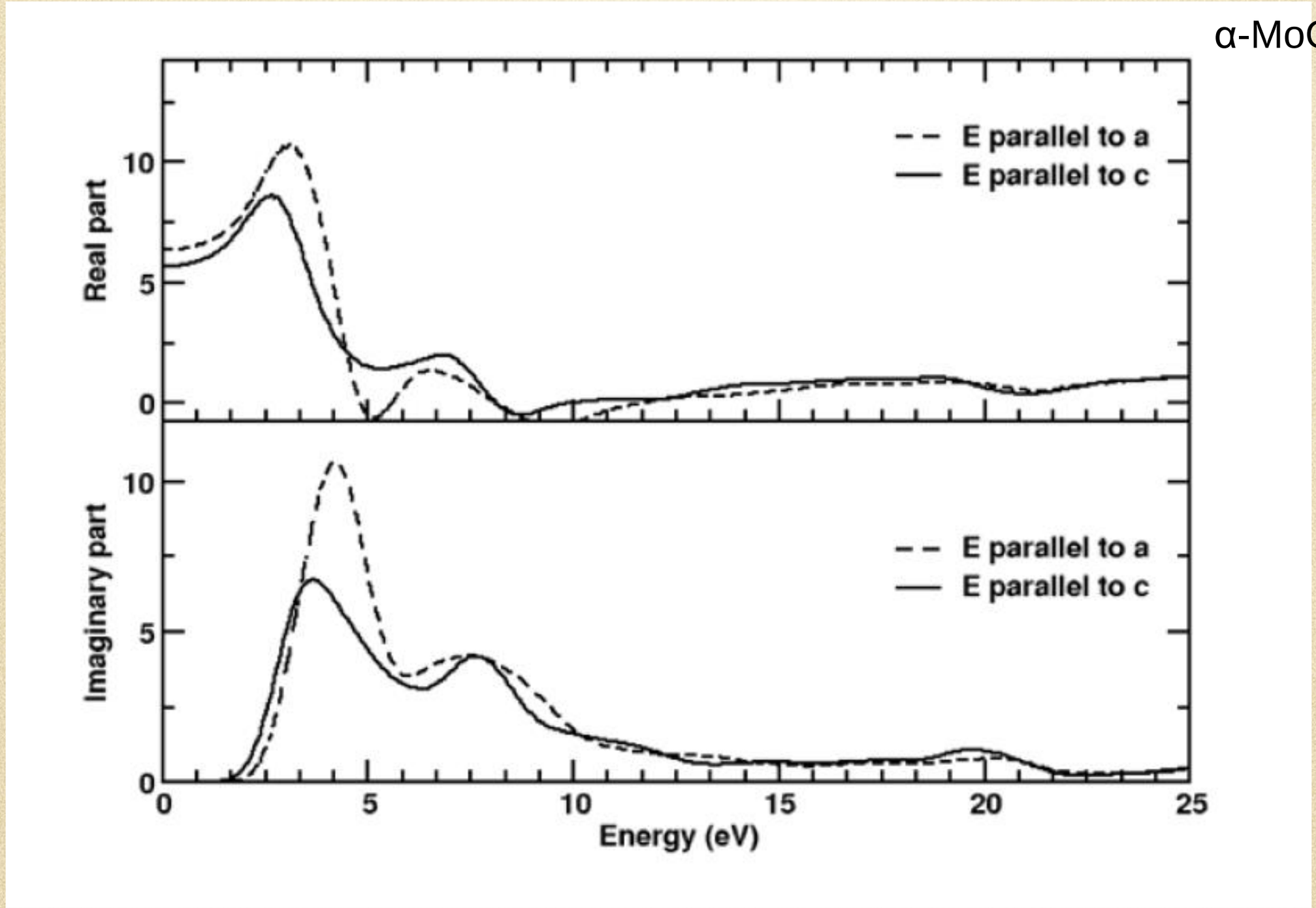

Dielectric Function ε

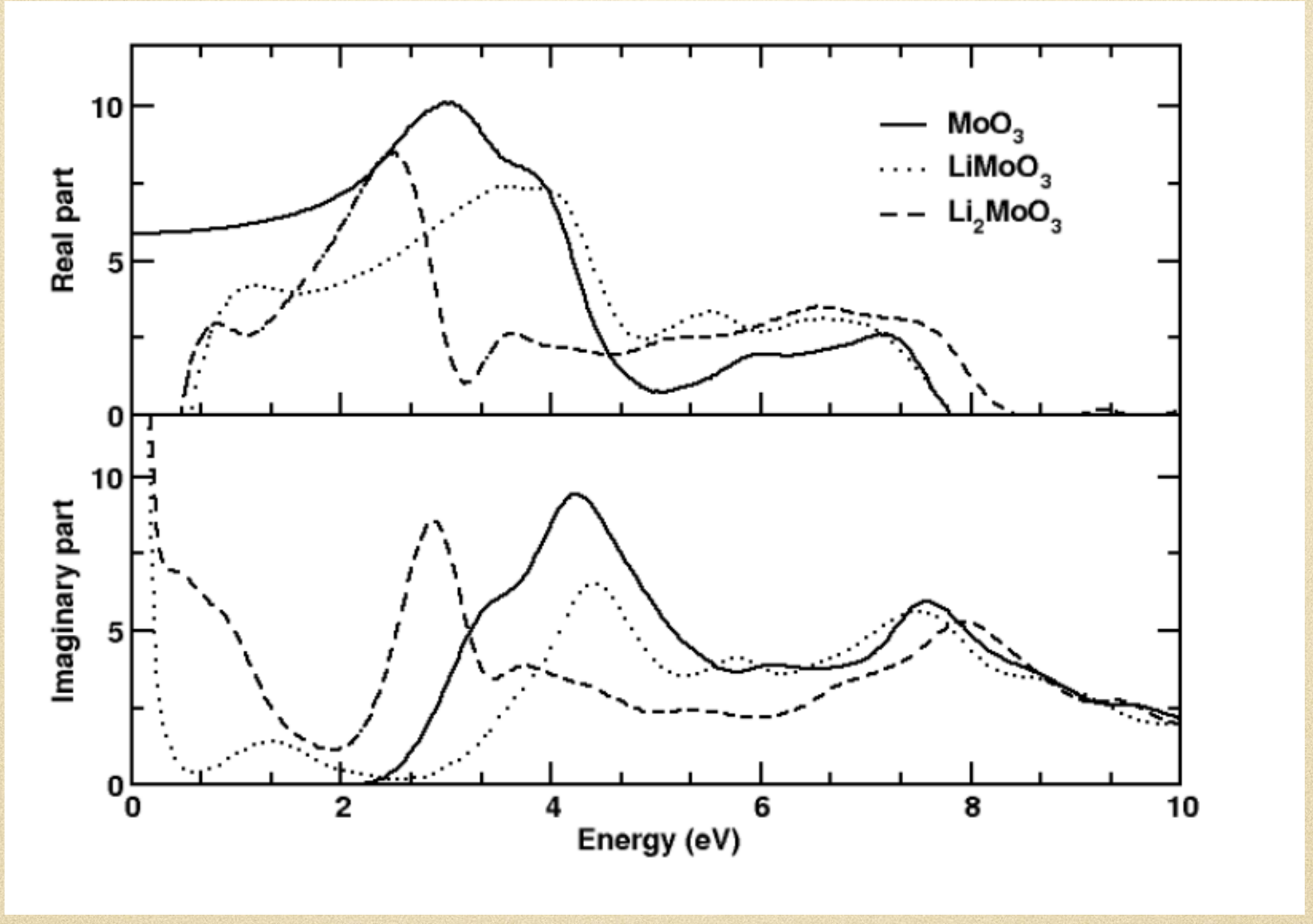

Voltage/Capacity

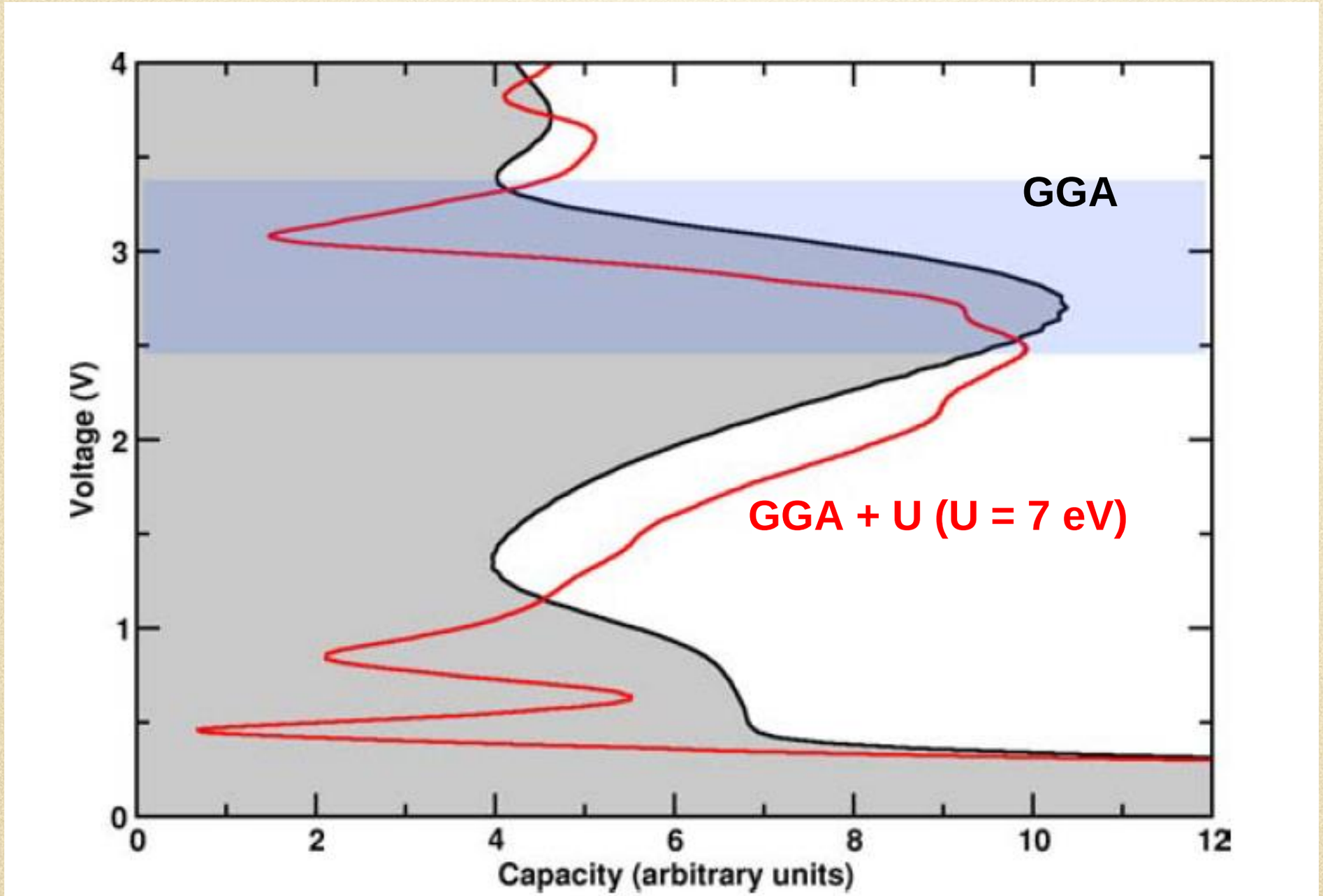

Dielectric Function ε

Li_2MoO_3

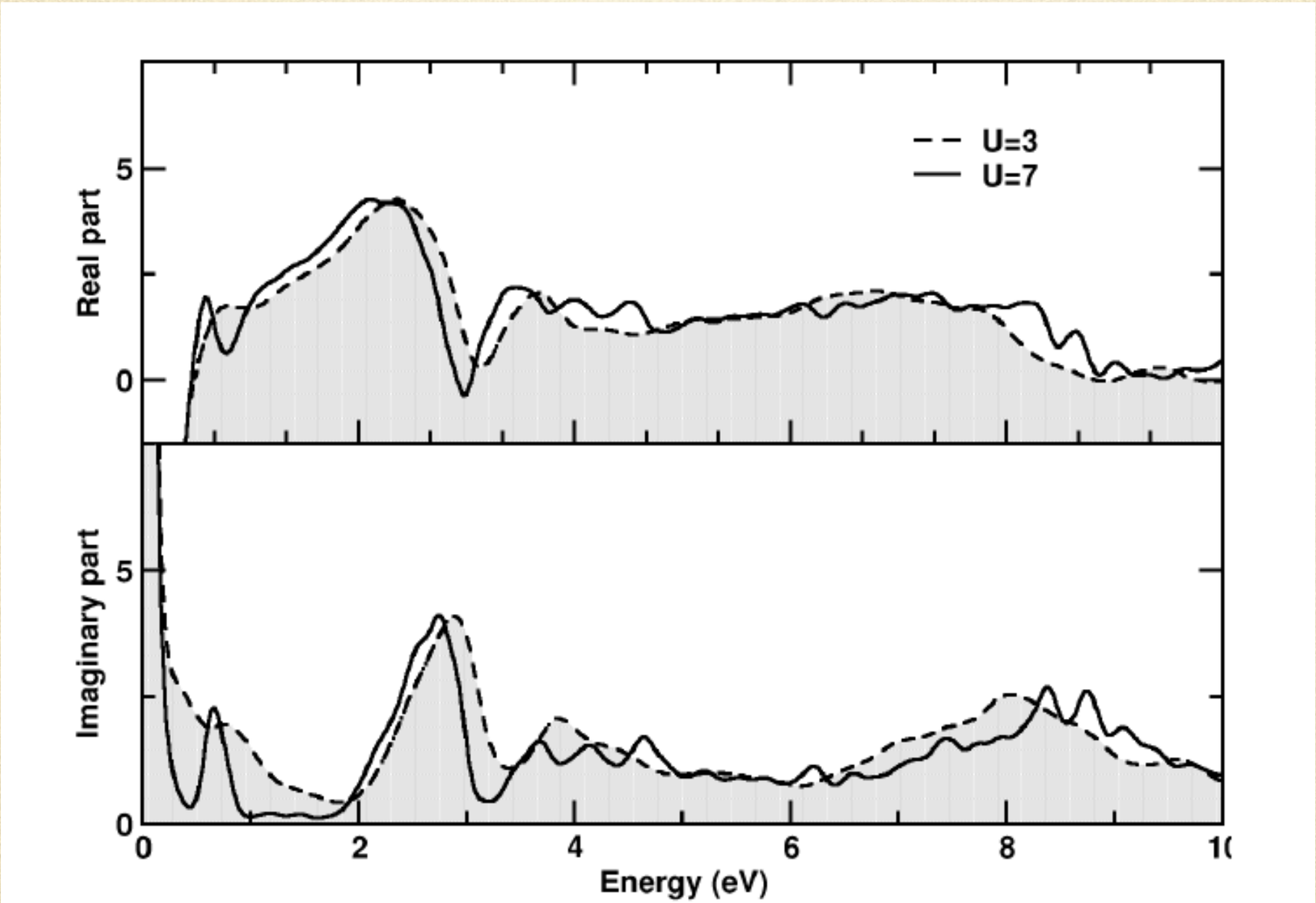

PDOS (4d)

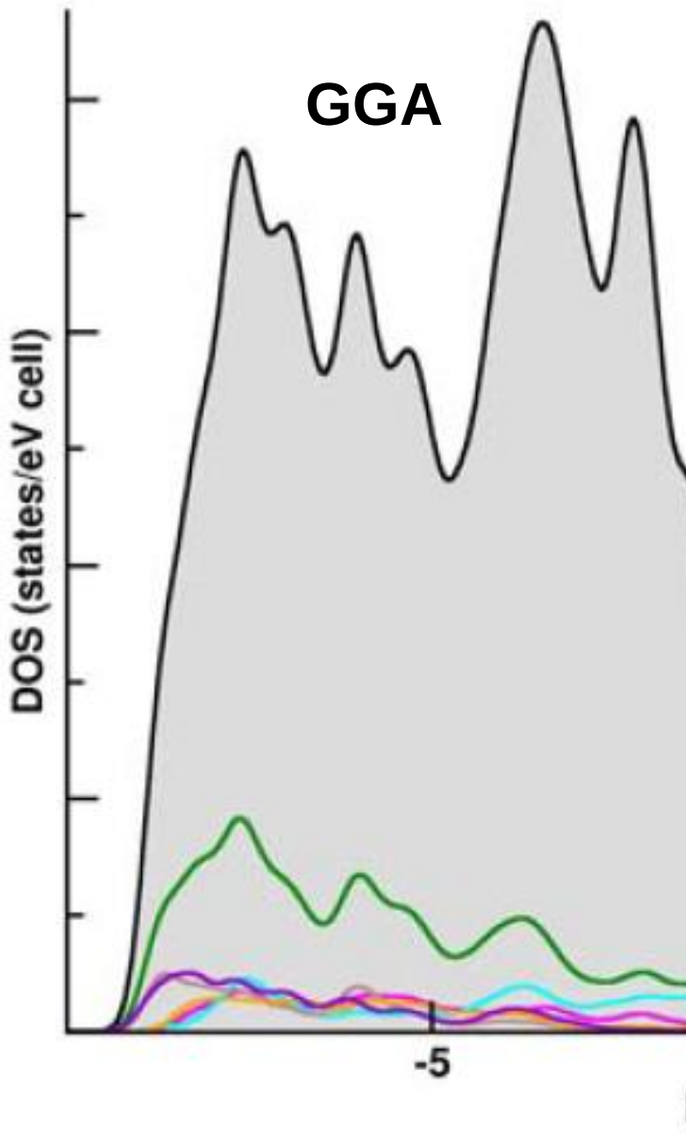
GGA
DOS (states/eV cell)
-5
0
5
Energy (eV)

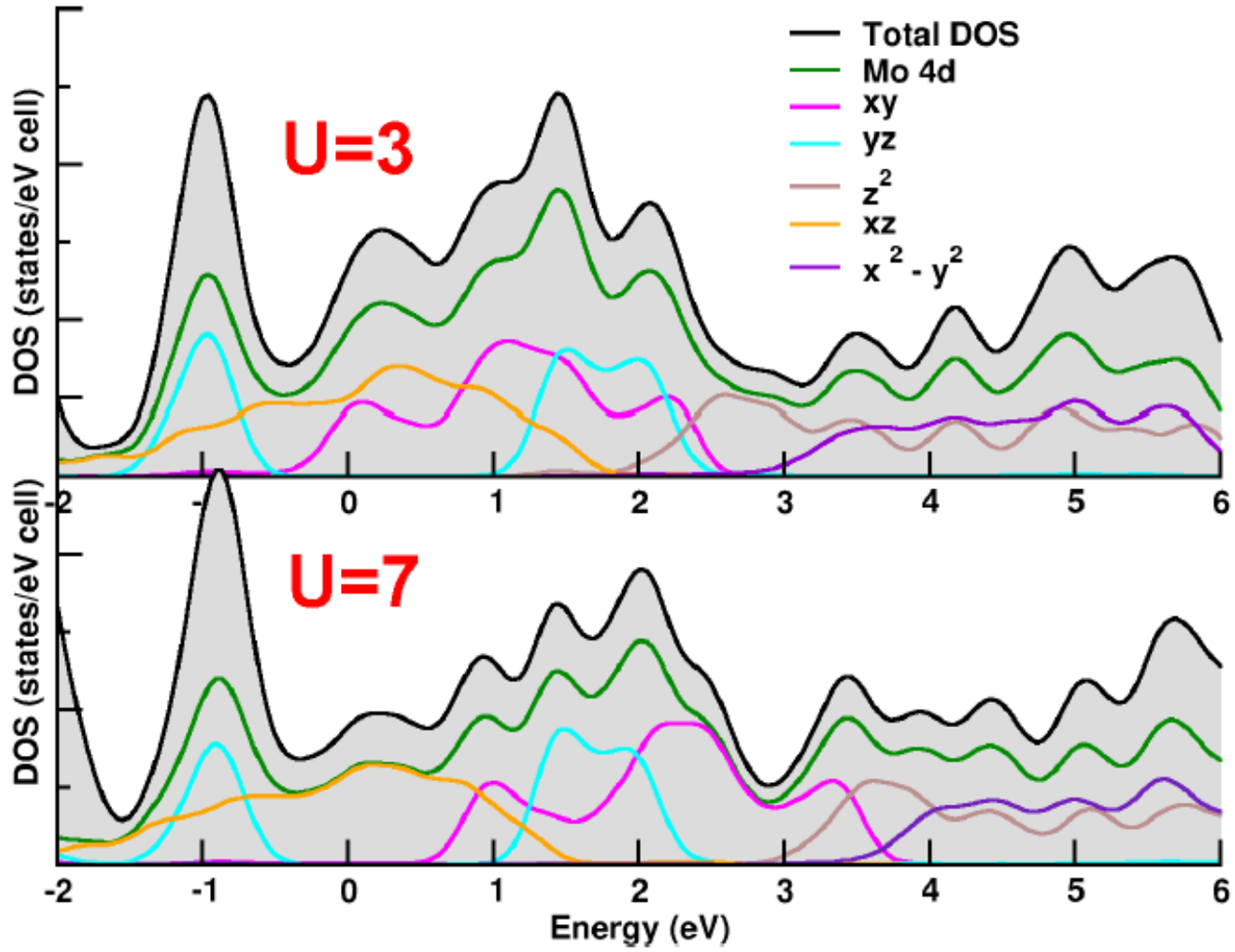
Total DOS
Mo 4d
xy
yz
z2
xz
x2 - y2
U=3
U=7
DOS (states/eV cell)
-2
-1
0
1
2
3
4
5
6
Energy (eV)

Comments

- Total dielectric function is characterized by peaks in the relevant EAM region, consistent with experiements.
- Peaks originate from intraband transitions within Mo 4d.
- Two electron transfer stabilizes the bonding-nonbonding gap between electronic states.
- This induces the stable voltage peak seen in galvanostatic experiments.
- Routes of divalet intercalated cations seems plausible.

Determination of Hubbard U

$$\hat{H} = -\sum_{I \neq J,\sigma} t_{IJ}\, \hat{c}^{\dagger}_{I\sigma}\, \hat{c}_{J\sigma} + U \sum_{I} \hat{n}_{I\uparrow}\, \hat{n}_{I\downarrow}$$

hopping term *on-site Coulomb interaction*

Hubbard Model

I and *J* are the atomic site indices

σ is the spin index

$\hat{c}^{\dagger}_{I\sigma}$ and $\hat{c}_{J\sigma}$ are the creation and annihilation operators

$\hat{n}_{I\sigma} = \hat{c}^{\dagger}_{I\sigma}\hat{c}_{I\sigma}$ is the particle-number operator

t_{IJ} is the hopping energy between sites *I* and *J*

U is the on-site Coulomb repulsion energy

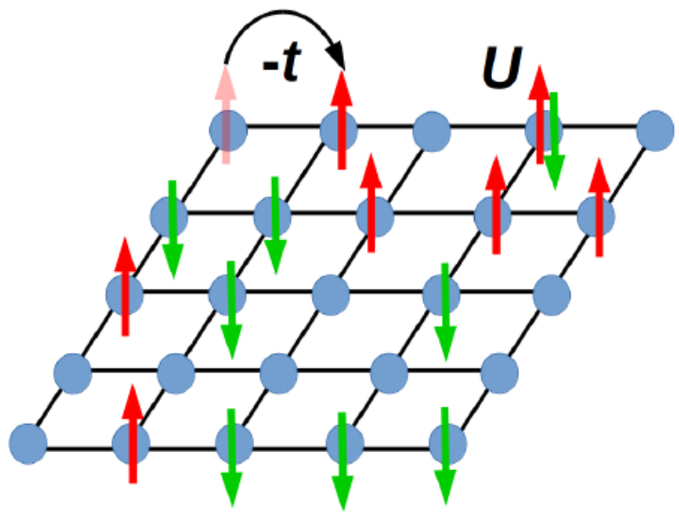

F. Lechermann, "Model Hamiltonians and Basic Techniques" (2011)
https://www.cond-mat.de/events/correl11/manuscripts/lechermann.pdf

Hubbard Model

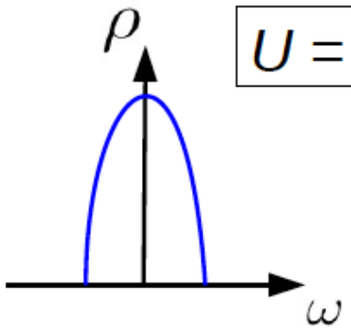

$U = 0$

$$\hat{H} = -\sum_{I \neq J,\sigma} t_{IJ}\, \hat{c}^{\dagger}_{I\sigma}\, \hat{c}_{J\sigma} + U \sum_{I} \hat{n}_{I\uparrow}\, \hat{n}_{I\downarrow}$$

Competition between *t* and *U*

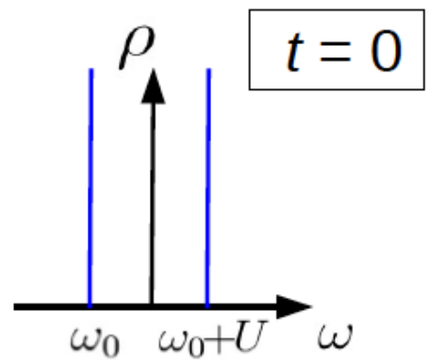

$t = 0$

band narrowing

band broadening

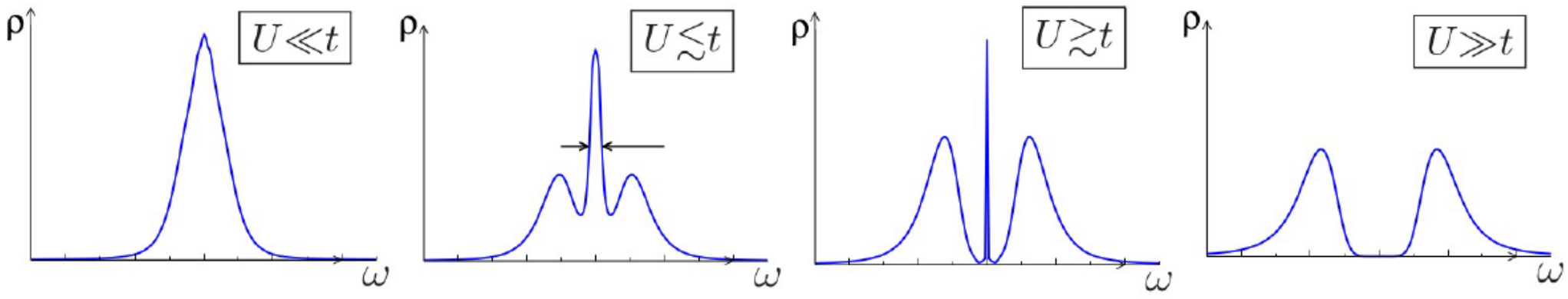

F. Lechermann, "Model Hamiltonians and Basic Techniques" (2011) https://www.cond-mat.de/events/correl11/manuscripts/lechermann.pdf

DFT+U

Original formulation:

V.I. Anisimov, J. Zaanen, O.K. Andersen, Phys. Rev. B **44**, 943 (1991)

Following papers:

V.I. Anisimov, I.V. Solovyev, M.A. Korotin, M.T. Czyzyk, G.A. Sawatzky, Phys. Rev. B **48**, 16929 (1993)

I.V. Solovyev, P.H. Dederichs, V.I. Anisimov, Phys. Rev. B **50**, 16861 (1994)

A.I. Liechtenstein, V.I. Anisimov, J. Zaanen, Phys. Rev. B **52**, R5467 (1995)

V.I. Anisimov, F. Aryasetiawan, A.I. Liechtenstein, J. Phys.: Condens. Matter **9**, 767 (1997)

S.L. Dudarev, G.A. Botton, S.Y. Savrasov, C.J. Humphreys, A.P. Sutton, Phys. Rev. B **57**, 1505 (1998)

W.E. Pickett, S.C. Erwin, E.C. Ethridge, Phys. Rev. B **58**, 1201 (1998)

LAD+U Concept

DFT+*U* total energy

DFT total energy

Hubbard-like term

double-counting term

$$E_{\mathrm{DFT}+U}[\rho^{\sigma}(\mathbf{r}),\{n_{Im\sigma}\}] = E_{\mathrm{DFT}}[\rho^{\sigma}(\mathbf{r})] + \underbrace{E_{\mathrm{Hub}}[\{n_{Im\sigma}\}] - E_{\mathrm{dc}}[\{n_{Im\sigma}\}]}_{E_U[\{n_{Im\sigma}\}]}$$

spin-charge density

occupation numbers

The resulting Hubbard correction

Consequences

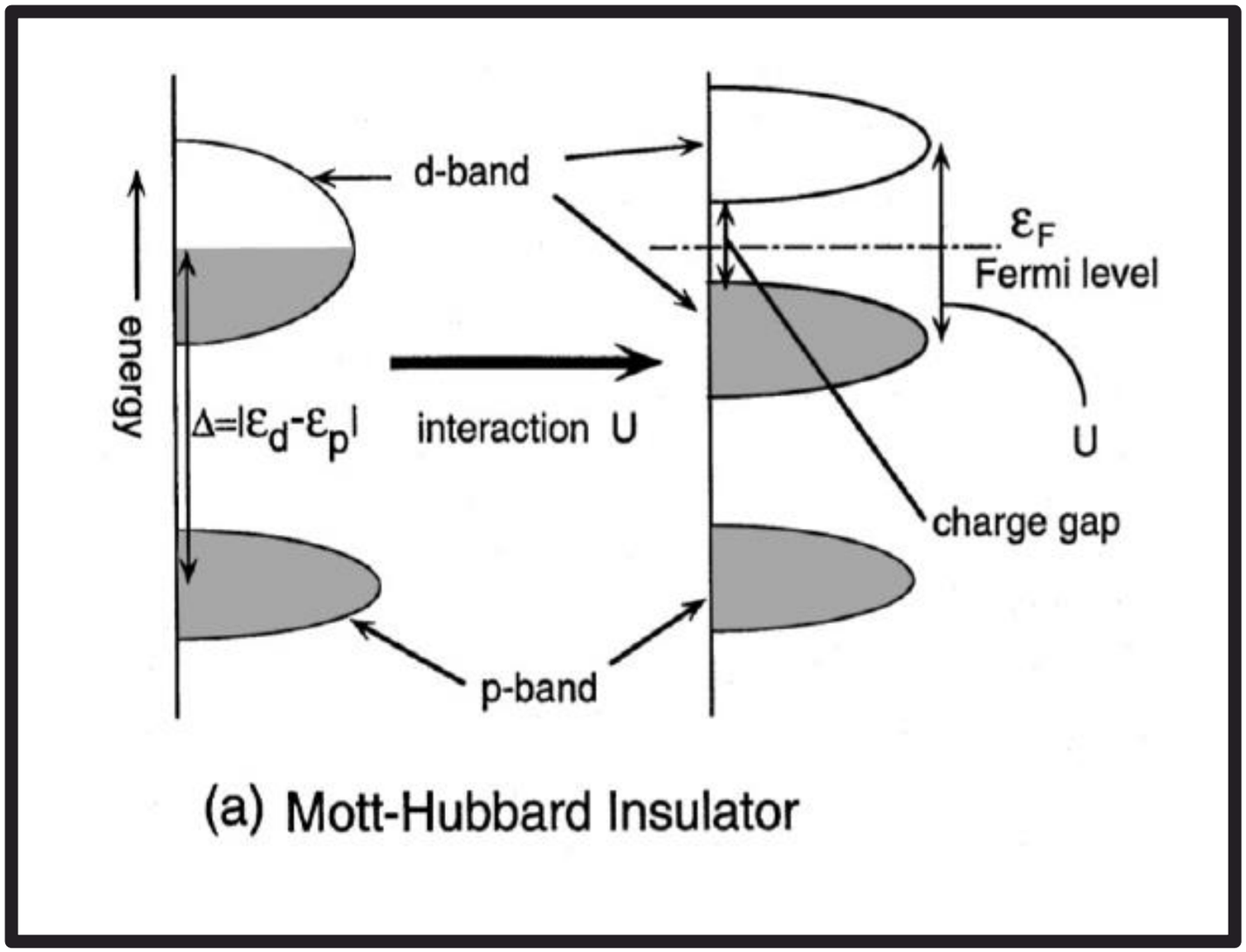

(a) Mott-Hubbard Insulator

M. Imada, A. Fujimori, and Y. Tokura, Rev. Mod. Phys. ***70****, 1039 (1998).*

Examples

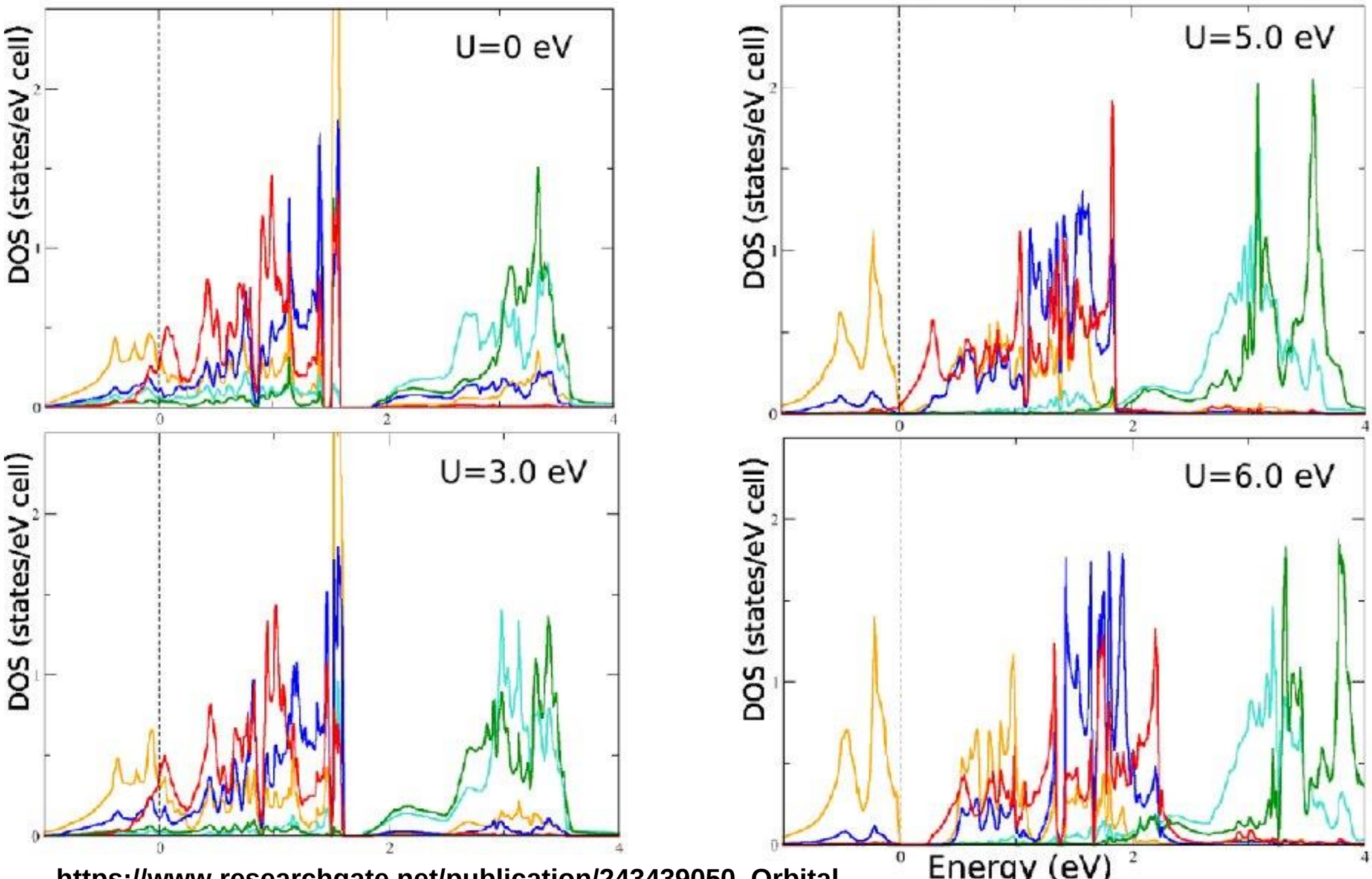

https://www.researchgate.net/publication/243439050_Orbital-spin_order_and_the_origin_of_structural_distortion_in_MgTi2O4/figures?lo=1

Orbital Order

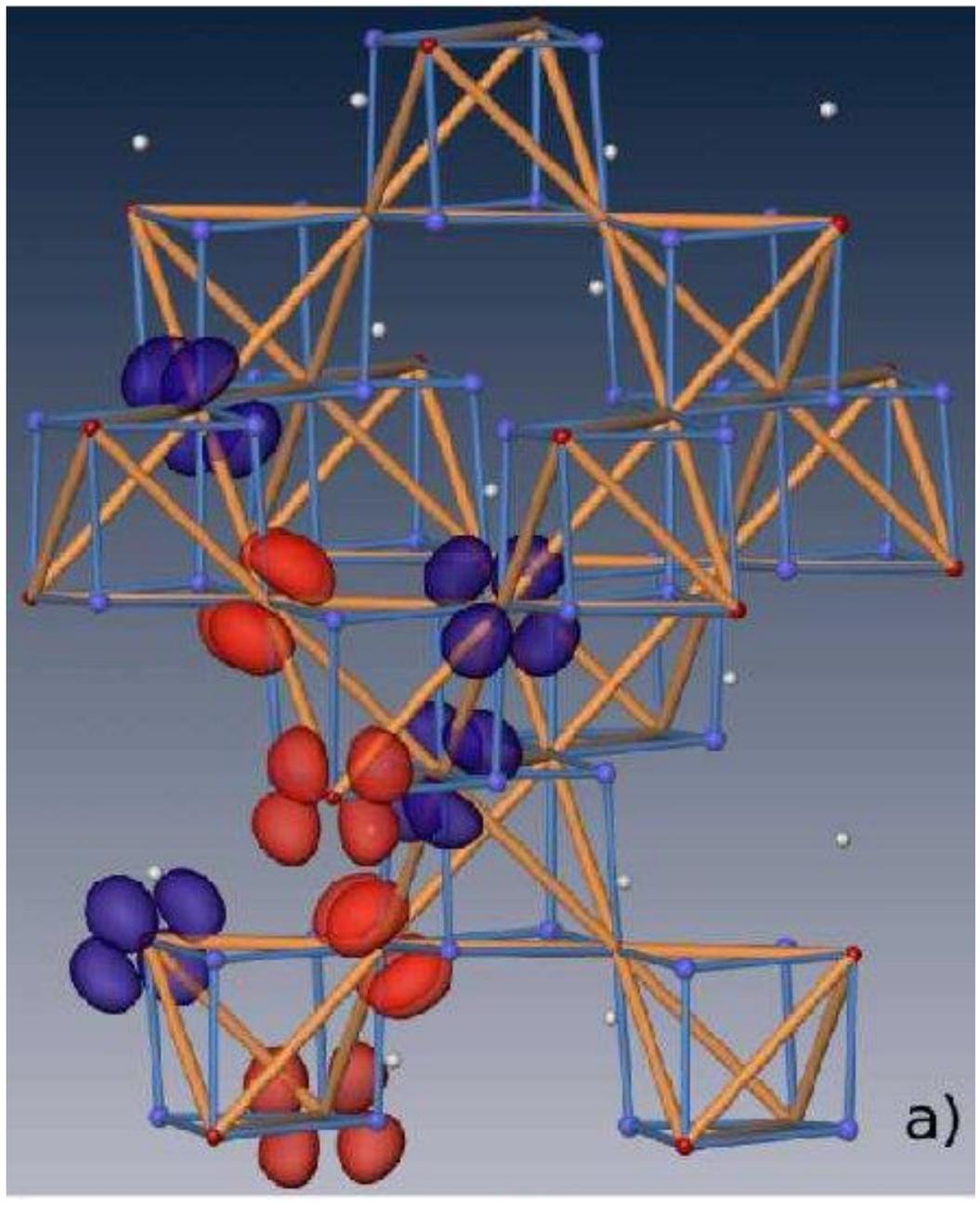

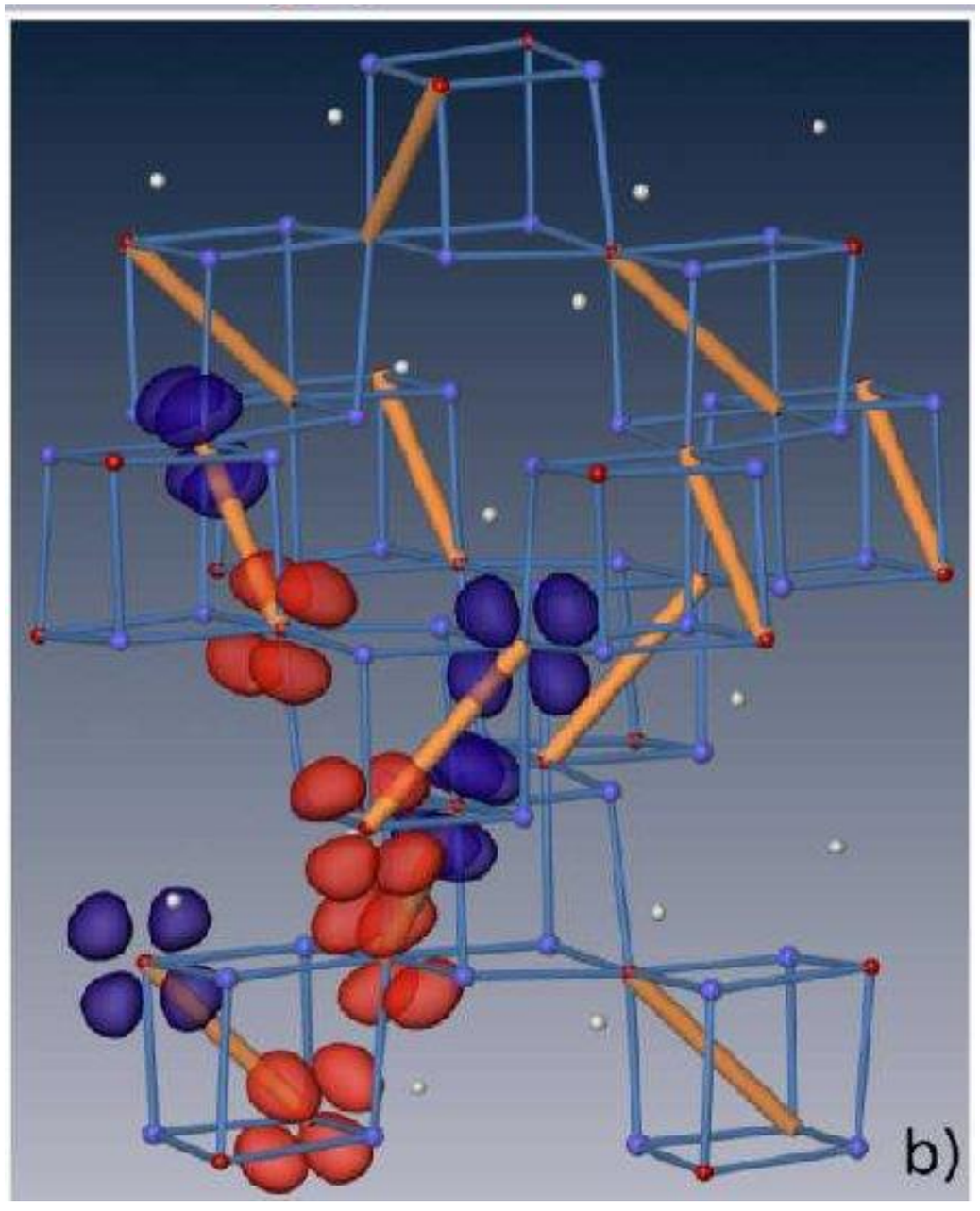

https://www.researchgate.net/publication/243439050_Orbital-spin_order_and_the_origin_of_structural_distortion_in_MgTi2O4/figures?lo=1

“ab initio” approaches - 1

Linear-response calculation of *U* using cDFT

The Kohn-Sham equations with a perturbing atomic potential:

$$\left[-\frac{1}{2}\nabla^2 + \hat{V}^{\sigma}_{\mathrm{KS}} + \hat{V}^{\sigma}_{U} + \alpha_J \sum_m |\varphi^J_m\rangle\langle\varphi^J_m|\right]\psi^{\sigma}_{v\mathbf{k}}(\mathbf{r}) = \varepsilon^{\sigma}_{v\mathbf{k}}\,\psi^{\sigma}_{v\mathbf{k}}(\mathbf{r})$$

Evaluate the change in occupation matrices: $\Delta n^{I\sigma}_{mm'}$

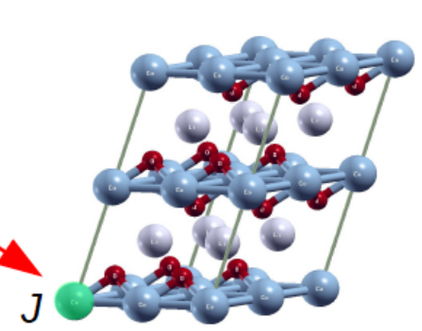

Compute the interacting and non-interacting response matrices:

$$\chi_{IJ} = \sum_{m,\sigma} \frac{\Delta n^{I\sigma}_{mm}}{\Delta\alpha_J}, \qquad \chi^0_{IJ} = \sum_{m,\sigma} \frac{\Delta n^{0\,I\sigma}_{mm}}{\Delta\alpha_J}$$

- supercells
- finite differences

On-site Hubbard U_{eff} parameters (diagonal matrix elements):

$$U^I_{\mathrm{eff}} = \left((\chi^0)^{-1} - \chi^{-1}\right)_{II}$$

All derivatives are computed using finite differences.

α_J is the amplitude of the perturbation of the *J*-th atom

Note: $\hat{V}^{\sigma}_{U}$ is fixed!

*M. Cococcioni and S. de Gironcoli, Phys. Rev. B **71**, 035105 (2005).*

Courtesy: Iurii Timrov

“ab initio” approaches - 2

DFPT for *U*eff : summary

Solve (self-consistently, iteratively) the linear-response Kohn-Sham equations for every **q**:

$$\left[-\frac{1}{2}\left[\nabla+i(\mathbf{k}+\mathbf{q})\right]^2+\hat{V}^{\sigma\,\circ}_{\mathrm{KS},\mathbf{k}+\mathbf{q}}+\hat{V}^{\sigma\,\circ}_{U,\mathbf{k}+\mathbf{q}}-\varepsilon^{\sigma\,\circ}_{v\mathbf{k}}\right]\Delta^{s}_{\mathbf{q}}u^{\sigma}_{v\mathbf{k}}(\mathbf{r})=-\hat{\mathcal{P}}^{\sigma}_{\mathbf{k}+\mathbf{q}}\left[\Delta^{s}_{\mathbf{q}}V^{\sigma}_{\mathrm{Hxc}}+\sum_{m}|\phi^{s}_{m\mathbf{k}+\mathbf{q}}\rangle\langle\phi^{s}_{m\mathbf{k}}|\right]u^{\sigma\,\circ}_{v\mathbf{k}}(\mathbf{r})$$

Compute linear-response occupation matrices:

$$\Delta^{s'}_{\mathbf{q}}n^{s\sigma}_{mm'}=\frac{1}{N}\sum_{v,\mathbf{k}}\left[\langle u^{\sigma\,\circ}_{v\mathbf{k}}|\phi^{s}_{m'\mathbf{k}}\rangle\langle\phi^{s}_{m\mathbf{k}+\mathbf{q}}|\Delta^{s'}_{\mathbf{q}}u^{\sigma}_{v\mathbf{k}}\rangle+\langle u^{\sigma\,\circ}_{v\mathbf{k}}|\phi^{s}_{m\mathbf{k}}\rangle\langle\phi^{s}_{m'\mathbf{k}+\mathbf{q}}|\Delta^{s'}_{\mathbf{q}}u^{\sigma}_{v\mathbf{k}}\rangle\right]$$

Sum up over **q** and compute the response matrices:

$$\chi_{IJ}=\sum_{m,\sigma}\frac{dn^{I\sigma}_{mm}}{d\alpha_J},\qquad \chi^{0}_{IJ}=\sum_{m,\sigma}\frac{dn^{0\,I\sigma}_{mm}}{d\alpha_J}$$

Compute Hubbard *U*eff : $U^{I}_{\mathrm{eff}}=\left((\chi^{0})^{-1}-\chi^{-1}\right)_{II}$

Implemented in

The **HP** code

Courtesy: Iurii Timrov

Approach

Calculation of Hubbard U_{eff}

self-consistent

So far: ~~"one-shot"~~ calculation of U_{eff}

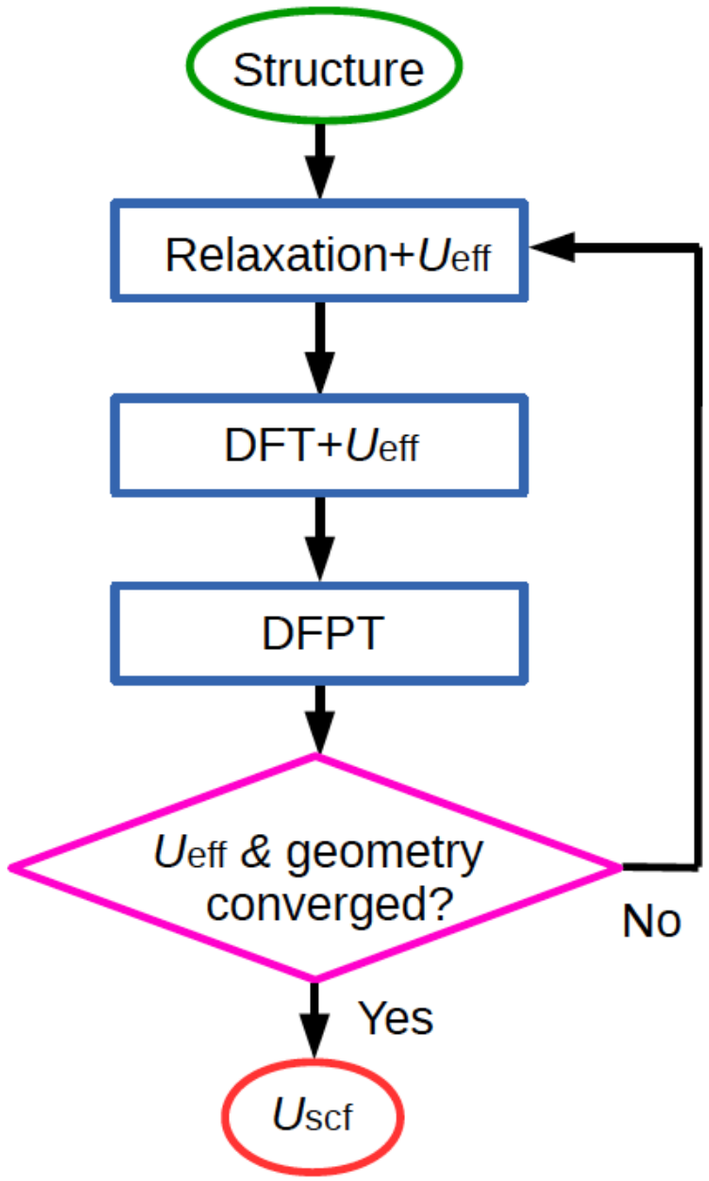

8. Repeat the cycle until convergence

The self-consistent cycle must be continued until the geometry does not change and until U_{eff} does not change with respect to previous iterations with a desired threshold.

*H. Hsu et al., Phys. Rev. B **79**, 125124 (2009).*

*H.J. Kulik and N. Marzari, J. Chem. Phys. **133**, 114103 (2010).*

I. Timrov, N. Marzari, and M. Cococcioni, in preparation.

Which directions are relevant ?

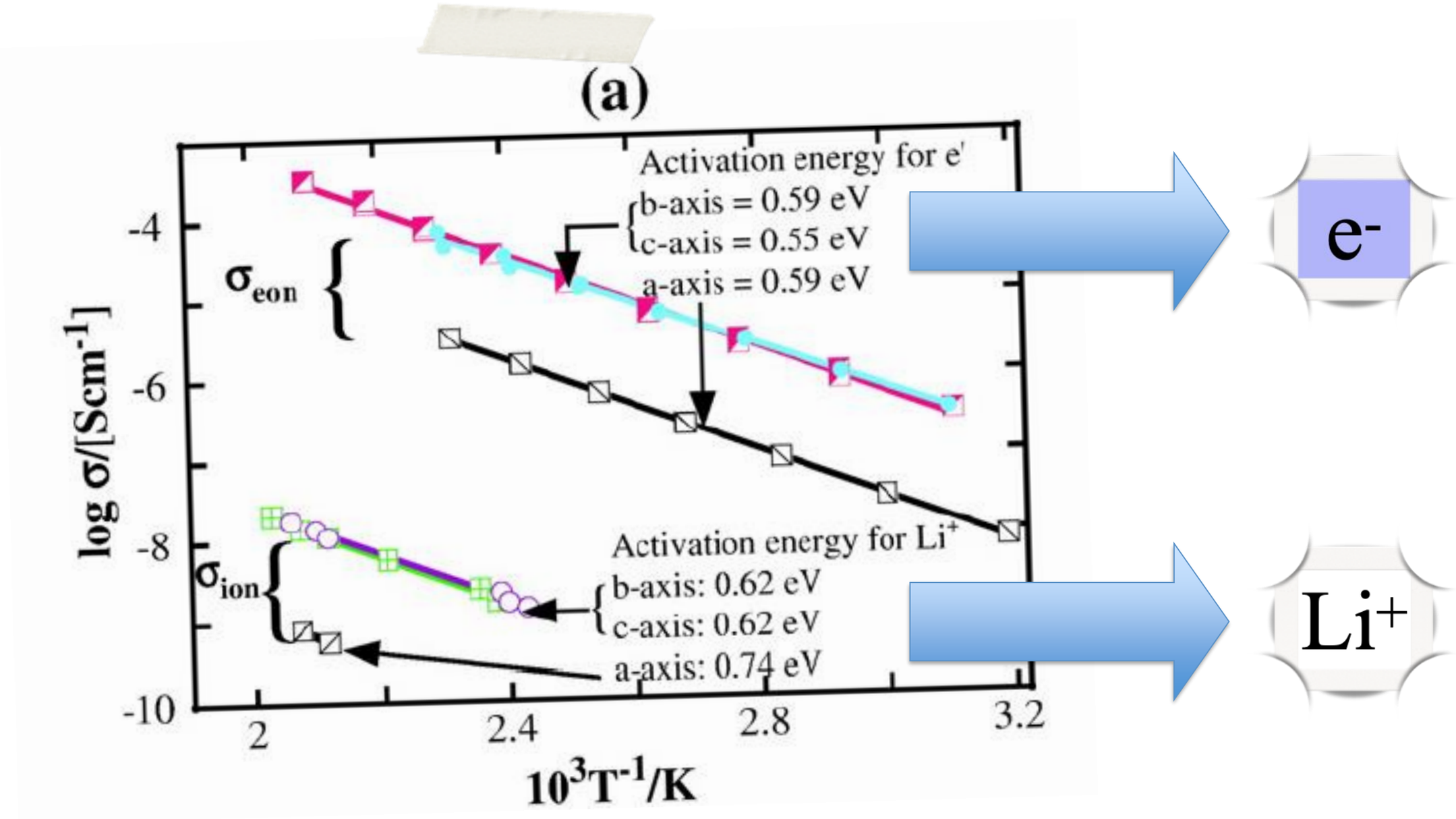

Amin et al. Solid State Ionics 179 (2008) 1683-1687

$LiFePO_4$, Mobility Pathways

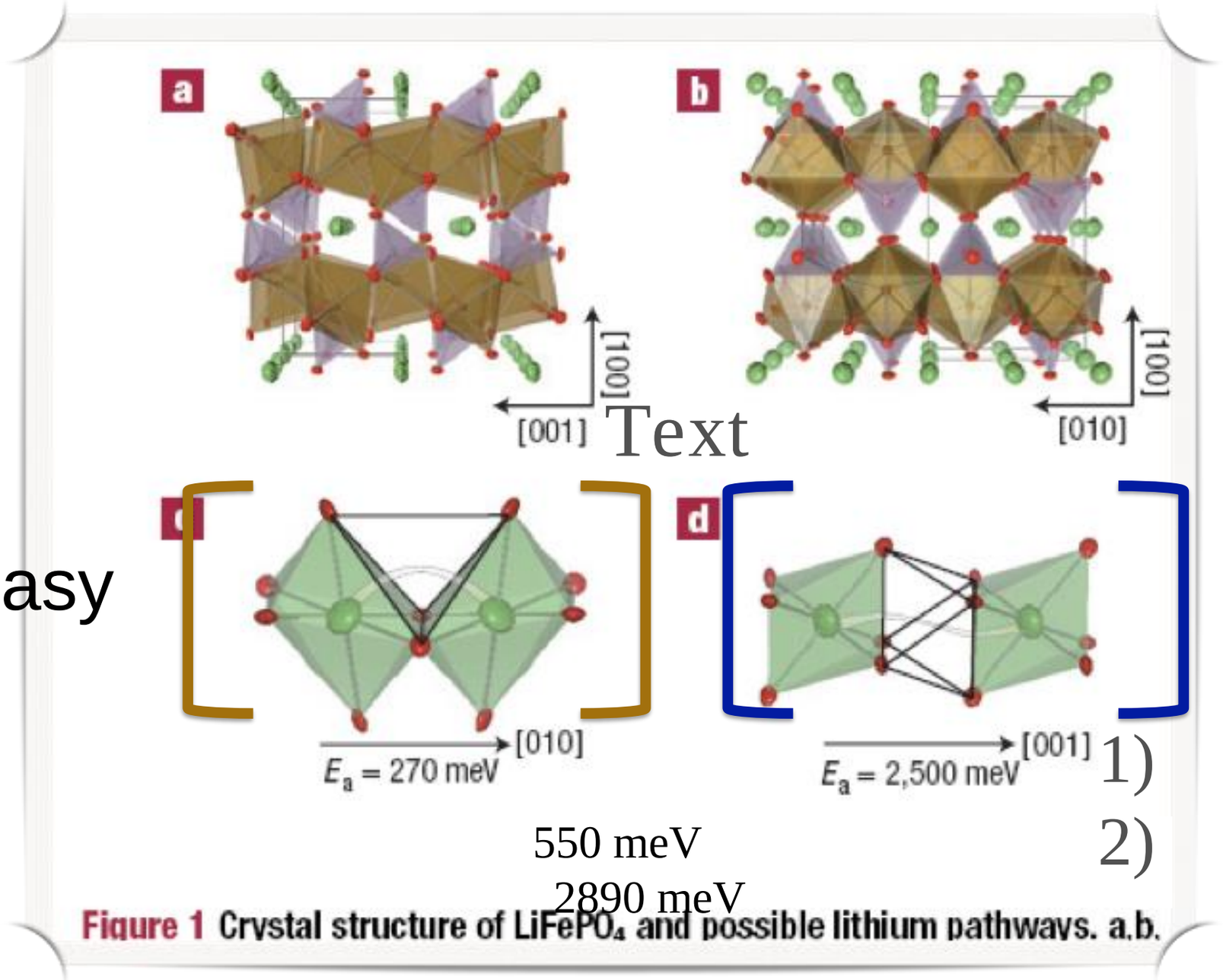

Figure 1 Crystal structure of $LiFePO_4$ and possible lithium pathways. a,b,

[010], easy

Text

[001], no go

1) 550 meV

2) 2890 meV

1) Yamada *et al.*, Nat. Mater. 7, 707 (2008)

2) M. S. Islam *et al.*, Chem. Mater. 17, 5085 (2005)

$LiFePO_4$ @ 1200 K

- Regular MD
- No jumps into adjacent voids
- Not even along [001]

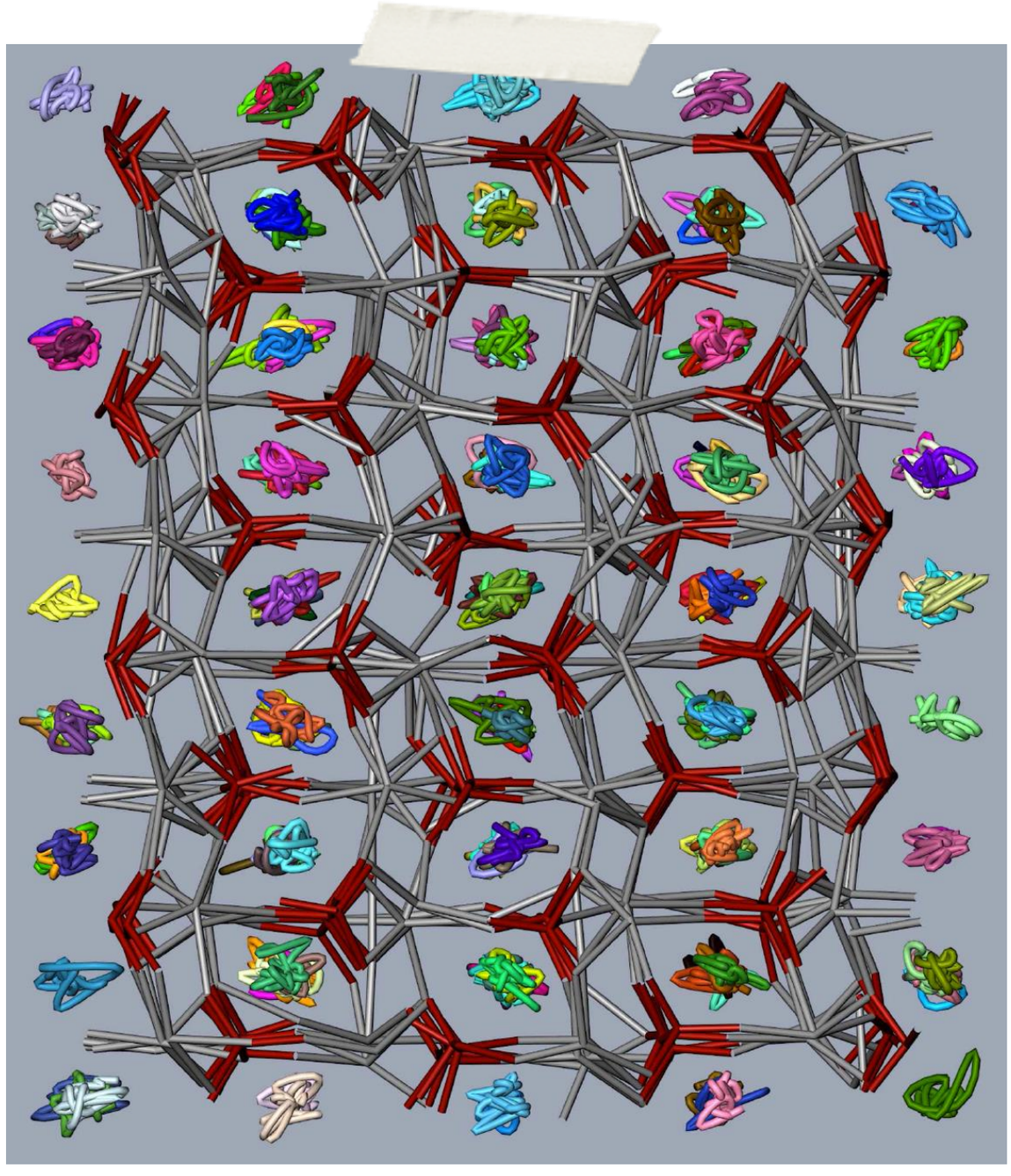

spline interpolation

How do the Li cations move ?

vent

Frequent events alone do not account for the complex potential energy landscape

Straightforward MD simulations typically incomplete

Time-Evolution of a System
Molecular Dynamics (MD)

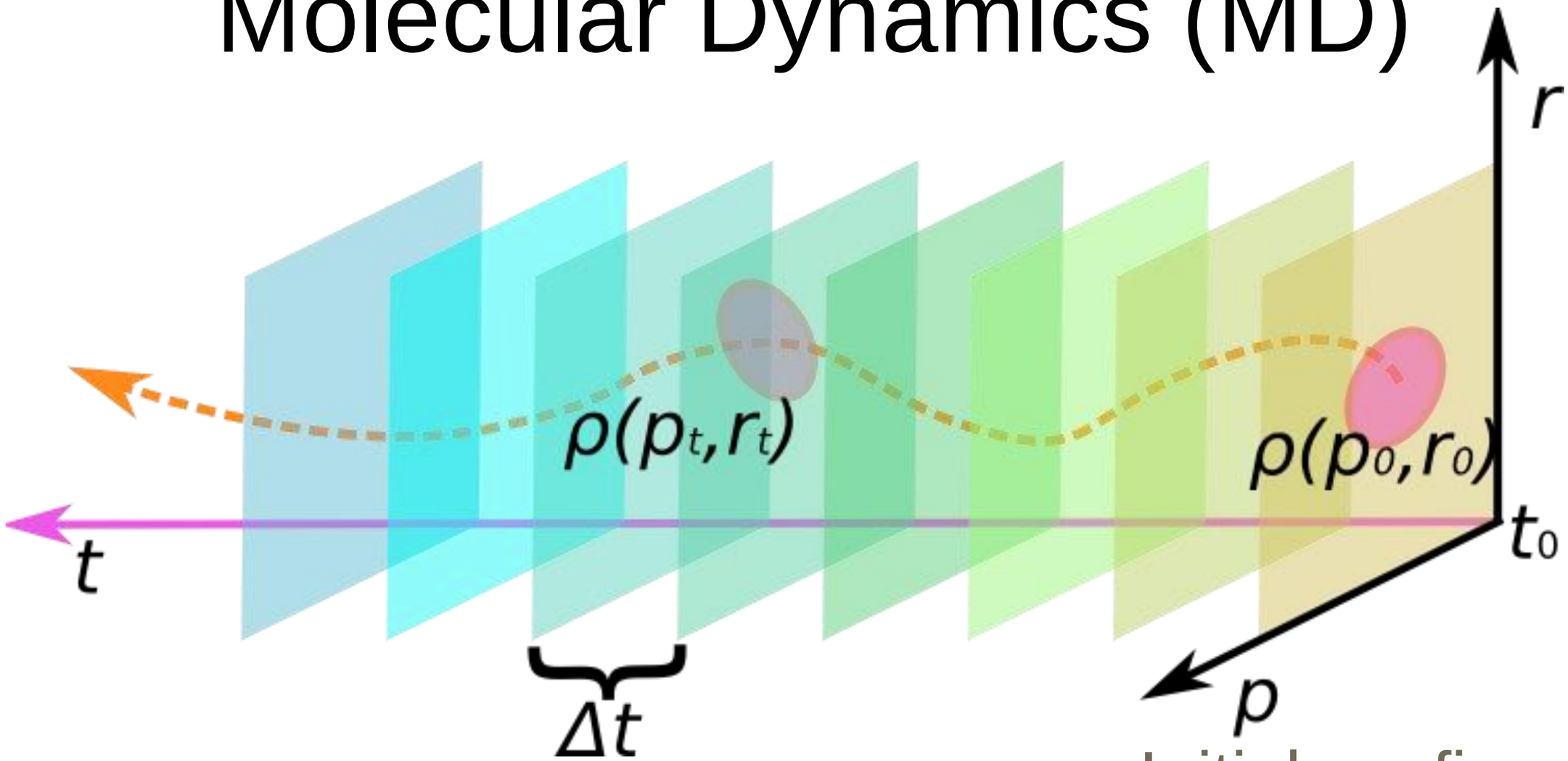

Calculate forces on atoms and time propagate, iteratively

Initial configuration: Specify positions and velocitiy distribution at temperature T.

„rare“ velocity distributions

Kinetic energy at time t

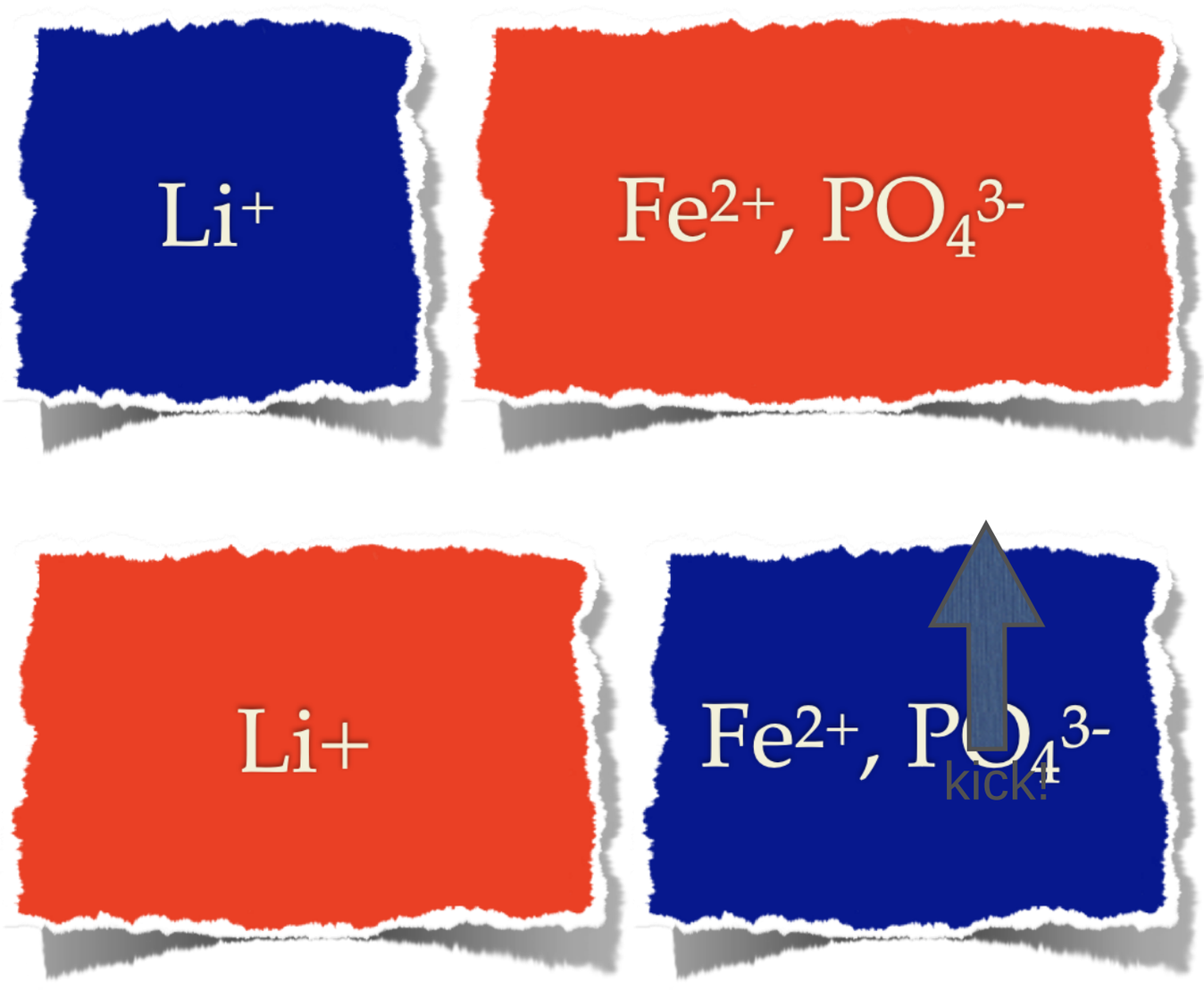

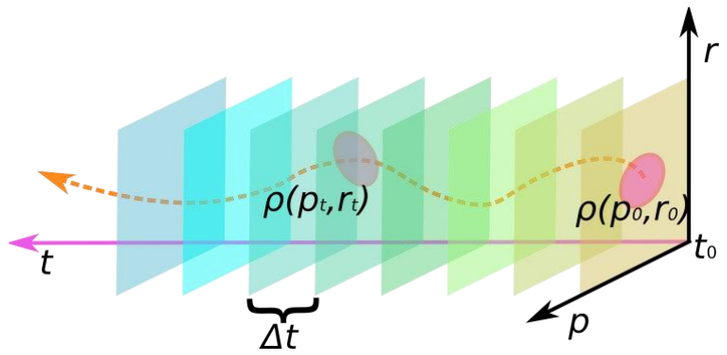

before

T(t) = const

Σ m(i)·v(i) = 0

kick! *after*

Internal redistribution of kinetic energy, „warming up“ of Li^+.

2D Diffusion Paths – [010] vs. [001]

500 K

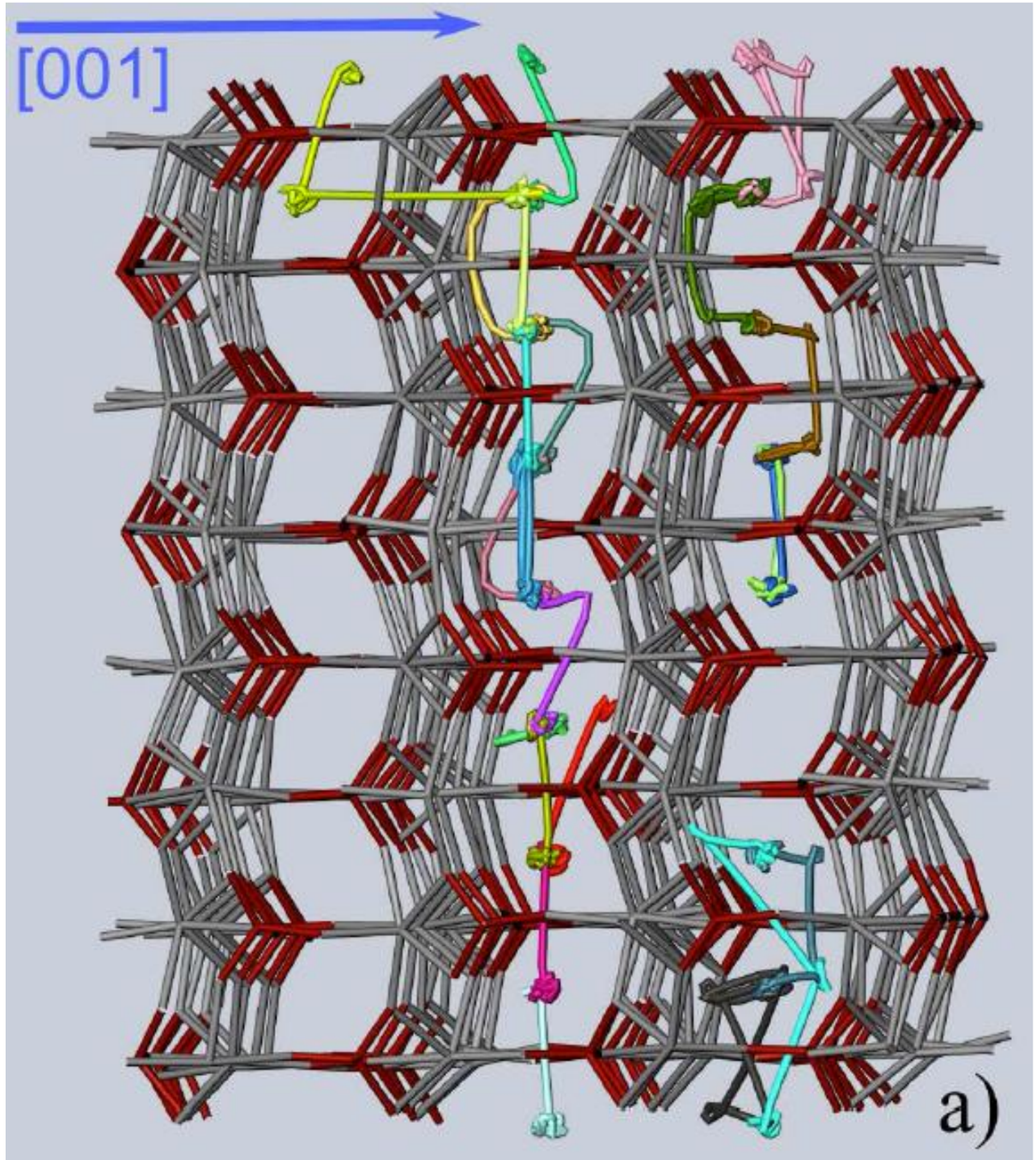

S.E. Boulfelfel, G. Seifert, S. Leoni, J. Mater. Chem. (2011)

Diffusion

- D is a macroscopic quantity;

- It can be related to (stepwise) microscopic displacements;

- A “time integration” of the Δr can be a way of assessing diffusion in MD simulations.

r $$\left\langle \Delta r(t)^2 \right\rangle = \frac{1}{N} \sum_{i=1}^{N} \Delta r_i(t)^2$$

Mean Squared Displacement

$$D = \frac{1}{6} \frac{MSD}{\Delta t}$$

p $$D = \int_0^{\infty} dt \left\langle v_x(t) v_x(0) \right\rangle, t = \Delta t$$

Total elapsed time

Velocity autocorrelation function

MSD vs VAC

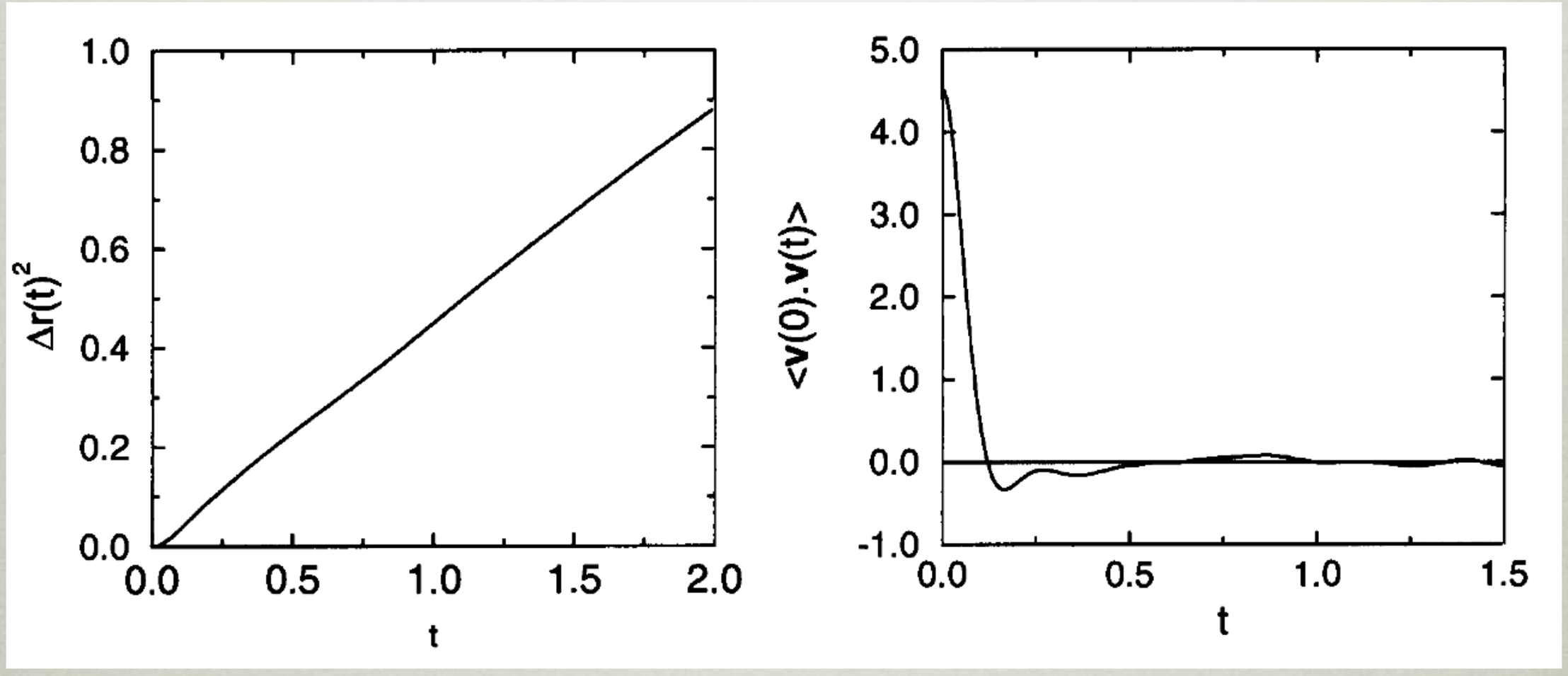
1.0
0.8
0.6
0.4
0.2
0.0
$\Delta r(t)^2$
0.0
0.5
1.0
1.5
2.0
t
5.0
4.0
3.0
2.0
1.0
0.0
-1.0
<v(0).v(t)>
0.0
0.5
1.0
1.5
t

Self-Diffusion Coefficients

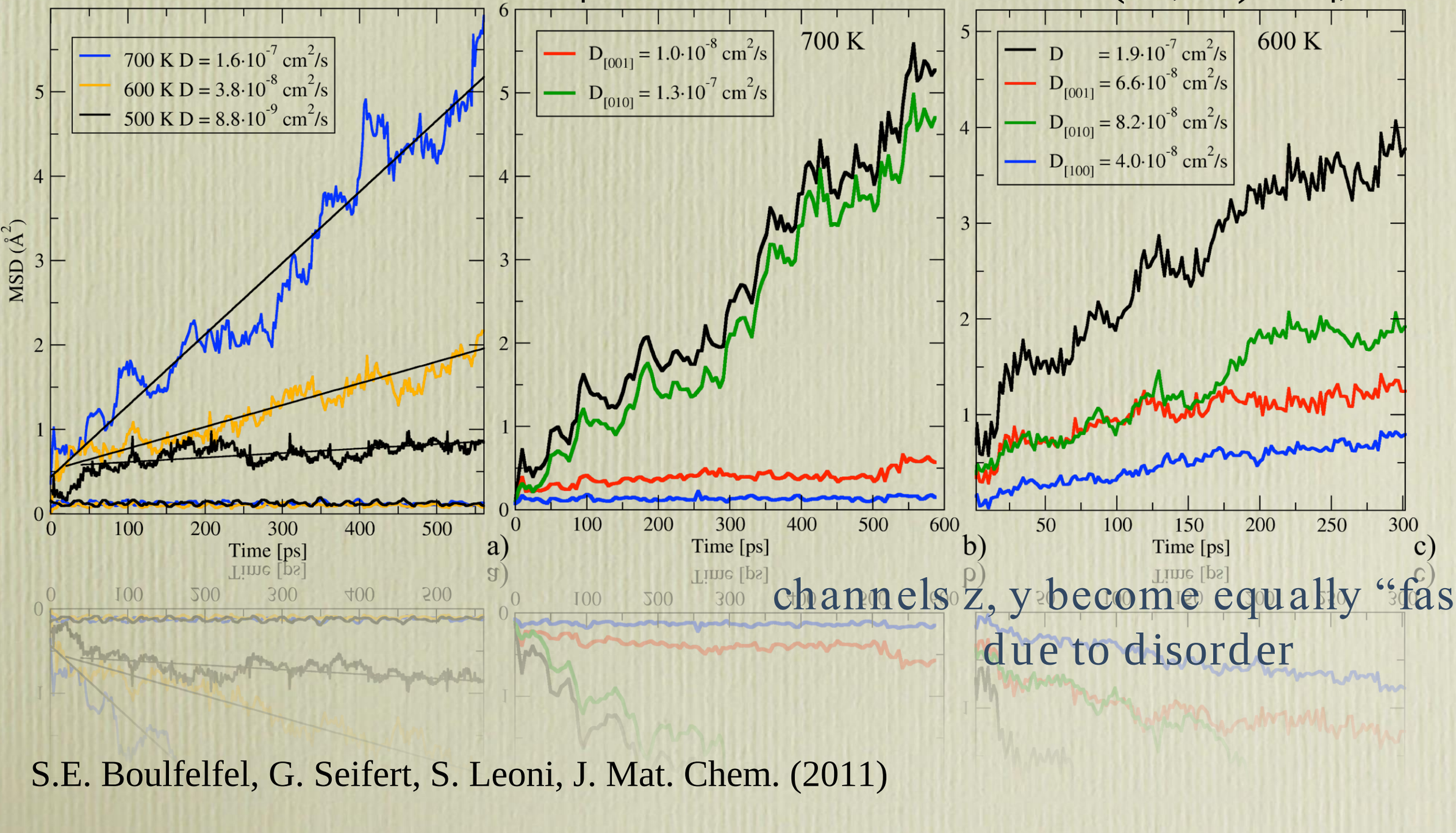

channels z, y become equally “fast” due to disorder

S.E. Boulfelfel, G. Seifert, S. Leoni, J. Mat. Chem. (2011)

What does enhance Li^+ mobility ?

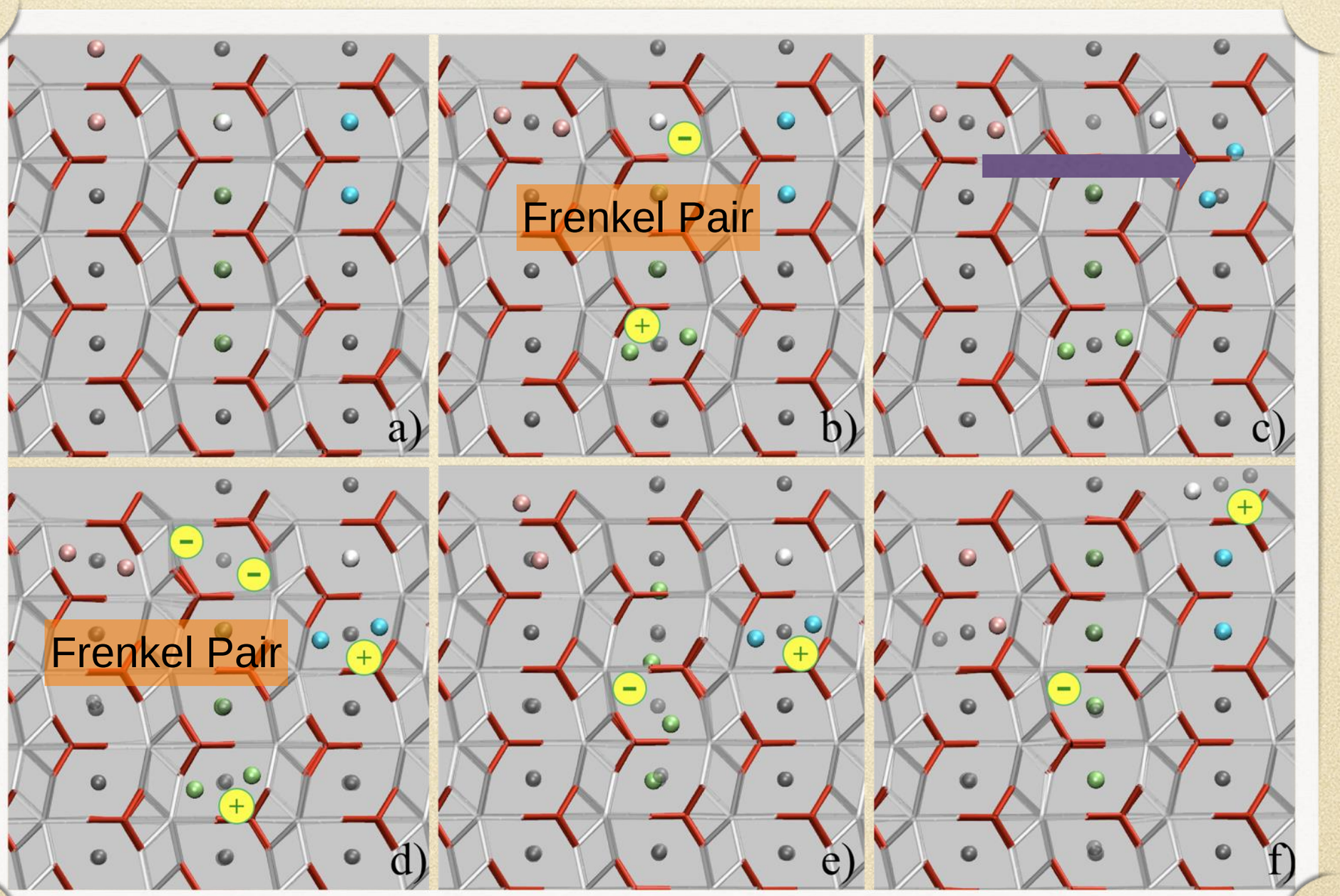

a fundamental yet elusive mechanism component!

Li vs. Na mobility in FePO4 olivine materials

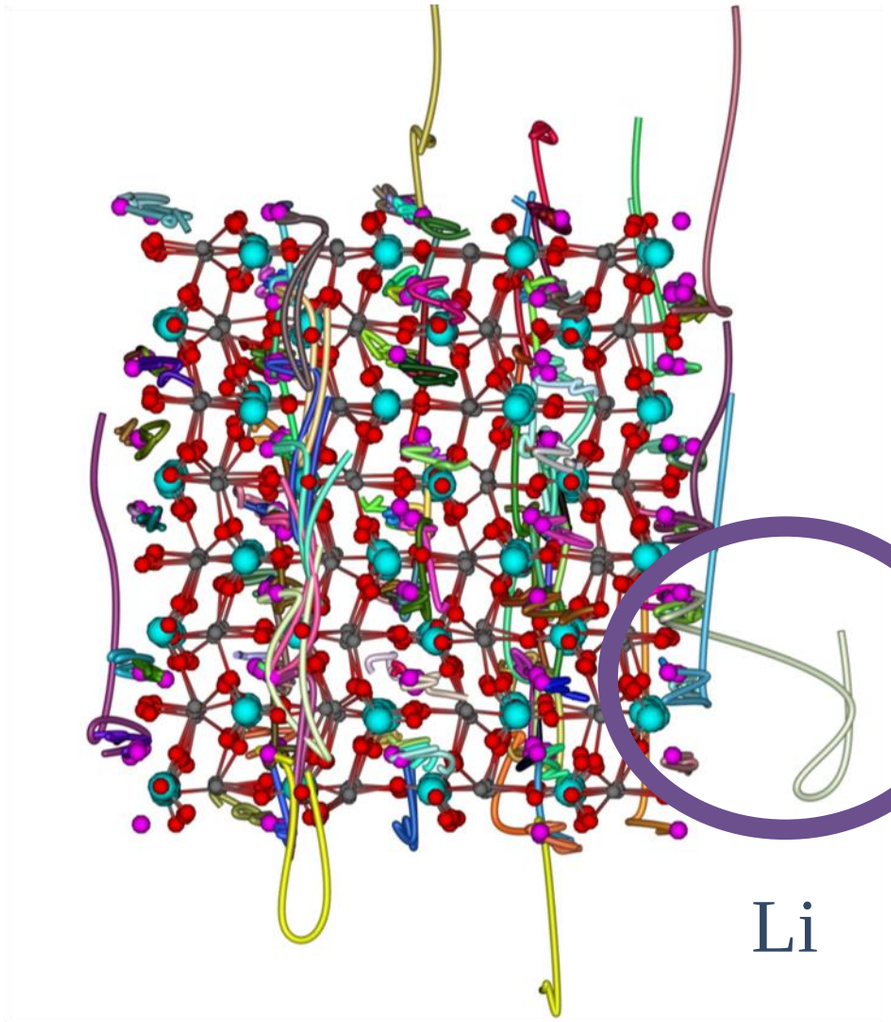

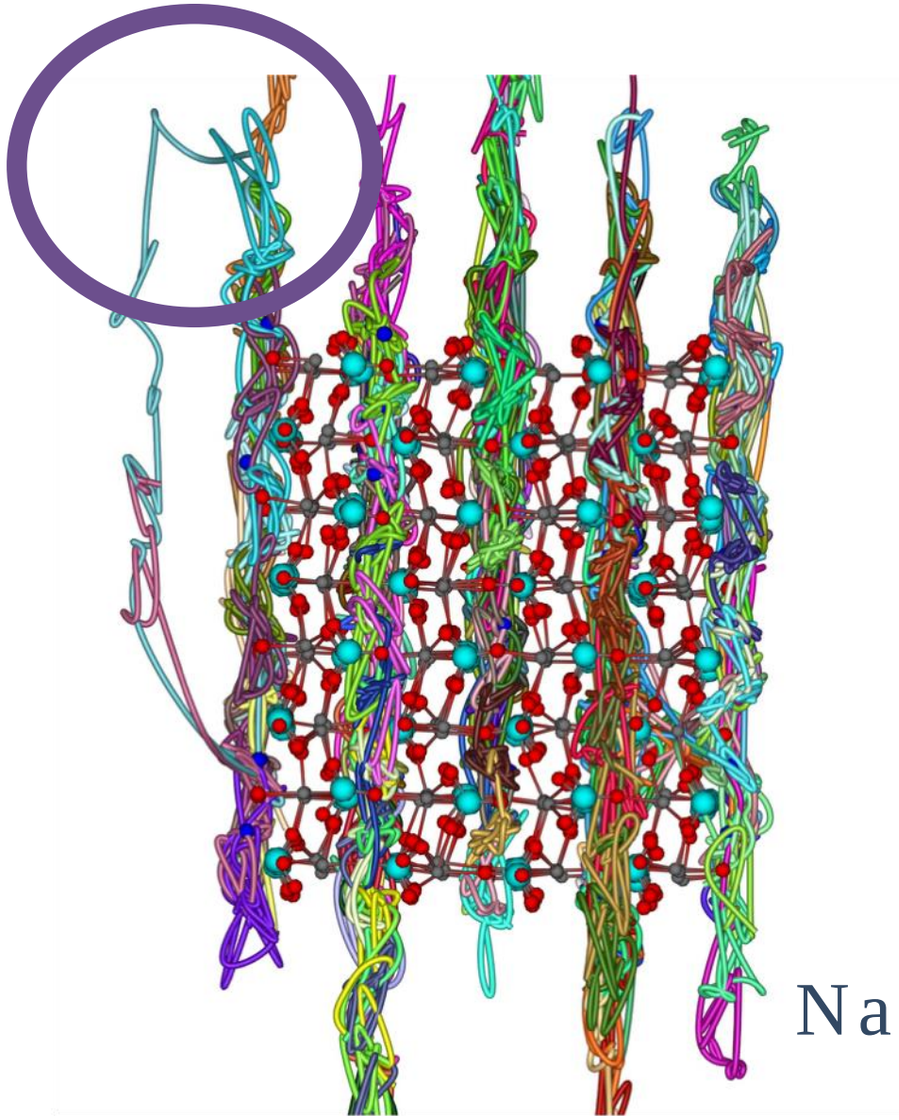

CATHODE MATERIAL	DIFFUSION COEFFICIENT / CM^2S^{-1}

T. Flack et al, in preparation (2018)

What CV for batteries

- Is it really diffusion ?
- In the spirit of MetaD, enhance appropriate collective variables to affect event probability.
- For crystallisation, a measure of “entropy” based on two body correlation was recently used.

$$S = -2\pi\rho k_B \int_0^\infty [g(r)\ln g(r) - g(r) + 1]r^2 dr$$

R. Nettleton and M. Green, *The Journal of Chemical Physics* **29**, 1365 (1958)

P.M. Piaggi, O. Valsson, M. Parrinello “Enhancing entropy and enthalpy fluctuations to drive crystallization in atomistic simulations”, PRL (2017)

“Diffusion” as Solid/Liquid Transition

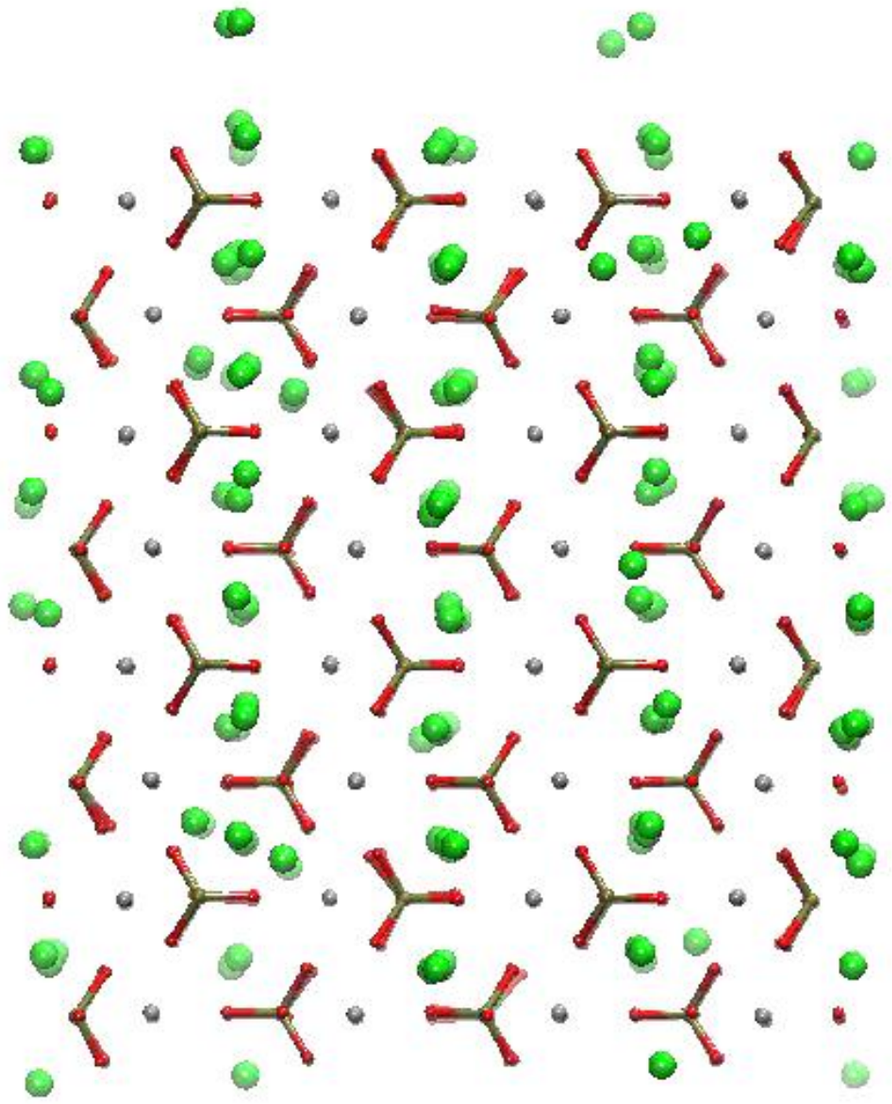

“entropy” as instantaneous measure of disorder

Defect formation

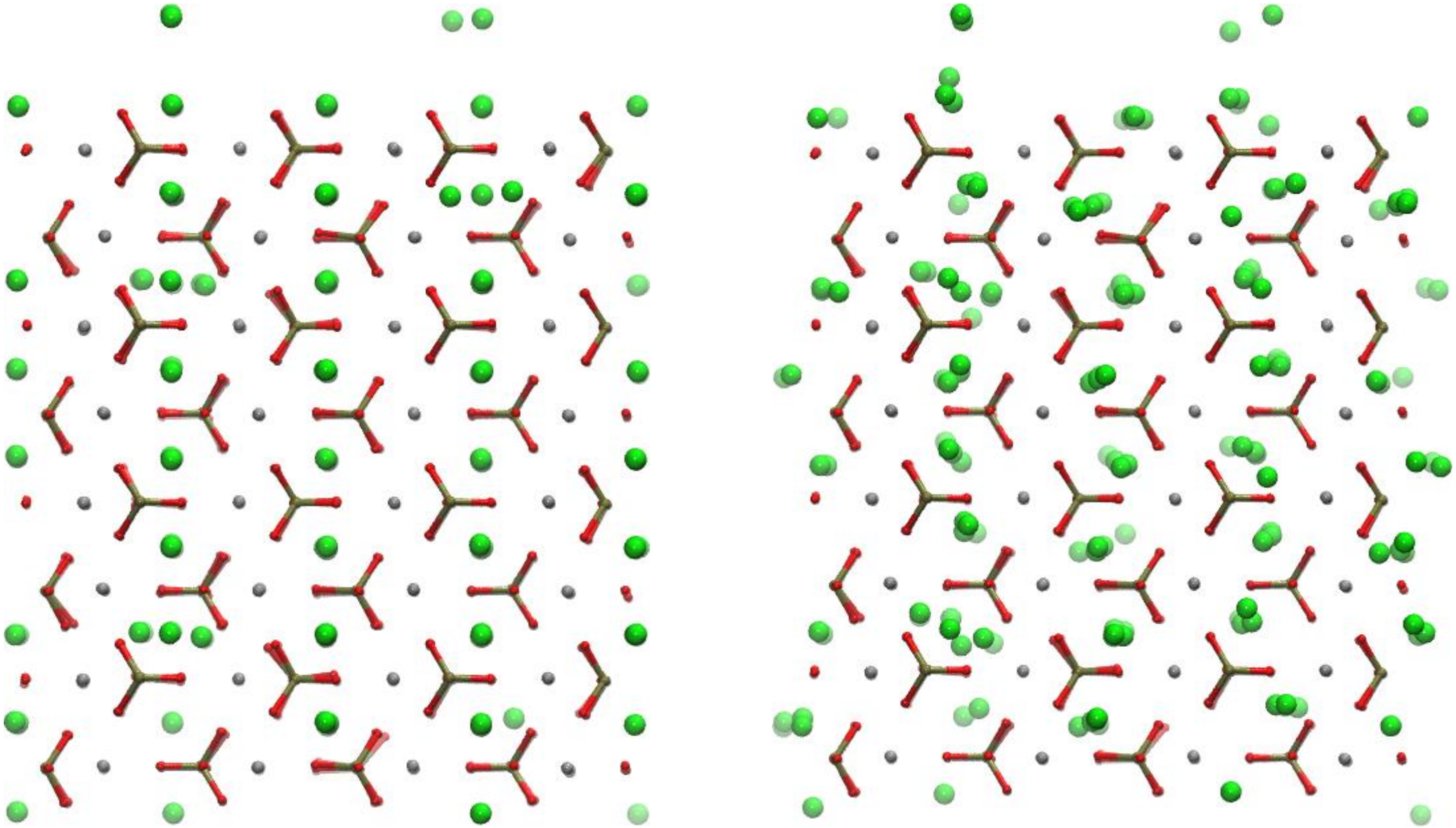

Defects promote translocation along easy axis

A different Approach

- “disorder” seems to fit the (necessary) formation of defects in battery materials.

- on the other hand, the existence of a structural scaffolding “funnels” chains of events.

- We designed a different CV with both periodicity and local order disruption in mind.

$$f(x) = \frac{\sum_{i=0}^{n} \sin(a\pi x_i)}{n}$$

S. Jobbins, S. Leoni, in preparation

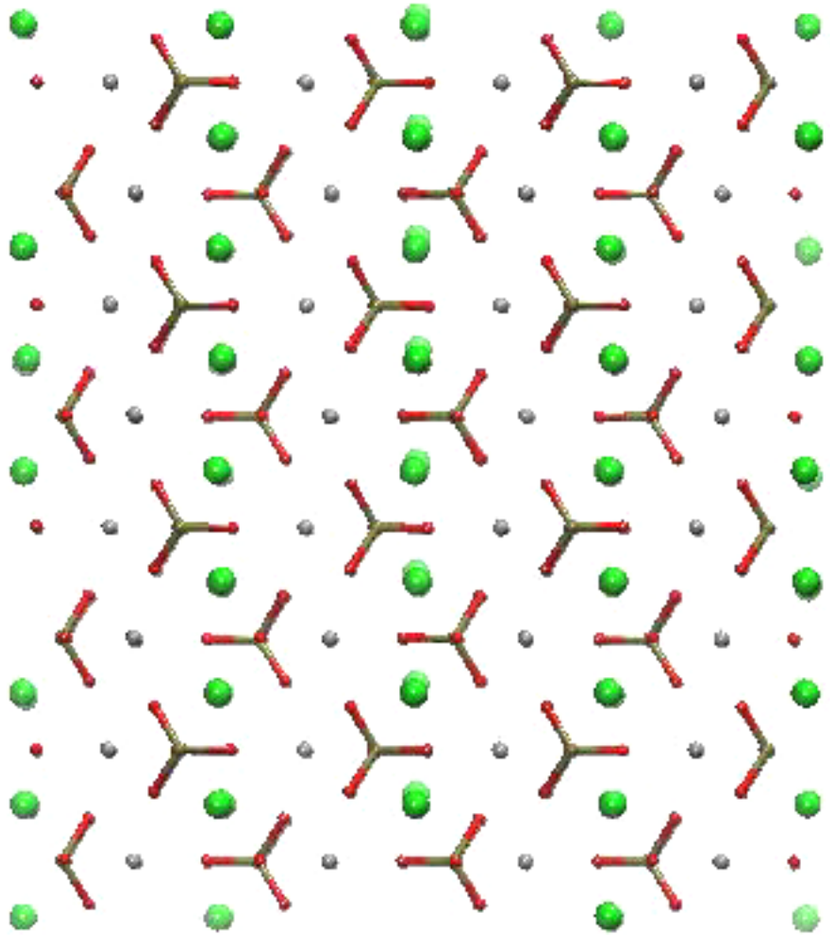

Comparison

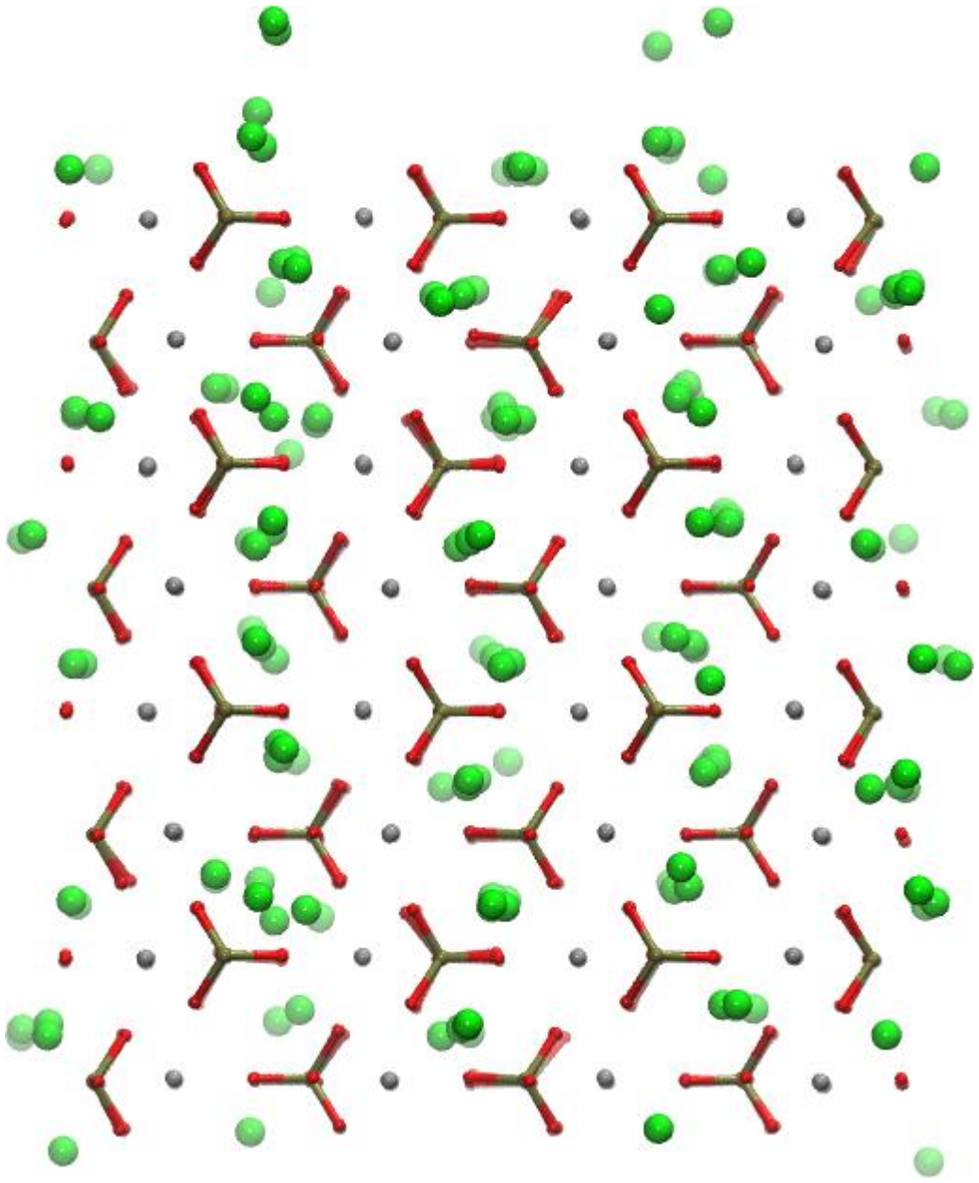

entropy

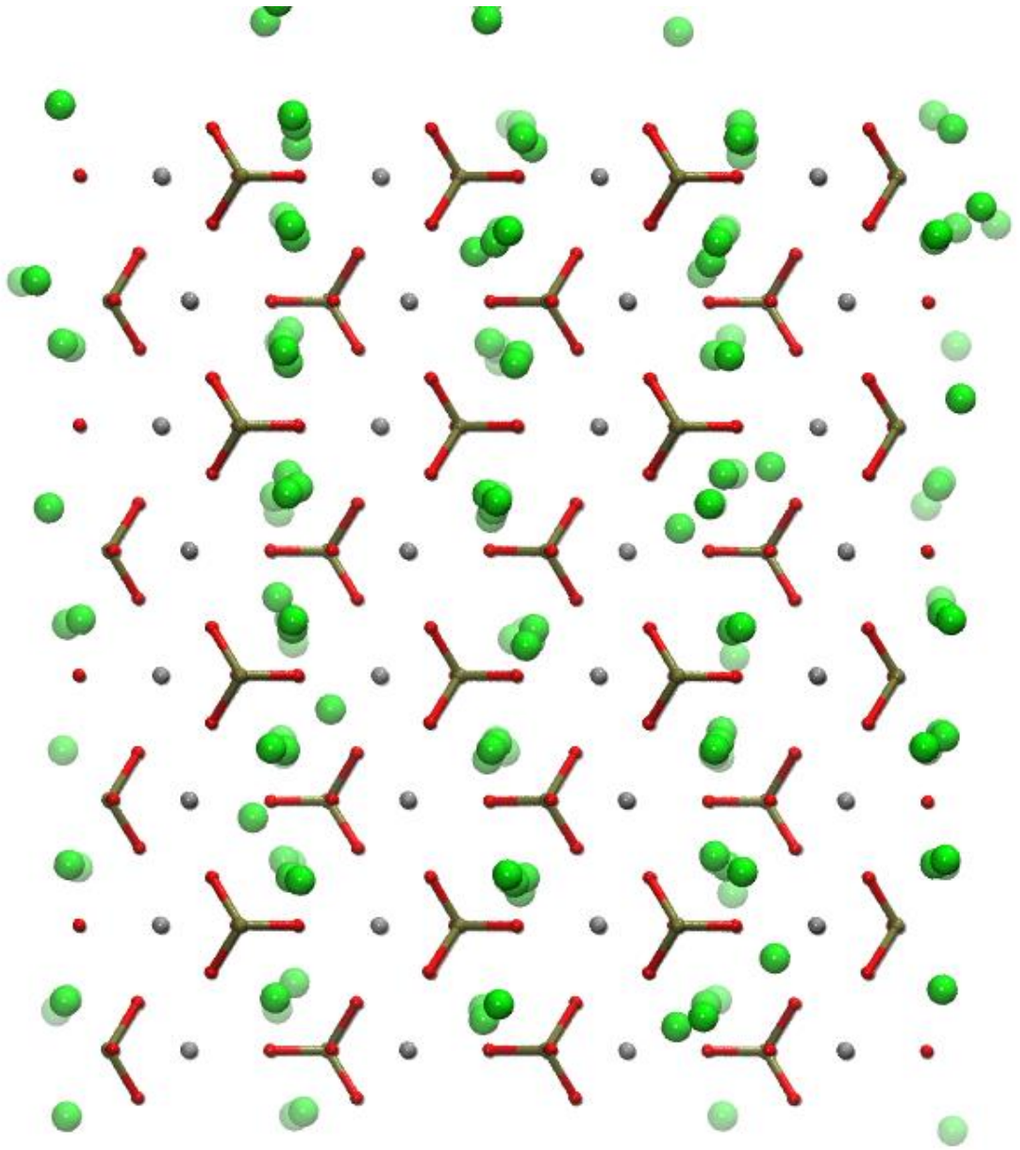

SFCV

Transversal translocations

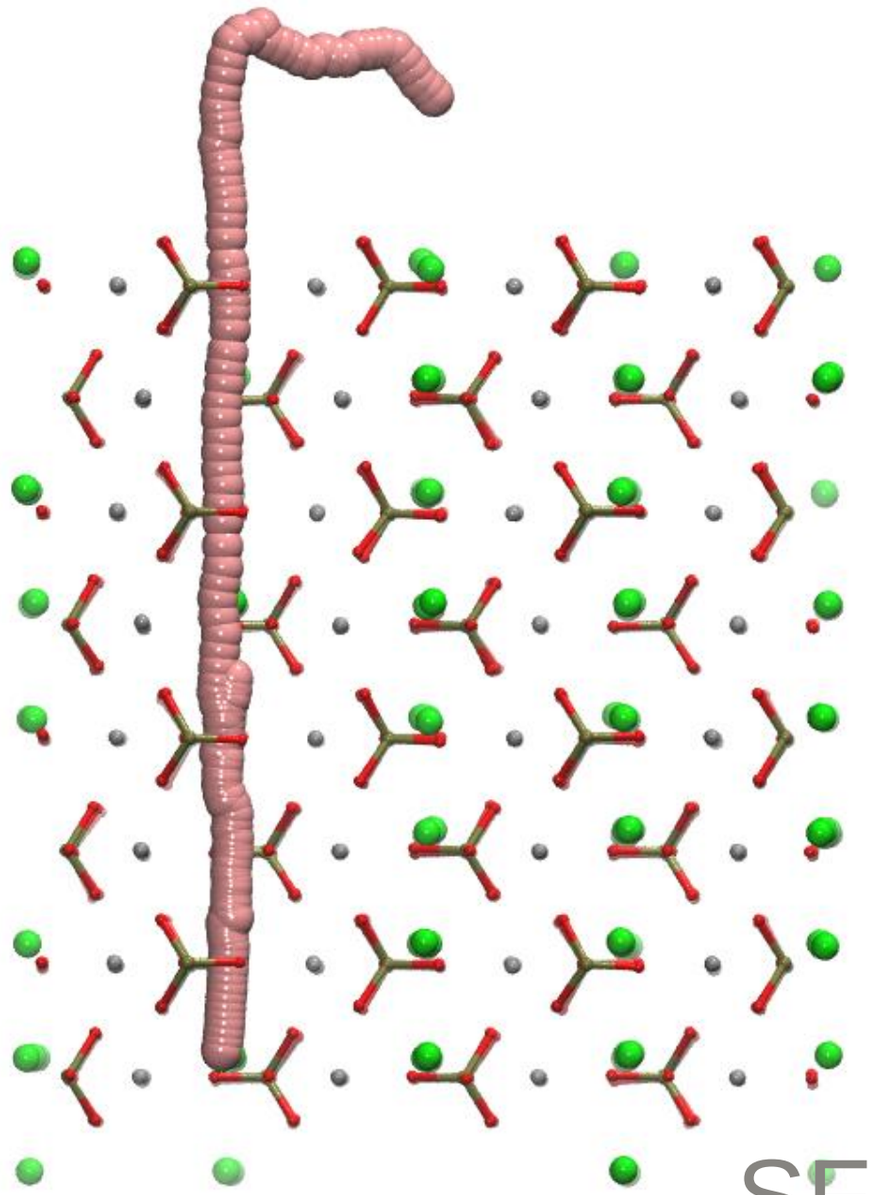

Events of lateral translocation are key to defect creation